

---

Theses and Dissertations

---

2012

# Regenerated cellulose for controlled oral drug delivery

Bhavik Janankumar Bhatt  
*University of Iowa*

Copyright 2012 Bhavik Bhatt

This dissertation is available at Iowa Research Online: <http://ir.uiowa.edu/etd/4577>

---

## Recommended Citation

Bhatt, Bhavik Janankumar. "Regenerated cellulose for controlled oral drug delivery." PhD (Doctor of Philosophy) thesis, University of Iowa, 2012.  
<http://ir.uiowa.edu/etd/4577>.

---

Follow this and additional works at: <http://ir.uiowa.edu/etd>

 Part of the [Pharmacy and Pharmaceutical Sciences Commons](#)

REGENERATED CELLULOSE FOR CONTROLLED ORAL DRUG DELIVERY

by

Bhavik Janankumar Bhatt

An Abstract

Of a thesis submitted in partial fulfillment  
of the requirements for the Doctor of  
Philosophy degree in Pharmacy  
(Pharmaceutics) in the Graduate College of  
The University of Iowa

May, 2013

Thesis Supervisor: Professor Maureen Donovan

## ABSTRACT

The performance of regenerated cellulose (RC) films and capsules was investigated for their applications in oral controlled drug delivery. Regenerated cellulose films were prepared by non-solvent-mediated, phase inversion of native and depolymerized cotton linter solutions (methylolcellulose; cellulose dissolved in dimethyl sulfoxide/ paraformaldehyde solvent system) in water as well as by phase inversion of native cotton linter solutions in organic non-solvents followed by thermal annealing. These films were monolithic in dry state and formed porous structures when hydrated. Irrespective of the degree of polymerization of the starting cellulose source or the use of organic non-solvents, the cellulose chain length was not significantly altered and cellulose was in an amorphous state. Flux analysis in diffusion cells, using ethanol-water mixtures as the solvent medium, indicated that the films take up solvent to form porous routes for transport of solute. The amount of solvent uptake required to form these routes was greater for films prepared from depolymerized cotton linter. Ionic and hydrophobic solutes traverse the films using the porous pathways following hydration of the film.

Blended RC films were prepared by combining native and depolymerized cotton linter solutions in varying ratios and phase-inverting in water, followed by thermal annealing. Porosity, pore size and water uptake of the hydrated films decreased, while the length of the transport pathway (tortuosity) increased, as the fraction of depolymerized cellulose increased in the blended films.

Differences in methylene blue dye adsorption on phase-inverted vs. phase-inverted and thermally annealed RC films indicated that the type of non-solvent utilized for phase-inversion does not affect the internal RC film structure during the phase-inversion process.

However, as the boiling point of the non-solvent increased, the amount of irreversible polymer consolidation and formation non-swelling domains (hornification) increased during the thermal annealing process. This, in turn, led to reduced porosity and solute flux through these RC films.

Two-piece cellulose capsules were fabricated by phase-inversion of methylolcellulose solutions in water using a dip-coating approach. Zero-order release rates for a number of drugs increased as their water solubility increased. The release of water soluble drugs occurred by osmotically-driven convection and diffusion through the pores in the capsule wall, while the release of moderate to poorly soluble drugs predominantly occurred by diffusion. Moreover, as the drug solubility increased, the apparent permeability of the drugs through the capsule wall decreased, which indicated that the inward osmotic flux of water reduced the diffusivity of the drug through the pores. The hydraulic permeability of the cellulose capsules was determined to be higher than for conventional ethylcellulose and cellulose acetate coated osmotic drug delivery systems, indicating that the cellulose-based capsules may be better suited for osmotic drug delivery.

Abstract Approved:

\_\_\_\_\_

Thesis Supervisor

\_\_\_\_\_

Title and Department

\_\_\_\_\_

Date

REGENERATED CELLULOSE FOR CONTROLLED ORAL DRUG DELIVERY

by

Bhavik Janankumar Bhatt

A thesis submitted in partial fulfillment of the  
requirements for the Doctor of Philosophy degree in  
Pharmacy (Pharmaceutics) in the Graduate College  
of The University of Iowa

May, 2013

Thesis Supervisor: Professor Maureen Donovan

Graduate College  
The University of Iowa  
Iowa City, Iowa

CERTIFICATE OF APPROVAL

---

PH.D. THESIS

---

This is to certify that the Ph. D. Thesis of

Bhavik Janankumar Bhatt

has been approved by the examining Committee for the  
thesis requirement for the Doctor of Philosophy degree in  
Pharmacy (Pharmaceutics) at the May 2013 graduation.

Thesis Committee:

---

Maureen Donovan, Thesis Supervisor

---

Douglas Flanagan

---

Dale Wurster

---

Jennifer Fiegel

---

Aliasger Salem

Dedicated to my family

Science is the one human activity that is truly progressive. The body of positive knowledge is transmitted from generation to generation

Edwin Hubble



## ACKNOWLEDGEMENTS

I want to thank the Department of Pharmaceutics and Translational Therapeutics at the College of Pharmacy for providing me the opportunity to pursue graduate studies. My sincerest appreciation goes to Dr. Kumar for sparking innovative ideas and research methods, and for his guidance and support through majority of my thesis. I hope you get well soon and back to the cheerful and insightful person you are.

My sincere gratitude goes to Dr. Donovan who helped me complete my graduate work, and for serving as a vital member on the dissertation committee. I also want to thank Dr. Flanagan, Dr. Wurster, Dr. Salem and Dr. Fiegel for serving on my dissertation committee. I would like to dedicate special acknowledgement to the Pharmacy Practice Lab, The University of Iowa Pharmaceuticals, Novartis Consumer Health and Syntrix Biopharmaceuticals Corporation for providing financial support through the course of my graduate study at the College of Pharmacy.

Acknowledgements would be incomplete without mentioning colleagues and friends who have made my stay memorable and enjoyable in Iowa City. Salil, Praveen and Raunaq, you were the greatest roommates anyone could ask for. I want to thank my lab mates Eduardo, John, Jinzhou, Dan and Andrew for their constant help and input of ideas and methodology for carrying out my experiments. Special thanks goes to my great friends Yogita, Maya, Vijaya and Varsha who have always provided me with amazing home cooked Indian dinners, at a moment's notice. Last, but not the least, I am thankful to my parents, Janakkumar and Ilaben, brothers Rajat and Vashishtha, sister-in-law Khyati, and lovely wife Pooja who have provided me with the strength, moral support

and encouragement through my stay in Iowa. They are the reason I am here and helped me succeed in my ambitions.

## TABLE OF CONTENTS

|                       |                                                                       |    |
|-----------------------|-----------------------------------------------------------------------|----|
| LIST OF TABLES        | ix                                                                    |    |
| LIST OF FIGURES       | xi                                                                    |    |
| LIST OF ABBREVIATIONS | xvi                                                                   |    |
| CHAPTER               |                                                                       |    |
| I                     | INTRODUCTION AND BACKGROUND                                           | 1  |
|                       | Controlled drug delivery                                              | 1  |
|                       | Cellulose                                                             | 2  |
|                       | 'Cellulosics' in controlled drug delivery                             | 4  |
|                       | Solvents for Unmodified cellulose utilized in biomedical applications | 7  |
|                       | Phase inversion\ immersion precipitation process                      | 15 |
|                       | Cellulose hornification and irreversible polymer consolidation        | 16 |
|                       | The capsule dosage form                                               | 17 |
|                       | Capsule based controlled drug delivery systems                        | 18 |
|                       | Determination of permeability of solute through membranes and films   | 20 |
|                       | Osmotic mechanism for drug release                                    | 21 |
| II                    | OBJECTIVES                                                            | 24 |
| III                   | CHARACTERISTICS OF REGENERATED CELLULOSE FILMS                        | 26 |
|                       | Introduction                                                          | 26 |
|                       | Experimental                                                          | 27 |
|                       | Materials                                                             | 27 |
|                       | De-polymerization of cellulose                                        | 28 |
|                       | Preparation of methylolcellulose solution                             | 29 |
|                       | Film casting by immersion precipitation and cellulose yield           | 29 |
|                       | Determination of degree of polymerization                             | 33 |
|                       | Fourier Transform Infrared (FTIR) spectroscopic analysis              | 35 |
|                       | Preparation of cellulose II crystallization standard                  | 35 |
|                       | X-ray diffraction analysis                                            | 36 |
|                       | Solvent uptake and volume fraction of solvents in swollen RC films    | 37 |
|                       | Porosity of cellulose films                                           | 38 |
|                       | Surface and cross-section analysis                                    | 39 |
|                       | Preparation of saturated solute solutions and                         | 40 |

|    |                                                                                             |     |
|----|---------------------------------------------------------------------------------------------|-----|
|    | determination of solubility                                                                 |     |
|    | Transport studies through RC films                                                          | 40  |
|    | Transport of acetaminophen through RC-W and RC-DP films in binary solvents                  | 41  |
|    | Influence of thermal curing on the flux of ethyl                                            | 43  |
|    | Transport of KCl and alkyl-p-aminobenzoates through RC blended films                        | 43  |
|    | Transport of LZY and BSA through RC blended films                                           | 44  |
|    | Estimation of irreversible polymer consolidation (hornification) by thermal treatment       | 44  |
|    | Analytical methods                                                                          | 45  |
|    | Results and Discussion                                                                      | 47  |
|    | Preparation of depolymerized cotton linters                                                 | 47  |
|    | Cellulose yield from precipitation of MC solution in various non-solvents                   | 48  |
|    | Polymer stability during film formation                                                     | 48  |
|    | X-Ray diffractograms of RC films                                                            | 56  |
|    | Visual examination of cellulose films formation                                             | 59  |
|    | Influence of degree of polymerization of cellulose                                          | 61  |
|    | Hydration and its influence on solute flux through thermally cured RC films                 | 66  |
|    | Transient effect of RC film hydration                                                       | 73  |
|    | Blending of MC and MC-DP solutions                                                          | 74  |
|    | Influence of non-solvents on RC film formation and solute flux                              | 92  |
|    | Modulation of RC film thickness and its impact on solute permeability                       | 96  |
|    | Conclusions                                                                                 | 103 |
| IV | PREPARATION AND IN-VITRO PERFORMANCE OF TWO-PIECE HARD SHELL REGENERATED CELLULOSE CAPSULES | 106 |
|    | Introduction                                                                                | 106 |
|    | Experimental                                                                                | 108 |
|    | Materials                                                                                   | 108 |
|    | Preparation of methylcellulose solutions                                                    | 108 |
|    | General method for preparing capsule halves                                                 | 108 |
|    | Improving reproducibility of capsules                                                       | 110 |
|    | Preparation of one component formulations for capsule filling                               | 113 |
|    | Capsule filling and sealing                                                                 | 115 |
|    | Determination of water solubility of the APIs                                               | 115 |
|    | In-vitro release studies from capsules                                                      | 115 |
|    | Osmotic pressure of urea and saturated API                                                  | 118 |

|                                                                                                                                |     |
|--------------------------------------------------------------------------------------------------------------------------------|-----|
| solutions                                                                                                                      |     |
| Permeability of APIs through RC films                                                                                          | 119 |
| Analytical methods                                                                                                             | 121 |
| Results and Discussion                                                                                                         | 123 |
| Fabrication of capsules                                                                                                        | 123 |
| Drug release and its dependence on enclosed API<br>solubility                                                                  | 127 |
| Process of API release from capsules                                                                                           | 130 |
| Verification of osmotic mechanism for release of<br>water soluble APIs                                                         | 134 |
| Contributions of osmotic and diffusive<br>mechanisms to water soluble API release<br>from capsules during the zero order phase | 141 |
| Evaluation of fluid permeability of cellulose<br>capsules and comparison to conventional<br>osmotic systems                    | 146 |
| Influence of osmotic flux on API diffusivity<br>through capsule walls                                                          | 148 |
| In-vitro conditions influencing API release                                                                                    | 154 |
| Conclusions                                                                                                                    | 157 |
| REFERENCES                                                                                                                     | 160 |

## LIST OF TABLES

| Table |                                                                                                                                                                                                                                                                               |    |
|-------|-------------------------------------------------------------------------------------------------------------------------------------------------------------------------------------------------------------------------------------------------------------------------------|----|
| 1     | Summary of typical X-ray diffractogram peak assignments reported for the four polymorphic forms of cellulose.                                                                                                                                                                 | 5  |
| 2     | Summary of advantages and disadvantages of solvents utilized for dissolution in order to prepare cellulose products for bio-medical applications.                                                                                                                             | 14 |
| 3     | Cellulose yield from MC-4 solution in various non-solvents                                                                                                                                                                                                                    | 50 |
| 4     | Summary of degree of polymerization of cellulose and viscosity average molecular weight of cellulose of cotton linter, depolymerized cotton linters and RC films from the linear fitting parameters of $\log\{(\eta_{rel}-1)/C\}$ vs. concentration plots.                    | 53 |
| 5     | Summary of solvent uptake (SU), volume fraction of solvent, solvent density and relative solvent volume ( ) in swollen RC-W and RC-DP films at 37°C, calculated using solvent uptake data                                                                                     | 69 |
| 6     | Summary of mass transfer rate, flux, solubility normalized flux and flux alteration factor of acetaminophen through RC-W and RC-DP films using Side-by-Side® diffusion cells in ethanol-water binary solvent systems with varying ethanol concentrations, at 37°C             | 71 |
| 7     | True density, porosity, degree of swelling and average pore size of RC-W, RC-4/1, RC-3/2, RC-2/3, RC-1/4 and RC-DP films                                                                                                                                                      | 79 |
| 8     | Flux parameters and calculated permeability coefficient as well as hindrance factors and tortuosity estimated from KCl flux through RC-W, RC-4/1, RC-3/2, RC-2/3, RC-1/4 and RC-DP films in Side-by-Side® diffusion cells, using purified water as solvent at 37°C            | 83 |
| 9     | Flux, permeability and hindrance factors of methyl-, ethyl-, propyl- and butyl-p-aminobenzoates through RC-W, RC-4/1, RC-3/2, RC-2/3, RC-1/4 and RC-DP films in water at 37°C, using Side-by-Side® diffusion cells.                                                           | 82 |
| 10    | Flux parameters and calculated permeability coefficient as well as hindrance factors for lysozyme chloride (LZY) in pH 4.5 buffer ( $\mu \approx 0.15$ ) and bovine serum albumin (BSA) in pH 7.4 buffer ( $\mu \approx 0.15$ ) through RC-W, RC-DP and blend films, at 37°C. | 90 |
| 11    | Methylene blue adsorption parameters determined by fitting Langmuir like equation to adsorption isotherms shown in Figure 28 for RC-A, RC-                                                                                                                                    |    |

|    |                                                                                                                                                                                                                                                                                                                                                           |     |
|----|-----------------------------------------------------------------------------------------------------------------------------------------------------------------------------------------------------------------------------------------------------------------------------------------------------------------------------------------------------------|-----|
|    | M, RC-E, RC-P, RC-W and RC-B freeze dried and thermally cured films.                                                                                                                                                                                                                                                                                      | 97  |
| 12 | Flux parameters of ethyl-p-aminobenzoate through RC -2T, RC-3T, RC-4T and RC-5T films, in purified water at 37°C.                                                                                                                                                                                                                                         | 102 |
| 13 | Composition of methylolcellulose solutions utilized in fabrication of capsules                                                                                                                                                                                                                                                                            | 109 |
| 14 | List of APIs, their molecular weight, literature reported water solubility, and maximum powder fill achieved in cellulose capsules.                                                                                                                                                                                                                       | 114 |
| 15 | Summary of HPLC settings and column specifications utilized in analysis of API concentrations                                                                                                                                                                                                                                                             | 122 |
| 16 | Measured capsule cap and body dimensions and estimation of core volume and exterior surface area of an assembled cellulose capsule.                                                                                                                                                                                                                       | 129 |
| 17 | Measured solubility and zero order release rates of the APIs from cellulose capsules, in purified water at 37°C.                                                                                                                                                                                                                                          | 132 |
| 18 | Measured vapor pressures of water vapor from saturated API solutions, known concentrations of urea aqueous solutions in three separate experimental runs and the estimated osmotic pressures of these solutions.                                                                                                                                          | 140 |
| 19 | Calculated osmotic pressure differences and corresponding zero order release rates of potassium chloride diphenhydramine HCl, tramadol HCl and niacinamide from cellulose capsules in aqueous urea solutions at 37 °C                                                                                                                                     | 142 |
| 20 | Estimation of osmotic component of zero order release rate and fluid permeability, calculated from the linear regression parameters of the total zero order release rate ' $(dM/dt)_T$ ' vs. osmotic pressure difference ' $\Delta\pi$ ' across the capsule shell when filled with potassium chloride, diphenhydramine HCl, tramadol HCl and niacinamide. | 145 |
| 21 | Permeability coefficients of APIs from cellulose capsules and through RC films obtained from diffusion cell experiments, and the calculated reduction in diffusive mechanism.                                                                                                                                                                             | 152 |

## LIST OF FIGURES

| Figure |                                                                                                                                                                                                                                                                                                                              |    |
|--------|------------------------------------------------------------------------------------------------------------------------------------------------------------------------------------------------------------------------------------------------------------------------------------------------------------------------------|----|
| 1      | Typical structure of cellulose polymer                                                                                                                                                                                                                                                                                       | 3  |
| 2      | Reaction schemes for modification of cellulose polymer. R <sub>1</sub> denotes the reducing end group, R <sub>2</sub> denotes the non-reducing end group and R <sub>3</sub> denotes the organic modification desired. Oxidation leads to mixed modifications which include addition of carboxyl, aldehyde and ketone groups. | 8  |
| 3      | Hypothesized structure of cellulose-DMSO/PF (methylolcellulose) meta-stable complex and its reversal back to cellulose in water and short chain alcohols. R <sub>1</sub> denotes the non-reducing end group and R <sub>2</sub> denotes the reducing end group.                                                               | 12 |
| 4      | Schematic representation of reaction setup utilized in preparing methylolcellulose solution (MC-4 and MC-DP)                                                                                                                                                                                                                 | 30 |
| 5      | Typical experimental setup of Side-by-Side® diffusion cells for analysis of RC film solute permeability.                                                                                                                                                                                                                     | 42 |
| 6      | Degree of polymerization vs. reaction time of cotton linters at 40°C in 2 N HCl. The degree of polymerization was determined by single point method.                                                                                                                                                                         | 50 |
| 7      | Relationship between $\log\{(\eta_{rel}-1)/C\}$ and the concentration of cellulose in 0.5 M cuen solution for (A) cotton linter, (B) depolymerized cotton linter, (C) RC-W, (D) RC-DP, (E) RC-A, (F) RC-M, (G) RC-E, (H) RC-P and (I) RC-B films in 0.5M cuen solution, at 25 °C.                                            | 52 |
| 8      | Fourier transformed infrared absorbance spectrum of (A) cotton linter, (B) RC-W film and (C) RC-DP film. The RC film samples were thermally cured at 120°C for 24 hours after precipitation in water.                                                                                                                        | 54 |
| 9      | Fourier transformed infrared spectra of (A) RC-A, (B) RC-M, (C) RC-E, (D) RC-P, and (E) RC-B films. The RC film samples were thermally cured in an oven at 120°C for 24 hours after precipitation in their respective non-solvents                                                                                           | 55 |
| 10     | X-ray diffractograms of (A) cotton linter sheets, (B) cellulose-II crystalline standard, (C) RC-DP and (D) RC-W films. The RC film samples were thermally cured in an oven at 120°C for 24 hours, after precipitation in water.                                                                                              | 57 |



|    |                                                                                                                                                                                                                                                                                                                                                                                                                                                              |    |
|----|--------------------------------------------------------------------------------------------------------------------------------------------------------------------------------------------------------------------------------------------------------------------------------------------------------------------------------------------------------------------------------------------------------------------------------------------------------------|----|
| 11 | X-ray diffractograms of (A) RC-4A, (B) RC-4M, (C) RC-4E, (D) RC-4P and (E) RC-4B. The RC film samples were thermally cured in an oven at 120°C for 24 hours after precipitation in their respective non-solvents.                                                                                                                                                                                                                                            | 58 |
| 12 | Scanning electron micrographs of RC-W films freeze dried immediately after precipitation in water: (A) Solvent non-solvent exchange interface, (B) cross section and, (C) test tube support facing interface.                                                                                                                                                                                                                                                | 62 |
| 13 | Scanning electron micrographs of RC-W films thermally cured at 105°C for 24 hours: (A) Solvent non-solvent exchange interface, (B) cross section and, (C) test tube support facing interface.                                                                                                                                                                                                                                                                | 63 |
| 14 | Scanning electron micrographs of RC-W films rehydrated after thermal curing: (A) Solvent non-solvent exchange interface, (B) cross section and, (C) test tube support facing interface.                                                                                                                                                                                                                                                                      | 64 |
| 15 | Scanning electron micrographs of (A) thermally cured and (B) rehydrated RC-DP film solvent/non-solvent exchange interface                                                                                                                                                                                                                                                                                                                                    | 65 |
| 16 | Equilibrium ethanol-water binary solvent uptake by RC-W and RC-DP films from ethanol-water mixtures with varying amounts of ethanol (% v/v), at 37°C, determined gravimetrically after 24 hours.                                                                                                                                                                                                                                                             | 68 |
| 17 | Flux profiles of acetaminophen through (A) RC-W and (B) RC-DP films, in Side-by-Side® diffusion cells containing varying amounts of ethanol in ethanol-water binary mixtures with saturated acetaminophen on the donor side, at 37°C.                                                                                                                                                                                                                        | 70 |
| 18 | Comparison of flux alteration factor ( $\Omega$ ) and relative solvent volume ( $\phi$ ) in swollen RC-W and RC-DP films, using acetaminophen as model solute.                                                                                                                                                                                                                                                                                               | 72 |
| 19 | Analysis of transient effect of ethanol acetaminophen flux through RC-W film in (A) 100 % water, (B) 100% ethanol, and (C) 100% water as solvent medium. The flux was measured through same set of films and the transition points for solvent exchange are marked by dashed lines. The donor cell concentration was maintained at 15 mg/cm <sup>3</sup> by periodically replacing the medium with fresh solution. Transport studies were conducted at 37°C. | 75 |
| 20 | Scanning electron micrographs of rehydrated solvent/ non-solvent exchange interfaces of (A) RC-4/1, (B) RC-3/2, (C) RC-2/3 and (D) RC-1/4 films                                                                                                                                                                                                                                                                                                              | 77 |

|    |                                                                                                                                                                                                                                                                                                                     |    |
|----|---------------------------------------------------------------------------------------------------------------------------------------------------------------------------------------------------------------------------------------------------------------------------------------------------------------------|----|
| 21 | Water uptake by RC-W, RC-DP and blend films. Water uptake was analyzed gravimetrically in 37°C purified water on thermally cured RC films that were precipitated in water.                                                                                                                                          | 78 |
| 22 | Thickness normalized flux profiles of KCl through RC-W, RC-DP and blended films in purified water at 37°C. Films were placed in purified water for 24 h prior to transport studies.                                                                                                                                 | 80 |
| 23 | Thickness normalized flux profiles of KCl through RC-W, RC-DP and blended films in purified water at 37°C. Films were pre equilibrated in purified water for 24 h prior to transport studies.                                                                                                                       | 83 |
| 24 | Thickness normalized flux profiles of (A) methyl-, (B) ethyl-, (C) propyl-, and (D) butyl-p-aminobenzoate in purified water at 37°C through RC-W, RC-4/1, RC-3/2, RC-2/3, RC-1/4 and RC-DP films, using Side-by-Side® diffusion cells.                                                                              | 85 |
| 25 | Comparison of hindrance factors ( $P/D_w$ ) of KCl, methyl-, ethyl-, propyl- and butyl-p-aminobenzoate through RC-W, RC-4/1, RC-3/2, RC-2/3, RC-1/4 and RC-DP films in purified water, at 37°C.                                                                                                                     | 87 |
| 26 | Flux profiles of (A) lysozyme chloride (LZY) in pH 4.5, and (B) bovine serum albumin (BSA) in pH 7.4, through RC-W, RC-DP and blended films at 37°C.                                                                                                                                                                | 89 |
| 27 | Fraction of pores greater than 5 nm and 10 nm as a function of fraction of depolymerized cellulose in RC films.                                                                                                                                                                                                     | 91 |
| 28 | Adsorption isotherms of methylene blue dye from pH 8.0 solution on (A) freeze dried and (B) thermally annealed RC-A, RCM, RC-E, RC-P, RC-W and RC-B films, after precipitation in respective non-solvents. Dashed lines represent curve fitting to Langmuir-like equation.                                          | 94 |
| 29 | Comparison of extent of polymer consolidation following thermal curing of RC films vs. the boiling of non-solvent utilized for phase inversion/precipitation of cellulose from MC-4 solution.                                                                                                                       | 98 |
| 30 | Thickness normalized flux profiles of ethyl-p-aminobenzoate in purified water at 37 °C through RC-A, RC-M, RC-E, RC-P and RC-B films (A) freeze dried immediately after phase inversion in their respective non-solvents and (B) after thermal treatment of wet films regenerated in their respective non-solvents. | 99 |

|    |                                                                                                                                                                                                                                                                                                                                                                                                     |     |
|----|-----------------------------------------------------------------------------------------------------------------------------------------------------------------------------------------------------------------------------------------------------------------------------------------------------------------------------------------------------------------------------------------------------|-----|
| 31 | Thickness normalized flux profiles of ethyl-p-aminobenzoate through RC-2T, RC-3T, RC-4T and RC-5T films in purified water at 37°C, using Side-by-Side® diffusion cells.                                                                                                                                                                                                                             | 101 |
| 32 | Schematic representation of capsule fabrication methodology employed for preparing two piece cellulose capsules                                                                                                                                                                                                                                                                                     | 111 |
| 33 | Schematic representation of method utilized in determining vapor pressure of water vapor above liquid gas interface of purified water, saturated API solutions and known concentrations of aqueous urea solutions.                                                                                                                                                                                  | 120 |
| 34 | Figure 34: (A) Influence of mold pin rotation time and cellulose concentration, on the capsule dry wall thickness, (B) Relative standard deviation (n=6) of capsule wall thickness as a function of mold pin rotation time using MC solution with 4.4, 3.3 and 2.2 % w/w cellulose. Green bars represent formation of intact capsule shell, yellow bars represent FTB and orange bars represent FTB | 124 |
| 35 | (A) Influence of no. of applications and cellulose concentration, on the capsule dry wall thickness, (B) Relative standard deviation (n=6) of capsule wall thickness as a function of no. of MC coating applications, using MC solutions with 4.4, 3.3 and 2.2% w/w cellulose. Green bars represent formation of intact capsule shell, yellow bars represent FTB and orange bars represent FTB      | 126 |
| 36 | (A) Photograph of regenerated cellulose telescoping capsule halves fabricated using dip coating approach followed by solvent non-solvent phase inversion/ precipitation process, and (B) schematic representation of capsule dimensions following assembly of the capsule ‘body’ and ‘cap’                                                                                                          | 128 |
| 37 | Release profiles of potassium chloride, diphenhydramine HCl, tramadol HCl, niacinamide, acetaminophen and ketoprofen from cellulose capsules, in purified water at 37 °C.                                                                                                                                                                                                                           | 131 |
| 38 | Comparison of API zero order release rates (moles/h) from cellulose capsules vs. their solubility (M), in purified water at 37 °C.                                                                                                                                                                                                                                                                  | 133 |
| 39 | Comparison of potassium chloride release profiles from capsule cores filled with 800 mg dry powder (solid fill), combination of 300 mg dry powder with 1 ml 350 mg/ml solution (suspension fill), and 1 ml of 350 mg/ml solution (liquid fill), in purified water at 37°C                                                                                                                           | 135 |

|    |                                                                                                                                                                                                                                                                          |     |
|----|--------------------------------------------------------------------------------------------------------------------------------------------------------------------------------------------------------------------------------------------------------------------------|-----|
| 40 | Comparison of acetaminophen release profiles from capsule cores filled with 450 mg dry powder (solid fill), combination of 300 mg dry powder with 1 ml 15 mg/ml solution (suspension fill), and 1 ml of 15 mg/ml solution (liquid fill), in 37°C water                   | 136 |
| 41 | Release profiles of (A) potassium chloride in media containing 1.25, 2.51, 3.75 and 4.55 M urea solutions and (B) diphenhydramine HCl in diffusing medium containing 1.24, 2.51 and 3.75 M urea solutions, at 37°C.                                                      | 138 |
| 42 | Release profiles of (A) tramadol HCl in media containing 0.66, 1.65 and 2.51 M urea solutions and (B) niacinamide in diffusing medium containing 0.25, 0.75 and 1.25 M urea solutions, at 37°C.                                                                          | 139 |
| 43 | Comparison of total zero order release rates (dM/dt) <sub>T</sub> of potassium chloride, diphenhydramine HCl, tramadol HCl and niacinamide with varying osmotic pressure difference 'Δπ' across cellulose capsule shell, at 37°C.                                        | 143 |
| 44 | Comparison of total zero order release rate, and osmotic and diffusive components of zero order release rates of potassium chloride, diphenhydramine HCl, Tramadol HCl and niacinamide from cellulose capsules vs. their measured solubility in purified water, at 37°C. | 147 |
| 45 | Flux profiles of KCl, diphenhydramine HCl, tramadol HCl, niacinamide, acetaminophen and ketoprofen through RC films (diffusion cell experiments), in purified water at 37 °C.                                                                                            | 150 |
| 46 | Comparison of diffusive mechanism reduction and solubility of the APIs.                                                                                                                                                                                                  | 153 |
| 47 | Release of potassium chloride from cellulose capsules in water with varying paddle speeds, at 37 °C.                                                                                                                                                                     | 155 |
| 48 | Release of acetaminophen from cellulose capsules in water with varying paddle speeds, at 37 °C.                                                                                                                                                                          | 156 |
| 49 | Influence of pH of the release medium on the release of ketoprofen from cellulose capsules, at 37 °C.                                                                                                                                                                    | 158 |

## LIST OF ABBREVIATIONS

|       |                                                                      |
|-------|----------------------------------------------------------------------|
| MC    | Methylolcellulose solution                                           |
| MC/DP | Methylolcellulose solution prepared with depolymerized cotton linter |
| RC    | Regenerated cellulose                                                |
| RC-A  | Regenerated cellulose film prepared in acetone                       |
| RC-B  | Regenerated cellulose film prepared in 1-butanol                     |
| RC-DP | Regenerated cellulose film prepared from MC/DP solution              |
| RC-E  | Regenerated cellulose film prepared in ethanol                       |
| RC-M  | Regenerated cellulose film prepared in methanol                      |
| RC-P  | Regenerated cellulose film prepared in 1-propanol                    |
| RC-W  | Regenerated cellulose film prepared in water                         |

## CHAPTER I

### INTRODUCTION AND BACKGROUND

The current global pharmaceutical industry is expected to be worth \$500 billion. Globalization of the pharmaceutical industry means more drugs are being marketed in more countries than ever before. The pharmaceutical industry is at a crossroad of traditional drug development and new approaches that can place more drugs in the hands of ever-demanding consumers. In this fast-changing new world, the new paradigm is based on more economical approaches to formulation development and shorter lead times to product manufacturing. For more economical approaches to pharmaceutical product development, the ingenuity in application of regulatory accepted biopolymers is gaining significant momentum. A leading trend in economical drug development is towards the use of controlled delivery devices which deliver the active pharmaceutical ingredients in the right therapeutic window with minimal loss.

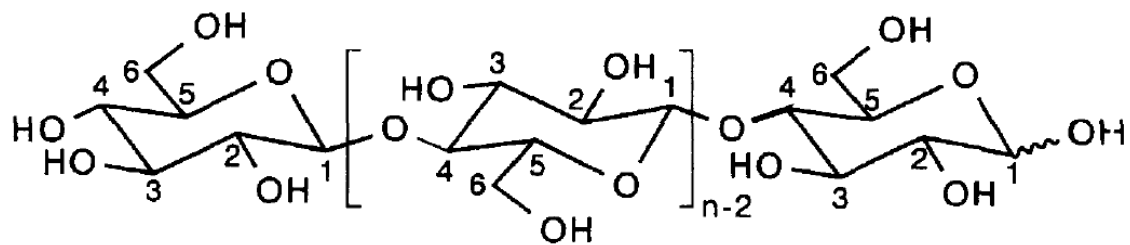
#### **Controlled drug delivery**

Controlled drug delivery has been a topic of great interest over the past three decades. The term “controlled drug delivery” is defined as the delivery of a therapeutic agent to the site of interest based on site specificity or rate of delivery. The term controlled release also implies predictability of pharmacologic action as well as reproducibility of the release kinetics [1]. The primary benefits of controlled drug delivery are (i) improved efficiency with lesser amount of API required (ii) minimized side effects (iii) decreased frequency of administration and (iv) increased patient compliance [2]. Disadvantages of controlled delivery systems include (i) high production

costs, (ii) leakage/dose dumping, (iii) difficulty in stopping drug release and (iv) biocompatibility of controlled release devices. Of these, high production costs and dose dumping are the major disadvantages pertaining to oral controlled release systems.

### **Cellulose**

Cellulose is the most abundant naturally occurring polymer. It is obtained from cotton plants, wood sources, bacterial sources etc[3]. Structurally, cellulose is homopolymer that consists of long chains of repeating anhydro-D-glucopyranose units linked together with  $\beta$  1-4 glycosidic bonds (Figure 1). Each anhydroglucose unit comprises of three hydroxyl groups, two primary and one secondary, with the exception for the terminal ends where a second secondary hydroxyl group is present on C<sub>1</sub> (reducing end) and on C<sub>4</sub> (non-reducing end). The primary hydroxyls are placed equatorially while the secondary hydroxyls are linked axially to the plane of the glucopyranose ring. The anhydroglucose units participate in extensive hydrogen bonding within the polymer and with the neighboring cellulose chains. The oxygen atom in the glucopyranose rings also participates in inter- and intra-molecular hydrogen bonds. Owing to the lowest free energy of the glucopyranose ring in the chair conformation, the bonding between neighboring anhydroglucose units occurs in  $\beta$  <sup>4</sup>C<sub>1</sub> configuration [3]. Physiologically, four principal polymorphic forms of cellulose exist: I, II, III and IV [3]. The Cellulose I polymorph occurs naturally in cellulosic raw materials and is the most abundant form. Cellulose II polymorphic form occurs when cellulose I source is transformed by dissolution/regeneration or mercerization [4]. The mercerization process involves swelling of cellulose in an alkaline medium, where the hydrogen bonds are



Non reducing end

Reducing end

Figure 1: Typical structure of cellulose polymer



disrupted by electrostatic repulsions followed by exposure to acidic environment, where the polymer realigns to a different configuration from the starting material. The transformation of cellulose I to cellulose II is irreversible. The irreversibility is attributed to the improved/ increased hydrogen bonding leading to increased stability and lower free energy of the polymeric rearrangement [5]. A similar process is of polymorphic transformation occurs during regeneration of cellulose from solvents. Cellulose III is obtained from cellulose I or II by treatment with liquid ammonia or other amine conjugates [3]. When ammonia treated cellulose III is treated at 260°C in glycerol, it converts to cellulose IV polymorphic form [3,4]. The conversions to cellulose III and IV are reversible depending on the type of starting crystalline structure of cellulose. Differentiation of cellulose crystalline motifs is usually performed by X-ray diffraction [3]. Table 1 summarizes the X-ray diffractogram peak assignments for cellulose polymorphs.

### **‘Cellulosics’ in controlled drug delivery**

Cellulose, while possessing large number of hydroxyl groups, is practically insoluble in water and most pharmaceutically acceptable solvents. Strong hydrogen bonding within cellulose supra-molecular structure makes the polymer insoluble in majority of the solvents [6]. The relatively low degradation temperature of cellulose (100 - 200°C) makes it difficult for use in melt processing techniques as the polymer decomposes before melting [3]. Hence, chemical modification of one or more of the hydroxyl groups has been the leading method to improve processibility and applicability of cellulose. The common pharmaceutically accepted and commercially utilized substitutions for pharmaceutical cellulosics involve etherification, esterification and

Table 1: Summary of typical X-ray diffractogram peak assignments reported for the four polymorphic forms of cellulose

| Cellulose<br>polymorphic form  | Observed 2 $\theta$ peaks for crystalline lattice planes |              |      |      |      |
|--------------------------------|----------------------------------------------------------|--------------|------|------|------|
|                                | 101                                                      | 10 $\bar{1}$ | 021  | 002  | 040  |
| I <sup>a</sup>                 | 14.7                                                     | 16.6         | 20.6 | 22.5 | -    |
| II <sup>a</sup>                | 12.3                                                     | 20.1         | -    | 21.9 | -    |
| III <sub>I</sub> <sup>b</sup>  | 11.7                                                     | 20.7         | -    | 20.7 | -    |
| III <sub>II</sub> <sup>b</sup> | 12.1                                                     | 20.6         | -    | 20.6 | -    |
| IV <sub>I</sub> <sup>b</sup>   | 15.6                                                     | 15.6         | -    | 22.2 | 34.7 |
| IV <sub>II</sub> <sup>b</sup>  | 15.6                                                     | 15.6         | 20.2 | 22.5 | 34.7 |

<sup>a</sup> obtained from reference [3,4]

<sup>b</sup> obtained from reference [7,8]

oxidation of one or all the hydroxyl groups.

Etherification of the hydroxyl groups is achieved by reacting raw cellulose with alkyl-chlorides or alkyl-sulfates, in an alkaline environment. The organic radical (alkyl group) of the chlorides and sulfates readily interacts with one or all the hydroxyl groups on cellulose to produce cellulose ether and the conjugate acid by product. Etherification has mixed effects on the solubility of the resultant modified cellulose. Minimally substituted ethers (degree of substitutions up to 1.0) are soluble in alkaline solutions, while mixed substitution ratios (degree of substitutions between 1.0 and 2.1) are soluble in water, and substitution of all hydroxyl groups (DS 3.0) makes them only soluble in organic solvents [9]. Cellulose ethers such as ethyl cellulose, methyl methyl cellulose, hydroxypropyl cellulose, hydroxypropylmethyl cellulose and salts of carboxymethyl cellulose are well known tablet matrix formers [10] [11]. Combinations of ethylcellulose and hydroxypropylmethyl cellulose are also used in forming porous tablet coatings [12].

Cellulose esters are typically manufactured using an alkyl anhydride treatment followed by acid hydrolysis. The end product of this multiphase reaction scheme is esterified cellulose and water. Strong mineral acids like nitric and phosphoric acid are utilized in order to promote swelling and even reaction throughout the polymer. Unlike cellulose ethers, cellulose esters such as cellulose acetate, cellulose acetate butyrate, cellulose acetate phthalate, etc. are predominantly utilized in the formulation of drug release effector films on solid dosage forms [13][14]. Their use as psuedolatex aqueous dispersions for spray coatings is widely accepted in the pharmaceutical and paint industry[15]. Cellulose esters are only soluble in organic solvents. Cellulose acetate phthalate usually contains 20 % acetyl groups and about 40 % phthalic acid groups. The

salt form makes it soluble in water and hence has been utilized as enteric coating. The pH dependent solubility can be modified by simply altering the phthalic acid group substitution in cellulose [16].

Oxidized celluloses are prepared from the treatment of cotton fibers with chlorine gases, peroxides, nitrous oxides, persulfates, permangantes, etc. The resulting cellulosic fibers contain hydroxyl groups substituted with carboxylic acids, ketones and aldehydes, depending on the type of reactant, reaction conditions and the extent of reaction [17].

Oxidized celluloses, owing to their biodegradable nature, have become a topic of interest in formulation of sustained release implantable matrix systems in conjunction with chitosan adducts [18]. There are no current applications of oxidized cellulose in oral controlled drug delivery. Figure 2 summarizes the reactions involved in the preparation of cellulose esters and ethers, and oxidized celluloses

### **Solvents for unmodified cellulose utilized in biomedical applications**

Although chemical modification of cellulose leads to improved processibility, the chemical processes are usually cumbersome and expensive. The need for fabrication of unmodified cellulose based products has led to the invention of numerous solvent systems over the past two decades. Cellulose products are usually extracted by a phase inversion/ immersion precipitation from these solvents [19]. Cellulose products prepared by this method include filtration membranes, dialysis tubing, textiles, synthetic scaffolds and tissue engineering backbones. The scope of the literature available is vast and hence the proceeding discussion only pertains to dissolution methods that are commonly employed in the biomedical field. It has been hypothesized and proven that by altering

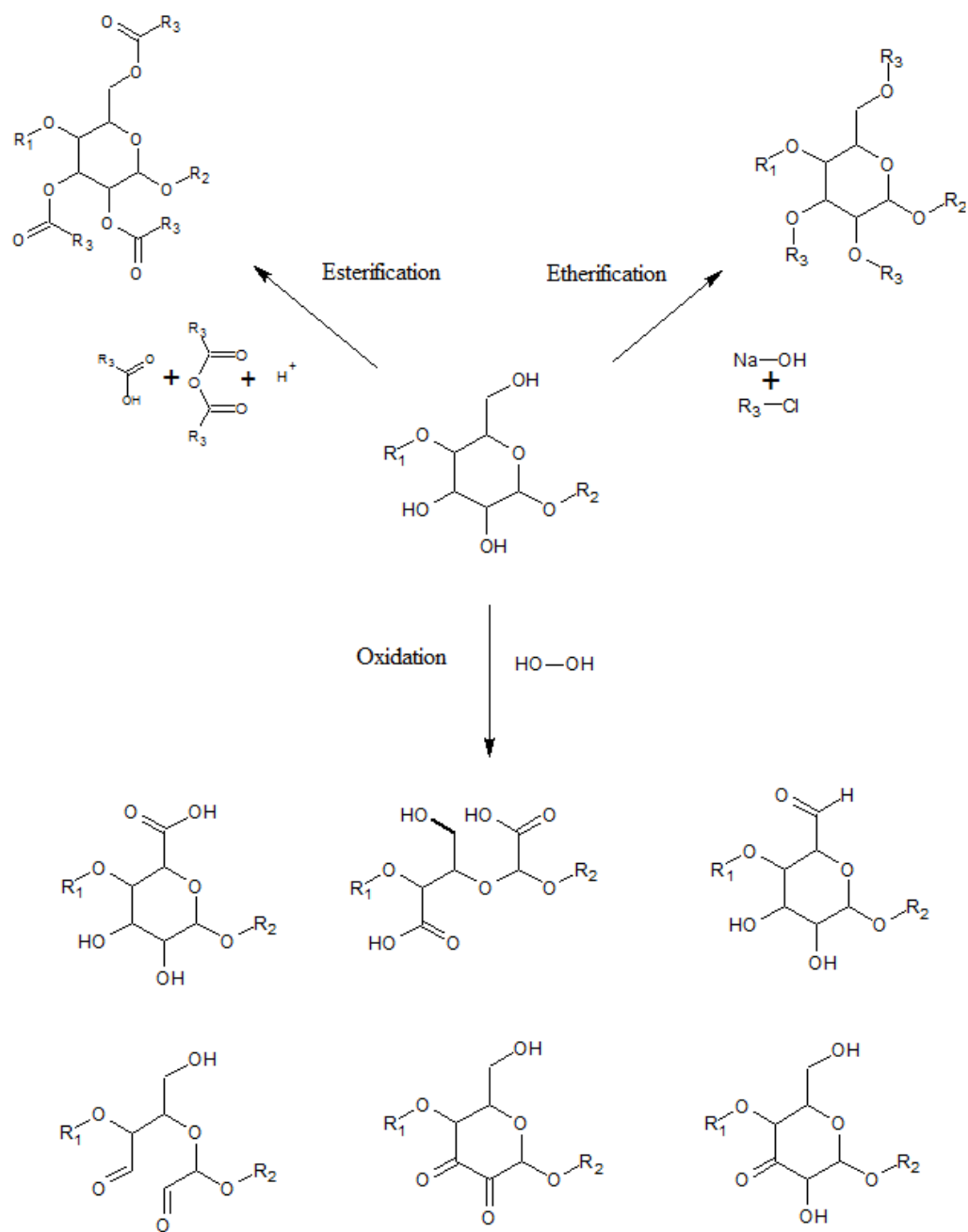


Figure 2: Reaction schemes for modification of cellulose polymer.  $R_1$  denotes the reducing end group,  $R_2$  denotes the non-reducing end group and  $R_3$  denotes the organic modification desired. Oxidation leads to mixed modifications which include addition of carboxyl, aldehyde and ketone groups.

the attractions involving hydrogen bonds between hydroxyl groups on neighboring cellulose chains, the polymer as a whole can be easily dispersed or dissolved in a particular solvent system [3]. This led to the advent of the viscose method where cellulose is treated with sodium hydroxide and carbon disulfide to form cellulose xanthate [20]. The 'xanthanation' of cellulose hydroxyls forces the chains apart due to electrostatic repulsion and allows water molecules to separate the chains and solvate the polymer completely. Although the process was simple and elegant in the dissolution of cellulose, the by-products formed after regeneration of cellulose are toxic and carcinogenic (sulfur derivatives), and this has led to the eventual decline in method implementation for fabrication of cellulosic materials.

The lyocell process was developed to combat the environmentally unfriendly effects of the viscose process. N-methylmorpholine-N-oxide monohydrate (NMMO) in combination with water is used as a solvent to dissolve cellulose [21]. The process involves high shear mixing of dispersed cellulose in water and NMMO at temperatures exceeding 170 °C. As water evaporates from the solvent, the amine oxide molecules dissociate the inter-cellulose hydrogen bonds and dissolve cellulose. Although the method is environmentally friendly in terms of reusability of the solvent, NMMO is considered to be relatively expensive and unstable, if not handled correctly. This method is also limited by the degree of polymerization (< 500) of cellulose that can be utilized as starting material [22]. Moreover, utilization of elevated temperatures and shear has been shown to reduce the degree of polymerization of cellulose by more than 10-20 % [23]. Rosenay et al. reported in a recent study that several side reactions occur even when dealing with this solvent in ambient conditions, which alter cellulose chemistry to some extent [24].

The work of Cai et al. is well known for the development of an aqueous alkali/urea based solvent system for cellulose. The process involves mixing cellulose (degree of polymerization less than 400) with 7% w/w NaOH and 12% w/w urea in pre-cooled water at  $-12^{\circ}\text{C}$ . At low temperatures, the dissolution of cellulose occurs due to the dynamic self-assembly process between sodium ions, water and cellulose macromolecules with urea acting as a stabilizer for the assembled complex. Cellulosic hydrogels are obtained by heating these solutions in the presence of a mineral acid to about  $50^{\circ}\text{C}$ , which destroys the metastable structure [25]. Based on the same complex formation, Zhang et al. developed another solvent system by replacing urea with thiourea. The resulting solvent system required 9% w/w NaOH, 4.5% w/w thiourea and pre-cooling to  $-5^{\circ}\text{C}$  [26]. The greatest drawback associated with these systems is the need for acidic solutions as regeneration medium in order to neutralize the alkali pretreatment of cellulose. The final acid solution treatment leads to hydrolysis of the glycosidic linkages which was shown to reduce the mechanical strength of the regenerated cellulose products[27].

The use of hydrophilic ionic liquids such as 1-butyl-3-methylimidazolium chloride [28] and 1-allyl-methylimidazolium chloride [29] with cellulose, have been utilized to form regenerated cellulose hemodialysis membranes. Both of these solvents are considered non-volatile and thermo-stable and can easily be recycled. The general method of dissolution of cellulose in ionic liquids involves the formation of a cation complex with the hydroxyl groups on cellulose. Regeneration of cellulose can also be carried out in water, ethanol or acetone for celluloses dissolved in ionic liquids. Several reports have shown the application of this solvent system in development of cellulose films, beads and gels [30]. The use of hydrophilic ionic liquids as solvents for cellulose

was conceived from the LiCl/ dimethyl acetamide solvent system, where after suitable pre-activation, usually by swelling in dimethyl acetamide, the chloride ions act as a base which interacts with the hydroxyl groups on cellulose causing repulsion of chains and dissolution by solvation [31]. Owing to the extreme electronegativity of chloride ions, the intermolecular repulsion forces the cellulose polymers to separate and undergo solvation. Two major drawbacks are associated with use of ionic liquids for dissolution of cellulose: (i) Ionic liquids are considerably expensive and require elaborate apparatuses to prepare, (ii) the maximum concentration of cellulose achieved in these liquids is 2 % w/w, and (iii) limitations to the maximum chain length of cellulose that can be dissolved (DP ~ 500) [30].

Nicholson developed a unique solvent system for dissolution of cellulose using dimethyl sulfoxide (DMSO) and paraformaldehyde (PF) [32]. Dissolution of cellulose in the DMSO/PF solvent system involves the formation of a hemiacetal derivative called methylolcellulose (MC) depicted in Figure 3. Dimethyl sulfoxide performs two major functions, (i) it interacts with the hydroxyl groups and disrupts intermolecular hydrogen bonding thereby causing swelling, and (ii) stabilizes the hemiacetal units once the formaldehyde has interacted with cellulose chains. The hemiacetal formation is preferred at the C<sub>6</sub> position [33]. The hemiacetal is less likely to be formed at the C<sub>2</sub> and C<sub>3</sub> positions due to steric effects. The resulting solution is clear and viscous which is stable in a sealed container as long as it is kept away from moisture. The advantage of this solvent system over other solvents is that cellulose can be regenerated easily by simply



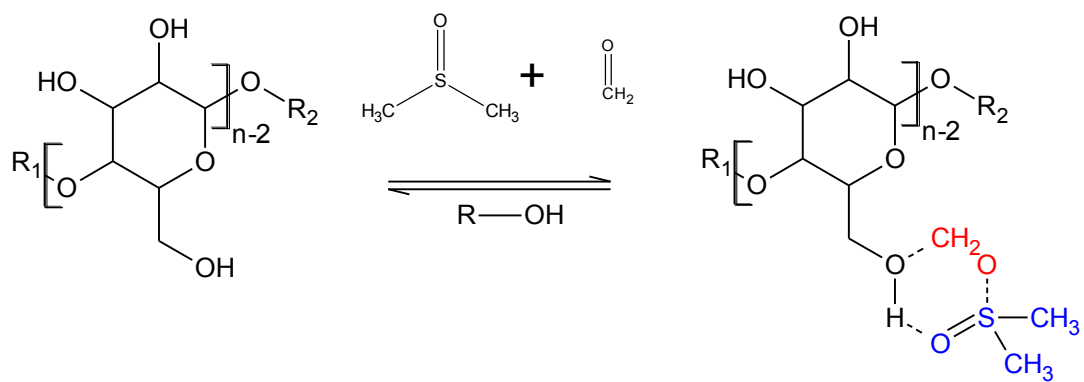


Figure 3: Hypothesized structure of cellulose-DMSO/PF (methylolcellulose) meta-stable complex and its reversal back to cellulose in water and short chain alcohols.  $R_1$  denotes the non-reducing end group and  $R_2$  denotes the reducing end group.

immersing the viscous solution in polar non-solvents, such as water, owing to the miscibility of DMSO and formaldehyde in these non-solvents. Also, DMSO is an inert compatible solvent that does not degrade/ hydrolyze cellulose. Moreover, this solvent system has been known to dissolve cellulose from wide variety of sources and with varying degrees of polymerization ( $> 10,000$ ) and in concentrations exceeding 10 % w/w cellulose [32] [34]. It was also observed that when the MC solution was cast on to molds of different shapes and sizes, the final RC film retained the shape of the mold [35]. Hei et al used this solvent to prepare filtration membranes and tested the flux of proteins and water through them as a function of concentration of cellulose [36]. Although the water flux remained constant through the membranes, the retention of proteins increased with increasing concentration of cellulose in solution. They also concluded that the flux of urea and creatinine remained essentially constant as a function of cellulose concentration in the regenerated cellulose membranes and proposed their use in preparation of synthetic dialysis tubing.

Cellulosic scaffolds as the base for tissue engineering [37], drug delivery [38] and other bio-medical applications have been developed from bacteria such as *Acetobacter xylinum*. The process of cellulose generation and scaffold fabrication involves the use of *xylinum* bacteria in a glucose rich environment to produce highly purified cellulose matrix with high degrees of swelling. Moreover, the physiochemical properties of cellulose matrix are controlled by changes in growth medium to obtain desired functionality. Cell seeding, tissue growth and addition of non-biological products can easily be achieved by placing living cells in the same growth medium as that of the

Table 2: Summary of advantages and disadvantages of solvents utilized for dissolution in order to prepare cellulose products for bio-medical applications.

| Solvent system                                                                                         | Advantage(s)                                                                                                                                                                                                                                                                                                                                                                                                  | Disadvantage(s)                                                                                                                                                                                    |
|--------------------------------------------------------------------------------------------------------|---------------------------------------------------------------------------------------------------------------------------------------------------------------------------------------------------------------------------------------------------------------------------------------------------------------------------------------------------------------------------------------------------------------|----------------------------------------------------------------------------------------------------------------------------------------------------------------------------------------------------|
| NaOH and CS <sub>2</sub> (viscose) in water                                                            | <ul style="list-style-type: none"> <li>• Fast dissolution</li> <li>• Ease of obtaining cellulose back</li> <li>• Possibility of chemical modification</li> </ul>                                                                                                                                                                                                                                              | <ul style="list-style-type: none"> <li>• By products are toxic and carcinogenic</li> </ul>                                                                                                         |
| Methylmorpholine-N-oxide monohydrate in water (NMMO, lyocell)                                          | <ul style="list-style-type: none"> <li>• Environmentally friendly</li> <li>• Reusable system</li> </ul>                                                                                                                                                                                                                                                                                                       | <ul style="list-style-type: none"> <li>• Unstable and expensive</li> <li>• Limited to cellulose degree of polymerization of 500</li> <li>• Cellulose degradation in elevated conditions</li> </ul> |
| Alkali (NaOH)/urea and thiourea system                                                                 | <ul style="list-style-type: none"> <li>• Inexpensive raw materials</li> <li>• Ease of obtaining cellulose back</li> </ul>                                                                                                                                                                                                                                                                                     | <ul style="list-style-type: none"> <li>• Requires mineral acids for regeneration which degrades the polymer</li> <li>• Limited to cellulose degree of polymerization of 400</li> </ul>             |
| Ionic liquids (1-butyl-3-methylimidazolium and 1-allyl-methylimidazolium) and LiCl/ dimethyl acetamide | <ul style="list-style-type: none"> <li>• Dissolution is as simple as mixing solvent and polymer at room temperature</li> </ul>                                                                                                                                                                                                                                                                                | <ul style="list-style-type: none"> <li>• Maximum cellulose concentration that can be achieved is 2.2 % w/w.</li> <li>• Ionic liquids are relatively expensive to prepare</li> </ul>                |
| Bacterial cellulose prepared from <i>Acetobacter xylinum</i>                                           | <ul style="list-style-type: none"> <li>• Inexpensive raw materials</li> <li>• Ability to modify cellulose matrix <i>in-situ</i> by manipulation of growth medium</li> </ul>                                                                                                                                                                                                                                   | <ul style="list-style-type: none"> <li>• Slow process of cellulose generation</li> </ul>                                                                                                           |
| Dimethyl sulfoxide and paraformaldehyde                                                                | <ul style="list-style-type: none"> <li>• Can dissolve cellulose from variety of sources</li> <li>• Cellulose degree of polymerization of upto 10,000 can be dissolved</li> <li>• Up to 10% w/w solutions of cellulose have been obtained</li> <li>• Rapid precipitation of cellulose in aqueous solutions as well as in short chain alcohols.</li> <li>• DMSO and PF are inexpensive raw materials</li> </ul> | <ul style="list-style-type: none"> <li>• Formaldehyde formation <i>in-situ</i>, during dissolution process, requires special handling of reaction and dissolution setup</li> </ul>                 |

bacterium [39]. Table 2 summarizes the advantages and disadvantages of solvent systems described.

### **Phase inversion\ immersion precipitation process**

The phase inversion\ precipitation process is the method of separating polymer from solution using a non-solvent. Phase separation\ precipitation of polymers from solutions can be achieved by three conventional techniques: (i) reaction, (ii) temperature and (iii) diffusion-induced phase separation [40]. In case of thermal induced phase separation, the solvent is evaporated from the system leaving behind a polymer rich phase. For reaction induced phase separation, the solution usually consists of monomers and certain reaction conditions induce polymerization of the monomers to a particular chain length at which point, due to loss in solubility, the polymer phase precipitates out of the solution. Irrespective of the method for dissolution of cellulose in organic or inorganic solvents, the thermal induced phase separation/ evaporation method is rarely used for precipitation of cellulose. It is likely that all the known solvents utilized for cellulose dissolution possess high boiling points and hence would prove detrimental to the stability of the polymer. Formation of bacterial cellulose membranes can be classified under reaction induced phase separation process as the monomer to form cellulose (glucose) is soluble in the culture medium. Diffusion induced phase separation in aqueous environments is usually employed owing to the ease of handling as well as solubility and miscibility of majority of the solvents and salts utilized in cellulose dissolution [19]. During phase inversion, the polymer solution is exposed to excess non-solvent (a medium or a combination of media in which the polymer is insoluble), where the presence of the non-solvent will lead to change in the local composition of the solution leading to precipitation of the polymer. Depending on the type of solvent and

non-solvent utilized as well as physiological conditions employed in polymer precipitation, such as temperature, non-solvent agitation, pH of the aqueous medium, etc., two types of films are obtained: (i) symmetric and (ii) asymmetric. These films can either be porous, dense or possibly contain both regions [41]. Symmetric membranes have a uniform structure throughout the membrane, while asymmetric membranes tend to possess a gradient. The gradient is usually observed in terms of a dense internal structure with an outer porous skin. Owing to this gradient nature, the solute permeation rate is usually governed by the permeation rate through the dense phase.

### **Cellulose hornification and irreversible polymer consolidation**

Cellulose hornification refers to the stiffening of the wet cellulose fibrils by thermal recycling for removal of solvents and non-solvents [42]. The cellulose fibril loses its water holding/swelling capacity owing to the formation of non-swelling domains that do not allow newly intruding water to penetrate. This is a common phenomenon observed in drying of wet wood pulps during paper manufacturing. This process was discovered by Jayme, G. who concluded that the water retention capability of thermally annealed cellulose fibers decreased from the original water volume retention prior to heating [43]. The process of hornification in lignocelluloses (cellulose, hemicellulose, lignin) containing materials has been associated with lactone bridge formation [44], where the hydroxycarboxylic groups of xylans in hemicelluloses can readily undergo intramolecular esterification to yield lactones [45] [46], while in pure cellulosic fabrics and paper products, hornification has been associated with hydrogen bonding between neighboring polymer fibrils [45]. In the case of pure cellulose fibers, the strong hydrogen bonding may be associated to the high cohesive energy of cellulose which leads to

formation of these irreversible domains [47]. The reversal of hornification has been investigated successfully under alkali treatment [48], and addition of bulking agents such as sucrose, lactose, glycerol, etc [49].

### **The capsule dosage form**

A capsule is shell or container that encloses one or more medicinal and/or inert substances. Gelatin has been at the heart of capsule dosage form for over 190 years. This dosage form can be subdivided into soft gelatin capsules and the two piece telescoping shells. Mothes and Dublanc are generally accredited to the invention of the soft gelatin capsule in 1834, while Murdock is accredited with the development of the telescoping variant in 1848 [50].

Soft gelatin capsules consist of a one-piece hermetically-sealed gelatin shell. These capsules are useful for encapsulation of non-aqueous liquids, suspensions and pastes of drug-excipient combinations which are considered volatile or are susceptible to deterioration in the presence of air. They are prepared by rotary die process where two thin gelatin ribbons are brought together between sandwiched twin rollers with metered fills of desired compositions injected between them. The hard shell telescoping capsule is made of two parts; the capsule 'body' and a shorter and slightly wider 'cap'. The 'cap' fits snugly over the open end of the capsule 'body'. Since the capsule shells have no affiliation with the type of ingredient that can be filled, this system can be considered as an *apriori* dosage form. The capsule halves are generally prepared by a dip coating procedure, where pre-fabricated dipping pins or pegs are immersed in a reservoir of melted gelatin mixture. The desired thickness of the coating is achieved by controlling,

gelatin concentration, mold pin rotation, temperature, water activity and/or by multiple dip coatings approach. Recently, the use of hydroxypropylmethyl cellulose as capsule shell former was introduced and approved by several regulatory authorities owing to certain challenges associated with gelatin.

One of the major drawbacks to gelatin is its instability in moderate to high temperature as (greater than 45 - 50°C) well as in humid environments (RH greater than 60%) [51]. Because gelatin is a mixture of water soluble proteins (derived from collagen), it is prone to Maillard reaction where the amine group on the amino acids react with carbonyl group on the (active pharmaceutical ingredients) APIs and/or excipients. Also, up to 15% w/w moisture content has been reported in the gelatin shell, which poses a concern when dealing with moisture sensitive drugs [52]. Recently, the use of gelatin from bovine sources has become a topic of debate due to the possibility of transfer of Bovine Spongiform Encephalopathy (BSE) and its association with variant Creutzfeldt-Jakob disease (CJD). Further, due to its high demand in the nutraceutical industry, the supply for pharmaceutical grade gelatin is becoming limited. Gelatin capsules are also not utilized by certain individuals or groups because of dietary and religious concerns.

### **Capsule based controlled drug delivery systems**

Enteric coated gelatin capsules [53], hydroxypropylmethylcellulose (HPMC) capsules [54], cross-linked dextran capsules [55], and starch capsules [56] have been commercialized for controlled delivery of APIs in the intestine and/or colon.

Osmotically-driven capsules, such as the OROS-CT<sup>®</sup> (OROS – Oral Release Osmotic System – Colon Targeting) [57], L-OROS<sup>®</sup> (Liquid fill – OROS) [58,59] and Telescopic osmotic capsule<sup>®</sup> [60,61] have been developed to deliver the API in a sustained- and/or

delayed-release manner. The OROS-CT<sup>®</sup> system consists of an enteric coated gelatin capsule comprised of multiple push-pull osmotically-driven units coated with a semi-permeable membrane. These units are released when the enteric coating dissolves in the large intestine. The L-OROS<sup>®</sup> system comprises of a hard gelatin capsule containing liquid fill (usually an emulsifier and a lipophilic drug), osmotic agent, and coated with an insoluble semi-permeable membrane. A macro-pore is mechanically drilled on the surface of the capsule. When the capsule comes in contact with the gastrointestinal (GI) fluid, water imbibes through the membrane and the hydrostatic pressure pushes the API out of the capsule through the macropore. The telescopic osmotic capsule device consists of two chambers; the first chamber contains the drug and an exit port, and the second chamber contains an osmotic agent. A layer of wax-like material forms a diaphragm that separates the two sections. As fluid is taken up in the housing enclosing the osmotic agent, it expands and exerts pressure on the sliding waxy layer present between the two chambers, which then forces the drug out of the first chamber through the pore.

The Pulsincap<sup>™</sup> system is a non-osmotic capsule-based controlled release dosage form. It was developed from gelatin capsules coated with an insoluble polymer on the body portion of the capsule containing drug formulation and plugged with an erodible polymer matrix. The erosion of the plug allows for pulse release of the API which is dependent on the amount of polymer in the plug [62,63]. Cross-linking of gelatin has also been explored to convert hard shell gelatin capsules into controlled release dosage forms[64].

Although the above devices are highly effective, their use to deliver APIs presents challenges because of the complexity of the design and development of not only the capsule itself but also the core formulation. Moreover, all the above systems that employ



hard gelatin shells require an additional coating stage which may impact the integrity of gelatin itself owing to its water sensitive nature. Cellulose derivatives (e.g., cellulose ethers and cellulose esters) have been extensively investigated in the encapsulation process. Researchers at Pfizer Inc. have developed a hard shell capsule system with cellulose acetate as the micro-porous semi-permeable barrier [65]. Since cellulose acetate is insoluble in water, these capsule shells serve as controlled-release membranes.

Cellulose acetate film has already been proven to be an effective drug release coating for tablet formulations [66]. Cellulose acetate capsules were fabricated by dip coating mold pins in a casting solution comprising of cellulose acetate, triethylcitrate and glycerin. The resulting capsule was asymmetric in composition with a thin dense homogenous inner layer and a porous thick outer layer [67]. Since cellulose acetate is a hydrophobic polymer, addition of pore formers during the fabrication stage was a necessity in order to facilitate water permeation and subsequent API release.

#### **Determination of permeability of solute through membranes and films**

The most common pharmaceutical approach to determining permeability of a solute through a membrane, *in-vitro*, is by utilizing “diffusion cells”. The film in question is placed between donor solution and receiver solution and flux of solute through the film is examined, typically under steady state conditions. The solute flux (J) at steady state is described by Fick’s second law as shown by the following relation [68]:

Equation 1

$$J = \frac{dM}{dt A} = \frac{P (C_d - C_r)}{h}$$

where, ‘dM/dt’ is the rate of solute flux, ‘A’ is the area of the film, ‘P’ is the permeability coefficient of the solute,  $C_d$  and  $C_r$  are donor and receiver concentrations of the solute, respectively and ‘h’ is the thickness of the film. In a typical experiment, the donor

concentration of the solute is held constant by utilizing saturated solutions, while the receiver solution is withdrawn periodically and the amount of solute transported across the barrier is plotted vs. time.

For a solute traversing across a porous barrier, the permeability coefficient is equivalent to the sum of diffusion occurring through polymeric phase and through the solvent filled porous pathways, as described by the following relation [69]:

$$\text{Equation 2} \quad P = D_0 \frac{\epsilon}{\tau} + D_m(1 - \epsilon)K$$

where, 'D<sub>0</sub>' is the diffusion coefficient of the solute in the solvent, 'ε' is the porosity of the barrier, 'τ' is the tortuosity factor of the barrier, 'D<sub>m</sub>' is the diffusivity of the solute in polymer phase and 'K' is the partition coefficient of the solute through the polymer phase.

### **Osmotic mechanism for drug release**

Osmosis is the movement of water from a region of low solute concentration to a region of high solute concentration, where the regions are separated by a semi-permeable membrane that only allows water to permeate through it. The osmotic flow of solvent across the semi-permeable membrane is directed to compensate differences in solvent activity. The amount of pressure required to prevent the movement of solvent across this semi-permeable membrane is described as the osmotic pressure.

The direct measurement of osmotic pressure requires that the semi-permeable membrane be impermeable to the solute in the solution and freely permeable to water. The direct measurement technique also requires that the semi-permeable membrane be rigid enough to withstand high pressures. All though ideal for dilute solutions of large dissolved solutes, the measurement of concentrated smaller sized solutes becomes

challenging owing to the difficulty in obtaining membranes that are only selective to water permeation. Moreover, concentrated solutions can generate high pressures that can be detrimental to the mechanical stability of semi-permeable membranes. Fortunately, like other colligative properties of solutions, the osmotic pressure also depends on the number of solute molecules in solution and can hence be determined by measuring solution colligative properties and comparing it to the colligative properties of pure water. Freezing point depression, boiling point elevation and vapor pressure depression are common indirect methods utilized in estimating osmotic pressures of solutions [70,71].

Osmosis is a common phenomenon observed in biological systems. Rose et al were the first investigators to implement osmotic principles towards controlled drug delivery [72]. Investigators at Alza Corporation (now owned by Johnson & Johnson) pioneered the incorporation of drug molecules into oral osmotic systems for controlled drug delivery [57, 58, 59]. Most osmotic systems contain a hygroscopic solute, enclosed within a semi-permeable coating that acts as osmotic driving force causing intake of water into the dosage form. This results in the buildup of internal hydrostatic pressure, which in turn forces the enclosed formulation to flow out of an intentionally created orifice or through numerous pores in the micro-porous coating. The volumetric flux rate of solution out of the device is well defined by the following relation [73]:

Equation 3 
$$\frac{dV}{dt} = A L_p (\sigma \Delta\pi - \alpha)$$

where, 'A' is the area of the polymeric barrier, 'L<sub>p</sub>' is the hydraulic permeability, 'σ' is the reflection coefficient of the solute, 'Δπ' is the absolute osmotic pressure difference across the membrane and 'α' is the external hydrostatic pressure overhead. The hydraulic

permeability describes the flow of solvent under pressure gradient, while the reflection coefficient corrects for the leakiness/ selectivity of the solute through the membrane. In oral drug delivery systems, the enclosed formulation is enclosed in a non-swelling system and the external hydrostatic pressure overhead is minimal. Hence, the solute mass transfer rate ' $\left\{\frac{dM}{dt}\right\}_o$ ' out of the osmotic system can be represented by the following relation:

$$\text{Equation 4} \quad \left\{\frac{dM}{dt}\right\}_o = \frac{dV}{dt} C = A k \Delta\pi C$$

where,  $C$  is the concentration of the solute in the core. The term ' $k$ ' (equivalent to  $L_p\sigma$ ) is also known as the 'fluid permeability' which describes the flow of solution under a pressure gradient. For osmotic drug delivery systems, Theeuwes described the total drug release rate ' $\left(\frac{dM}{dt}\right)_T$ ' as the sum of release rates from osmotic contribution ' $\left(\frac{dM}{dt}\right)_o$ ' and diffusive contributions ' $\left(\frac{dM}{dt}\right)_D$ ', by the following relationship [74,75]:

$$\text{Equation 5} \quad \left\{\frac{dM}{dt}\right\}_T = \left\{\frac{dM}{dt}\right\}_o + \left\{\frac{dM}{dt}\right\}_D$$

The diffusion of the solute can occur either through the polymer phase or through the pore(s) in the semi-permeable membrane.

## CHAPTER II

### OBJECTIVES

Unmodified cellulose is a pharmaceutically acceptable and compendial polymer for tableting and capsule filling [76]. However, this robust polymer is not utilized in modified and/or controlled release owing to the difficulty associated with incorporating known cellulose dissolution methods into pharmaceutical unit operations. This work proposes the use of regenerated cellulose in the form of an *a priori* two piece hard shell capsule for oral controlled drug delivery. Dimethyl sulfoxide /paraformaldehyde solvent system was chosen for dissolution of cellulose owing to the ability to form clear and transparent films and membranes, when thermally annealed after phase-inversion of the cellulose solution in water. The objectives of this research were:

- 1) Investigate the formation of regenerated cellulose films from dimethyl sulfoxide / paraformaldehyde solvent system by phase inversion in water as well as in various non-solvents and analyze their physiochemical properties.
- 2) Investigate the differences in films formed by using native cotton linters and depolymerized cotton linters as starting materials in terms of hydration and solute permeability.
- 3) Study the impact of blending native and depolymerized solutions on film properties such as porosity, tortuosity, pore size, and the influence of solute hydrophobicity on their permeability through these films.
- 4) Develop a suitable method for fabrication of cellulose two-piece hard shell capsules using dip coating approach.

- 5) Study the process of one component formulation release from cellulose capsules and investigate the contributions of osmotic and diffusive mechanisms of enclosed solutes with varying solubility.
- 6) Investigate in-vitro conditions that can influence solute release from cellulose capsules.

## CHAPTER III

### PHYSIOCHEMICAL ATTRIBUTES OF REGENERATED CELLULOSE FILMS

#### **Introduction**

Cellulose is a naturally occurring polymer composed of repeating anhydroglucose units linked together by  $\beta$  1-4 glycosidic linkages. This inexpensive and abundant polymer is routinely applied in the powdered form as a tablet binder and filler. It is chemically and mechanically stable as well as completely insoluble in physiological conditions, which makes it an ideal candidate for oral controlled drug delivery systems. However, to date, there are no known applications of cellulose membranes and films in controlled release dosage forms owing to the difficulty associated with dissolution of this polymer in physiologically relevant or pharmaceutically-accepted solvent systems.

Regenerated cellulose membranes are commonly utilized in protein separation and reverse osmosis processes. Majority of these membranes are produced by precipitation (diffusion induced phase separation) of cellulose solutions in aqueous environments. The structure and properties of these membranes depends on the type of the solvent(s) utilized for cellulose dissolution as well as the non-solvents utilized for precipitation. Following immersion precipitation, most of these membranes are stored in aqueous environments to maintain their porous structure or are freeze-dried for further processing.

Although the dissolution of cellulose in dimethyl sulfoxide/ paraformaldehyde solvent system is well characterized, there is very little information on the properties of the films and membranes formed after phase inversion of methylolcellulose solution. In

this work, cellulose film formation was investigated from this solvent system, by the immersion precipitation/ phase-inversion process, followed by thermal annealing. Solvent and non-solvent-free elegant films were easily prepared by thermal annealing of the wet precipitated membranes. Flux of solute was examined under controlled hydration conditions in order to characterize the influence of water uptake on solute permeability. Blended films were prepared from native cotton linters and depolymerized cotton linters in order to alter film properties such as water uptake, porosity and tortuosity. The changes in solute size and hydrophobicity were examined through these blended films. The effect of thermal annealing was examined on cellulose films regenerated in various organic non-solvents and the extent of polymer consolidation by hornification was indirectly quantified by dye adsorption method. The thickness of the films was altered by lamination approach and the changes in the film tortuosity were analyzed as a function of thickness.

## **Experimental**

### Materials

Cellulose raw materials used in the preparation of various films were cotton linter sheets obtained from Southern Cellulose Products Inc. (Grade R270; Chattanooga, TN), paraformaldehyde, methanol (99.9%), 1-propanol (99.9%), 1-butanol (99.9%), acetone (99.7%), potassium chloride and hydrochloric acid (12.1 N) was obtained from Fisher Chemicals (Fair Lawn, NJ). Dimethyl sulfoxide was purchased from Sigma Aldrich (St. Louis, MO), methyl *p*-aminobenzoate from Aldrich Chemical Co. Inc. (Milwaukee, WI), ethyl *p*-aminobenzoate from ICN Biomedicals Inc. (Aurora, OH), propyl-*p*-aminobenzoate from Pfaltz and Bauer Inc. (Waterbury, CT) and butyl-*p*-aminobenzoate



was obtained from Sigma Life Sciences (St. Louis, MO). Ethanol (200 proof) was obtained from Decan Labs (King of Prussia, PA), glacial acetic acid (A.C.S grade, 99.7%) from Research Products International Corp. (Mt. Prospect, IL), copper(II)-ethylenediamine complex reagent (1 M) from Acros Organics (Geel, Belgium), and triethylamine from Mallinckrodt (St. Louis, MO). Bovine Serum Albumin (BSA) and Lysozyme chloride (LZY) were purchased from Sigma Life Sciences (St. Louis, MO). The protein assay kit (Micro BCA kit) for analysis of BSA and LZY was purchased from Thermo Scientific (Rockford, IL). All materials and chemicals were stored and utilized as received except for BSA and LZY which were initially stored at 4°C and -20°C, respectively, prior to their use.

#### Depolymerization / Hydrolysis of cellulose

Cellulose from cotton linter sheets was depolymerized according to the mineral acid hydrolysis method [77]. Briefly, cotton linter sheets, shredded into 1 cm x 1 cm pieces and weighing approximately 50 g, were placed in a 1 L Erlenmeyer flask filled with 500 ml of 2 N hydrochloric acid and agitated using a magnetic stir bar at 40°C in a thermostatic water bath for up to 72 hrs (RM 6 Lauda, Lauda Brinkmann L.L.C, Delran, NJ). At predetermined time intervals, approximately 1 to 5 g samples were removed from the flask and rinsed in running water for 2 hours, followed by washing in acetone and finally placed in an oven at 105°C for 24 hours. At the end of 72 hrs, the remaining cellulose slurry was rinsed and dehydrated by the same method. Depolymerization studies were carried out in three separate flasks.

### Preparation of methylolcellulose solution

Methylolcellulose (MC) solutions were prepared according to the procedure described by Johnson et al [32,34,35]. Briefly, for 4.5% w/w cellulose solution, 24 g of cotton linter sheets, cut up into 1 cm x 1 cm pieces, were dispersed in a 1 L three-neck round bottom flask containing 500 ml dimethyl sulfoxide (DMSO). One of the necks on the round bottom flask was connected to a 50 cm x 3 cm glass condenser and a solvent trap containing amorphous calcium silicate as a desiccant; the second neck was closed off with a rubber stopper attached to a mercury thermometer, and the third neck was connected to a dropping funnel which contained 60 g paraformaldehyde powder. The cellulose suspension was heated and maintained at 120°C using a thermostatic heating mantle for 2 hours, at which point 60 g of paraformaldehyde (PF) was added geometrically using a dropping funnel while gently mixing the suspension with a magnetic stir bar. The mixture was allowed to react for 4 to 6 hrs at 120°C, or until the suspension became a clear viscous solution. The resulting solution was then transferred to a sealed container prior to further analysis. Methylolcellulose solution with 4.5% w/w 72 hours depolymerized cotton linter (MC-DP) was also prepared by the same method. Figure 4 shows the schematic of the reaction system used in preparation of MC and MC-DP solution

### Film casting by regeneration and phase inversion and cellulose yield

Regenerated cellulose films from MC (native cotton linters) and MC-DP (depolymerized cotton linters) solutions were prepared by dip coating glass test tubes (20 mm diameter) in the respective methylolcellulose solutions and rotating the tubes at 70-100 rpm on an electric motor (GKH model GT-21, G. K. Keller Corp, Floral Park, N.Y.)

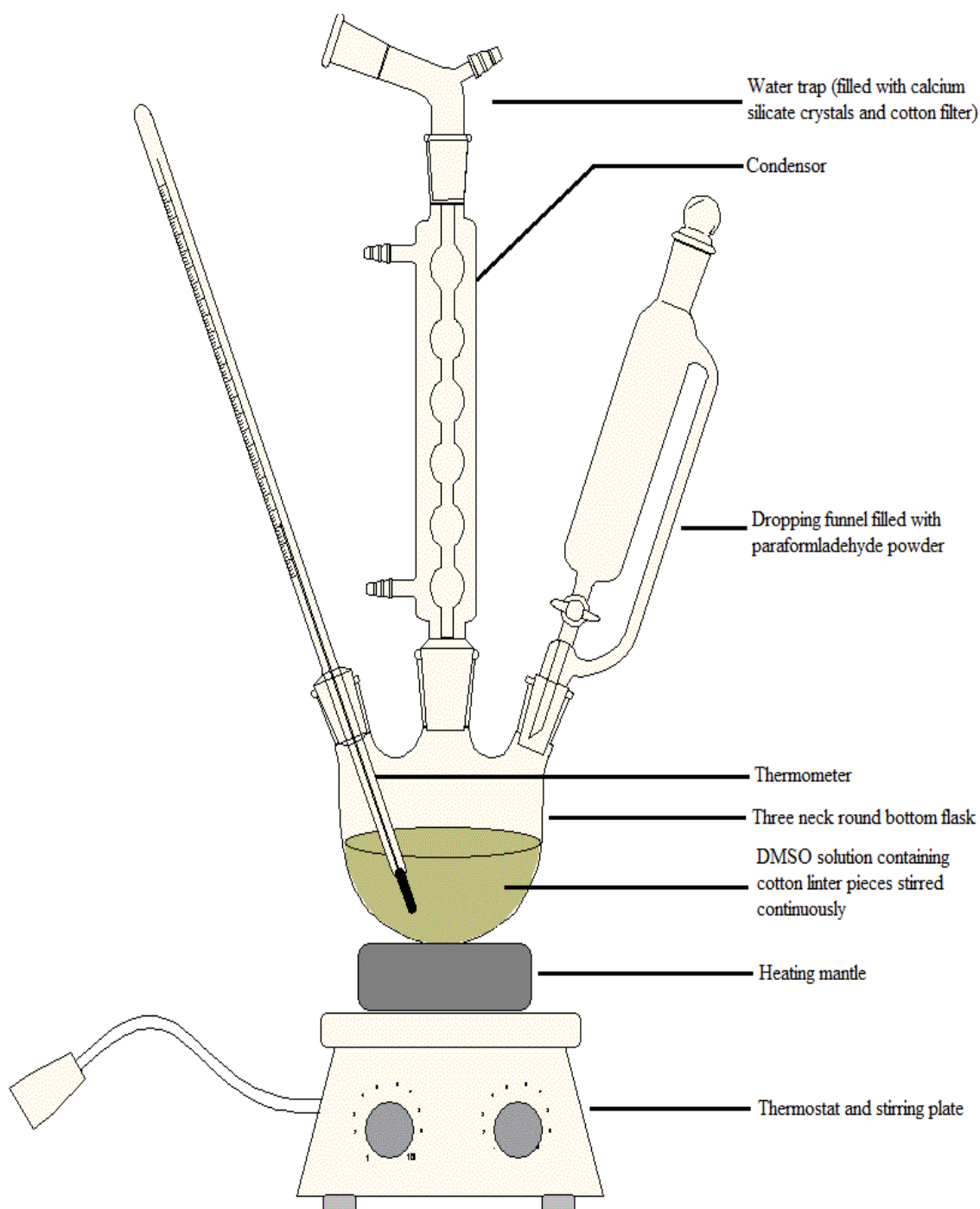


Figure 4: Schematic representation of reaction setup utilized in preparing methylolcellulose solution (MC-4 and MC-DP)

regulated by an electrical voltage regulator (GKH model GR-45, G. K. Keller Corp, Floral Park, N.Y.), for about 10 min or until evenly coated. These test tubes were then placed in 5 L water bath at room temperature for 3 days (regeneration\ phase inversion). The water was replaced in the precipitation bath every 6 to 12 hours. Regenerated cellulose films were then annealed in a thermostatic oven at 105 - 120°C for 24 hours. Annealed films were peeled from the glass tubes and placed in 20 ml scintillation vials, sealed with screw caps, and stored in a vacuum desiccator prior to further analysis.

Regenerated cellulose films were also prepared by precipitating MC solution in excess (> 5L) acetone, methanol, ethanol, 1-propanol and 1-butanol and the resulting thermally annealed films are referred to as RC-A, RC-M, RC-E, RC-P and RC-B, respectively.

Blended films were also prepared by mixing MC and MC-DP solutions in 50 ml beakers in the following ratios; MC: MC-DP, 4:1 (RC-4/1), 3:2 (RC-3/2), 2:3 (RC-2/3) and 1:4 (RC-1/4). All solutions were heated up to 50°C and blended using a magnetic stirrer operating at 200 rpm for 30 minutes. Film preparation, precipitation and annealing were performed as mentioned above.

Regenerated cellulose films of varying thicknesses were prepared with 5 (RC-5T), 4 (RC-4T), 3 (RC-3T) and 2 (RC-2T) applications of MC solutions via a multiple dip coating approach. After each application, the solution coated test tubes were immersed in acetone for a period of 10 min, followed by drying at room temperature for 10 min and re-immersing them in MC solution. After each application of MC solution, the test tubes were rotated in order to achieve even distribution of MC solution. After the final application of the solution, the test tubes were immersed in 5 L purified water and the

films were allowed to precipitate over 3 days. After precipitation in water, films were annealed in a thermostatic oven at 105 – 120°C for 24 hours, removed from the tubes and stored in sealed vials prior to analysis.

The amount of cellulose retrieved after precipitation was estimated by weighing the amount of dry mass obtained following precipitation of MC solution in various non-solvents. Approximately 50 grams of the solution was poured into a glass petri dish and weighed on a micro balance (Model R200D, Sartorius Corp., Bohemia, NY.) prior to placing in excess non-solvent medium. Precipitation of cellulose was carried out by placing these petri dishes in 1 L 100 % acetone, methanol, water, ethanol, 1-propanol and 1-butanol as non-solvents for 3 days. The non-solvent medium was continuously agitated using a stainless steel stirring rod attached to an electric rotor (GKH model GT-21, G. K. Keller Corp, Floral Park, N.Y.). At the end of 3 days, the petri dish was removed from the non-solvent bath and placed in a thermostatic vacuum oven at 120°C, for 24 hrs (Model 5831 vacuum oven, Napco, Tulatin, OR, and vacuum pump, Welch Duoseal, Skokie, IL). The amount of dry mass retrieved was weighed and the fraction of cellulose obtained was calculated by the following equation:

$$\text{Equation 6} \quad \% \text{ Cellulose yeild} = \frac{W_{RC}}{C_{MC} \times W_{MC}}$$

Where, ' $W_{RC}$ ' is the weight of dried regenerated cellulose obtained after precipitation and thermal annealing, ' $C_{MC}$ ' is the concentration of cellulose in MC solution and ' $W_{MC}$ ' is the weight MC solution utilized prior to precipitation. All measurements were carried out in triplicates.

### Determination of degree of polymerization

Single-point method:

The degree of polymerization of cellulose during depolymerization / hydrolysis was determined by viscometric method adapted by the American Standards for Testing Materials, at  $25 \pm 0.5^\circ\text{C}$  using a Cannon-Fenske capillary viscometer (size 100; Fisher Scientific, Fair Lawn, NJ) [78,79]. Briefly, 0.15 to 0.7 g/dl solutions of cellulose and of RC films were prepared by dissolving them in 0.5 M copper(II)-ethylenediamine (cuen) solution. This solution was thoroughly mixed using a magnetic stirrer and equilibrated to  $25^\circ\text{C}$  in a water bath, under nitrogen purge. Approximately 6 to 7 ml of this solution was filled into the lower bulb of the viscometer (immersed in a water bath at  $25^\circ\text{C}$ ) and pulled to the upper bulb using capillary vacuum bulb. The solution was then allowed to flow from the upper to the lower markings on the viscometer and the time for efflux recorded. Efflux time of pure 0.5M cuen solution was also measured. The relative viscosity of the cellulose solution was determined by the following equation:

Equation 7  $\eta_{\text{rel}} = \frac{t}{t_0}$

where ' $\eta_{\text{rel}}$ ' is the relative viscosity, ' $t$ ' and ' $t_0$ ' are the efflux times of cellulose solution and that of the pure 0.5 M cuen solution. The intrinsic viscosity was calculated from the ASTM tables for intrinsic viscosity  $[\eta]$  which lists predetermined values of the product of intrinsic viscosity and concentration ( $[\eta] C$ ), for samples exhibiting relative viscosities between 1.1 to 9.9. The degree of polymerization was calculated by multiplying  $[\eta]$  with 190 [78,79]. This method is herein referred to as the "one point method" for molecular weight determination. The one-point method was utilized in the determination of the

degree of polymerization of cellulose during hydrolysis of cotton linters. All measurements were carried out in triplicates.

Multi-point method:

The degree of polymerization of cellulose in cotton linters, depolymerized cotton linters, and RC films was also determined by multi-point method. The relative viscosity of these samples, dissolved in 0.5M cuen solution (as described in single point method), was determined according to the above method for three different concentrations. Since the cellulose solution in cuen is reported to behave as a Newtonian liquid at low concentrations (< 1 g/dL), relative viscosity was converted to reduced viscosity ( $\eta_{red}$ ) by the following equation <sup>84</sup>:

Equation 8 
$$\eta_{red} = \frac{\eta_{rel} - 1}{C}$$

where 'C' is the concentration of cellulose in cuen. Reduced viscosity was converted to intrinsic viscosity by the following relation:

Equation 9 
$$[\eta] = \left[ \frac{\eta_{rel} - 1}{C} \right]_{C \rightarrow 0}$$

A plot of the following equation would hence yield  $[\eta]$  at the y-intercept:

Equation 10 
$$\log \left\{ \frac{\eta_{rel} - 1}{C} \right\} = \log[\eta] + K[\eta]C$$

The degree of polymerization of the samples was calculated by multiplying  $[\eta]$  (obtained with 190, a constant previously determined by other reports [78,79]). The viscosity average molecular weight of cellulose was determined by the multiplying the degree of polymerization obtained above by 162 (molecular weight of single anhydroglucose repeat

unit).

#### Fourier-Transform Infrared (FTIR) spectroscopic analysis

Infrared spectroscopic analyses were carried out by grinding approximately 2 - 5 mg of film sample or cotton linter fibers, previously oven dried at 105°C for 24 hours, with 300 mg of anhydrous potassium bromide (KBr) on an agate mortar and pestle. Two hundred milligrams of this mixture were compressed into flat discs using a flat faced 12.5 mm diameter punch and die set on a Caver press (Model C, Fred S. Carver Press, Menomonee Falls, WI) between 10,000 and 16,000 lbs force with a maximum dwell time of 0.75 to 1 min. The compression parameters were varied in order to prepare near transparent discs. Spectra were obtained by placing the compressed sample disc in the sample holder of a Nicolet 210 FT-IR spectrophotometer (Nicolet Instrument Corp, Madison, WI), equipped with an IBM compatible computer and Omnic<sup>®</sup> data processing software (Nicolet Instrument Corp, Madison, WI). Infrared spectra were collected over the 4000 to 650  $\text{cm}^{-1}$  range with the number of scans set at 16 and a resolution of 8  $\text{cm}^{-1}$ .

#### Preparation of cellulose II crystalline standard

Cellulose II crystalline standard was prepared by the method reported by Patil et al [80]. Briefly, 50 g of cotton linters were immersed in 1L 5 N NaOH and stirred for 30 minutes at 50°C, using a stainless steel blade attached to a motor. These linters were then removed and washed in water using a Buchner funnel until the pH of the washing solution was near neutral. Neutralized linters were re-exposed to the 1L 5N NaOH solution for 2 hours and washed again in running water until the pH of the washing solution was near neutral. The final neutralized linters were hydrolyzed in 1L 2N HCl



solution at 105°C for 10 hrs. Hydrolyzed linters were once again neutralized by rinsing in running water and dehydrated using acetone washing, followed by heating in an oven for 24 hours at 105°C. The dehydrated linters (now in cellulose II polymorphic form) were stored in vacuum desiccators until further analysis.

#### X-ray diffraction analysis

X-ray diffraction analysis was carried out on flat film samples using a specialized sample holder (stainless steel filling in traditional well plate sample holder), while samples of cellulose II standard and cotton linters was analyzed using a traditional well plate sample holder. All samples were pre-treated in an oven at 105°C for 24 hours and placed in sealed scintillation vials prior to analysis. A small amount of white petrolatum jelly (Aquaphor, Beiersdorf, Inc., Wilton, CT) was applied on the flat surface of the sample holder and the film was lightly placed on the surface using forceps. The film sample was further flattened by placing a glass slide over its surface and lightly compressing until all the air bubbles were removed between the sample holder surface and the film. The X-ray diffraction measurements were carried out between 10° and 40° 2 $\theta$  with a 0.05° 2 $\theta$  step width and time constant of 0.5 seconds. The samples were irradiated with monochromatic CuK $\alpha$  X-rays at a wavelength of 1.5059 Å on a Siemens D5000 X-ray diffractometer operating at 40 kV and 30 mA (Siemens Energy & Automation, Inc., Madison, WI). The diffractograms were processed using an IBM compatible computer with Diffrac<sup>plus</sup> X-ray software (EVA, version 2.0a, Siemens Energy & Automation, Inc., Madison, WI).

#### Solvent uptake and volume fraction of solvents in swollen RC films

Water uptake:

The water uptake of RC films, as circular discs, was determined gravimetrically at 37°C, in the form of circular discs. Briefly, RC film discs were placed in 500 ml beaker containing purified water. The beaker was placed in a thermostatic bath at 37°C (RM 6 Lauda, Lauda Brinkmann L.L.C, Delran, NJ). The solvent uptake (SU) was calculated at the end of 24 hours using the following equation:

$$\text{Equation 11} \quad \text{SU (\%)} = \left\{ \frac{W_{\text{wet}} - W_{\text{dry}}}{W_{\text{wet}}} \right\} \times 100$$

where ‘ $W_{\text{wet}}$ ’ is the weight of the hydrated disc and ‘ $W_{\text{dry}}$ ’ is the weight of the dry discs prior to immersing in water. All solvent uptake studies were conducted in triplicates.

Time dependent solvent uptake was also examined in RC-W, RC-DP and blended films by calculating the water uptake at predetermined time intervals. At each pre-determined time point, the film disc was removed from the beaker, surface water removed by blotting with dry tissue, and weighed in pre-calibrated petri dish. After weighing, the film discs were replaced in the water bath and the process repeated. All studies were conducted in triplicates.

Volume fractions of water-ethanol binary mixtures:

The hydration of RC and RC-DP films was also analyzed in water-ethanol mixtures with varying ethanol contents using the same method as described above. The volume fraction of the binary solvent mixtures ( $V_f$ ) in RC films was determined by the following relation:

$$\text{Equation 12} \quad V_f = \frac{V_s}{V_s + V_c}$$

where ‘ $V_s$ ’ is the volume of the solvent and ‘ $V_c$ ’ is the volume of the polymer. Since the volume of individual components cannot be measured directly, Equation 12 can be converted to the following relation:

$$\text{Equation 13} \quad V_f = \frac{\frac{SU}{100} \rho_c}{\rho_s \left\{ 1 - \frac{SU}{100} \right\} + \frac{SU}{100} \rho_c}$$

where, ‘SU’ is the solvent uptake at equilibrium, ‘ $\rho_c$ ’ is the true density of cellulose and ‘ $\rho_s$ ’ is the density of the solvent. The true density of cellulose in RC films was determined using a helium pycnometer as described in the next section. Solvent uptake (SU) of the binary mixtures by RC films was determined using Equation 11.

#### Porosity of cellulose films

Porosity ( $\epsilon$ ) of various RC films prepared, in the form of circular discs, was determined by the following equation:

$$\text{Equation 14} \quad \epsilon = \left\{ 1 - \frac{\rho_{app}}{\rho_{true}} \right\}$$

where ‘ $\rho_{app}$ ’ is the apparent density of the discs and ‘ $\rho_{true}$ ’ is the true density of cellulose film. The film discs were prepared by regenerating respective methylolcellulose solutions placed in a circular glass petri dish and regenerating in excess non-solvent medium for 3 to 4 days. Regenerated cellulose membranes were carved into circular sheets using a 1 cm diameter circular plastic mold and a surgical blade. The apparent density of the circular discs was determined by the following relationship:

$$\text{Equation 15} \quad \rho_{app} = \frac{W_{dry}}{\pi r^2 h}$$

where, 'r' and 'h' are the radius and thickness of the regenerated cellulose circular sheets. All dimensional measurements were carried out using a digital caliper (Marathon Management Company Ltd., Richmond Hill, Ontario, Canada). The apparent densities were determined for cellulose film discs in the dry state after thermal annealing and after hydration in water for 24 hrs.

The true density of cellulose in RC films was determined in lyophilized RC film discs. Briefly, RC circular sheets were placed in excess water for 24 hours, followed by flash freezing in liquid nitrogen and finally by vacuum drying them for 24 hours (Labconco Freezone 4.5, Labconco Corp, Kansas City, MO). The true density was determined using a helium micropycnometer (Quantachrome micropycnometer-2, Quantachrome Corp., Boyton Beach, FL) at ambient temperature. All measurements were carried out in replicates of 5 or 6.

#### Surface and cross-section analysis

The morphology of the RC films were examined at three different stages: (i) regenerated film on test tube support following regeneration / phase inversion in water (ii) thermally annealed RC film at 105°C for 24 hours, after removal from precipitation bath, and (iii) rehydrated RC films after thermal annealing for 24 hours. All film samples were stored in vacuum desiccators prior to further sample processing. The hydrated samples (i and iii) were flash frozen in liquid nitrogen and then dried in a vacuum (Labconco Freezone 4.5, Labconco Corp, Kansas City, MO), while the non-hydrated samples were dried for 24 h at 105°C, prior to analysis. The heat-dried and freeze-dried samples were loaded on aluminum stubs and sputter coated with gold using an Emitech K550 sputter coater (Emitech Products, Inc., Houston, TX). Images of the surface and the

cross-section of the RC films were captured using a Hitachi S-4800 scanning electron microscope (Hitachi Ltd., Tokyo, Japan) at magnifications between 1,000 X and 10,000 X. All the images were captured at an accelerating voltage of 10 to 15 kV.

#### Preparation of saturated solutions and determination of solubility

Saturated solutions of acetaminophen in water as well as in ethanol-water binary mixtures of 20, 40, 60, 80 and 100 % v/v ethanol were prepared by loading excess solid acetaminophen in 25 ml Elmeyer flasks containing the described binary solvents. These flasks were sealed and shaken in a 37°C water bath for 72 hrs. Excess solid was added until white precipitate was observed visually. The saturated solutions were used in determining solubility as well as in transport studies. For solubility analysis, one milliliter of the saturated solution was removed using a syringe and passed through 0.45 µm filter (Nylon Acrodisc<sup>®</sup>, Gelman, Ann Arbor, MI), diluted in pure ethanol, and the acetaminophen content analyzed by the HPLC method described in a later section. Solubility of alkyl-p-aminobenzoates in pure water at 37°C was also determined by the same method. All solubility measurements were carried out in triplicate. For transport studies, 8-10 ml of the solution, equilibrated at 37°C, was removed using a syringe and the solution ejected in the donor cell.

#### Transport studies through RC films

Transport studies of various solutes through RC films were investigated using dual chambered 'Side-Bi-Side' horizontal glass diffusion cells (Figure 5, PermeGear Inc., Hellertown, PA) with an orifice opening of 1.7 cm<sup>2</sup> and a cell volume of 8 ml. The temperature in each cell was maintained at 37 ± 0.5°C using circulating water from an external self-contained heater reservoir (RM 6 Lauda, Lauda Brinkmann L.L.C, Delran,

NJ). The stirring rate within the diffusion cells was maintained at approximately 600 rpm using magnetic stir bars. The flux 'J' of solutes through RC films was calculated from the slope of the linear portion of the cumulative amount of solute transported versus time, by the following relation:

Equation 16 
$$J = \frac{dM}{A dt}$$

where, 'dM/dt' is the rate of solute transfer and 'A' is the area of the exposed film in the diffusion cell.

#### Transport of acetaminophen through RC-W and RC-DP films in binary solvents

Transport of acetaminophen was examined through RC-W and RC-DP films using 0, 20, 40, 60, 80 and 100% ethanol v/v with co-solvents in the donor and receiver cells. Thermally annealed RC-W and RC-DP films were pre-treated in the respective binary solvent mixtures by placing them in sealed 20 ml glass scintillation vials containing the respective binary mixtures and equilibrated in a water bath at 37°C for 24-48 hours. After equilibration, the films were immediately mounted between diffusion cells and a transport study initiated. Saturated acetaminophen solutions were placed in the donor cell while the receiver cell was emptied at pre-determined time intervals and replenished with fresh medium in order to maintain sink condition.

Reversibility of swelling and its effect on permeability was examined in RC-W films by first observing acetaminophen flux using purified water as the solvent medium in both cells, followed by ethanol as the solvent medium and, finally again in purified water. The donor concentration was held constant at 15 mg/cm<sup>3</sup>. The time required between medium exchanges in the diffusion cells was less than 5 minutes.

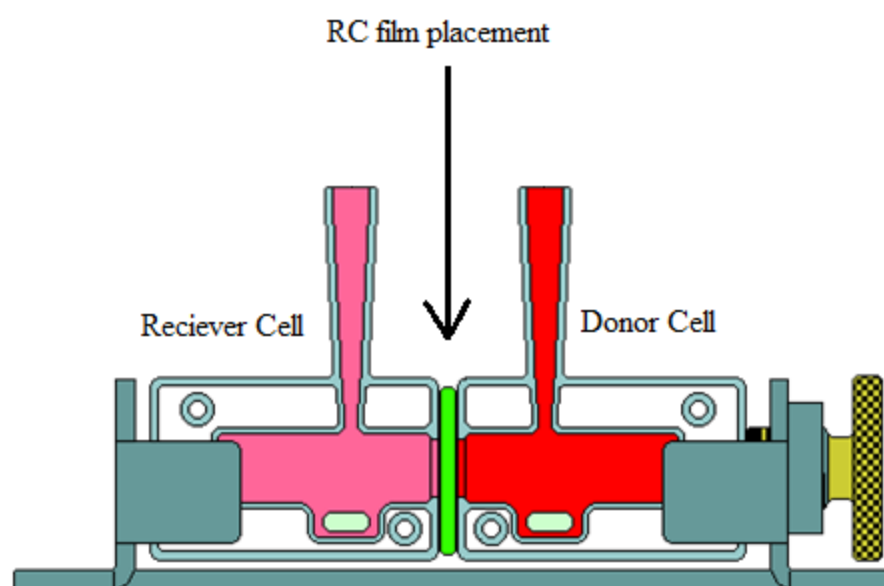


Figure 5: Typical experimental setup of Side-by-Side<sup>®</sup> diffusion cells for analysis of RC film solute permeability.

### Influence of thermal annealing on the flux of ethyl-*p*-aminobenzoate

To study the influence of thermal annealing on the flux of solutes, the transport of ethyl-*p*-aminobenzoate was examined through RC-A, RC-M, RC-W, RC-E, RC-P and RC-B films that were freeze dried immediately after precipitation, and through same set of films that were thermally annealed at 120°C for 24 hours after precipitation in their respective non-solvents. Saturated solutions of ethyl-*p*-aminobenzoate were filled on the donor side while the receiver cell was emptied and replenished with purified water at predetermined time intervals. Transport studies were conducted at 37°C in triplicate.

### Transport of KCl and alkyl-*p*-aminobenzoates through RC blended films

Transport of KCl was examined through RC-W, RC-DP and RC blended films. In all cases, the films utilized were thermally annealed at 105°C for 24 hours prior to initiating transport study. The amount of KCl transported through the RC film was examined by analyzing KCl concentration in the receiver cell which was emptied at predetermined time points and replenished with purified water, in order to maintain sink conditions. The donor concentration was set at 0.1 M KCl and held constant by periodically replacing the donor cell with fresh 0.1 M KCl solution as well. Concentration of KCl was determined using a potentiometric method described in the analytical section.

Fluxes of methyl-, ethyl-, propyl- and butyl-*p*-aminobenzoate were also examined through RC-W, RC-DP and RC blended films. In all cases, saturated solutions of the alkyl-*p*-aminobenzoates were utilized in the donor cell. Saturated solutions were prepared by the method described in the previous section. The receiver cell was emptied at predetermined time intervals and replaced with purified water. Alkyl-*p*-amino benzoates in the receiver cell volumes were assayed using the HPLC method described in the



analytical section.

#### Transport of LZY and BSA through RC blended films

In order to study the pore sizes as a function of the fraction of depolymerized cellulose in the film, the flux of lysozyme chloride (LZY) and bovine serum albumin (BSA) was examined at steady state through RC-W, RC-DP and RC blended films. The solvent medium utilized to study LZY flux was pH 4.5 acetate buffer medium, while BSA flux was examined in pH 7.4 phosphate buffer medium. The donor concentrations of LZY and BSA were maintained at 1.0 mg/ml by periodically replacing the donor cell contents with fresh protein solutions in their respective buffer. The receiver cell was emptied at pre-determined time intervals and replenished with fresh buffer in order to maintain sink conditions.

Buffer solutions were prepared in accordance with USP 23 specifications [81]. Briefly, for phosphate buffer, 50 ml of 0.2 M monobasic potassium phosphate solution (27.22 grams in 1 L purified water) was mixed with 39.1 ml of 0.2 M NaOH solution (8.00 grams in 1L purified water) and the mixture diluted to 200 ml. The acetate buffer medium was prepared by dissolving 2.95 grams of sodium acetate in 100 ml purified water and placing 14.0 ml of 2N acetic acid in the same medium. The mixture was diluted to 1L using purified water. The pHs of the solutions were adjusted by adding excess NaOH or acetic acid and verified using a pH meter.

#### Estimation of irreversible polymer consolidation (hornification) by thermal treatment

Wet cellulose fibers have been shown to undergo irreversible cohesion when thermally treated [42,45]. The irreversibility is associated with the inability of newly intruding water to penetrate the dry cotton fabrics and induce swelling. The tight cohesion is brought about by hydrogen bonding and to some extent by hydrophobic

interactions involving the glucopyranose rings. The extent of irreversible polymer consolidation following thermal treatment of wet precipitated RC films was analyzed by measuring the amount of methylene blue adsorbed on RC-DP, RC-A, RC-M, RC-W, RC-E, RC-P and RC-B membranes which were freeze dried immediately after precipitation of cellulose membranes in their respective non-solvents, and thermal annealing of the wet membranes after precipitation. Membranes were prepared by pouring 50 g of MC solution into 22 cm x 22 cm square ceramic well plates. The solution filled plates were placed in 1 L non-solvents and the cellulose membranes were allowed to regenerate for 3 days, with constant replacement of the non-solvent every 8 – 12 hours. Two sets of membranes were prepared from each non-solvent, one set was immediately freeze dried following regeneration while the second set was thermally annealed at 120°C in an oven for 24 hours. The dried membranes were then placed in 250 ml Erlenmeyer flasks filled with methylene blue solution (0.4 to 6 µg/ml, pH adjusted to 8.5 using 0.01 M NaOH solution). These flasks were allowed to stand undisturbed for 5 days at 25°C in a temperature controlled oven. The concentration of methylene blue in the flasks was analyzed using a Hewlett-Packard 8450-A diode array UV spectrophotometer (Palo Alto, CA) at 658 nm.

#### Analytical methods

Potassium chloride assay:

Potassium chloride (KCl) concentration was determined conductively using a potassium ion-selective electrode (Cole Parmer, Vernon Hills, IL) attached to a pH meter (Orion™ Model 420A, Cole Parmer, Vernon Hills, IL). All samples obtained were equilibrated at room temperature prior to analysis.

Alkyl-p-aminobenzoate and acetaminophen assay:

The concentrations of alkyl-p-amino benzoates were determined by a modified reversed phase high performance liquid chromatographic (RP-HPLC) method reported by Grouls [82]. A Shimadzu HPLC system was employed for analysis of solute concentrations (Shimadzu Corporation, Kyoto, Japan). The system consisted of a system controller (LC-6A), a pump (SIL-6), an automated sample injector (SIL-9B), an ultraviolet-visible spectrophotometric detector (SPD -6AV) and an analog data processor/recorder (CR-5A). The samples were eluted (isocratic) through a reverse phase (RP) C<sub>18</sub> column (150 x 3 mm, 110 Å, particle size 3 µ; Phenomenex Gemini, Torrance, CA). The mobile phase contained a 3:0.99:0.01 (v/v) ratio of pH 3.5 glacial acetic acid solution, methanol and triethylamine. The glacial acetic acid solution was prepared by mixing 20 ml of glacial acetic acid with 980 ml of purified de-ionized water. The pH of the solution was adjusted to 3.5 by further addition of acetic acid. All components of the mobile phase were thoroughly mixed for 10 minutes and filtered through a 0.45 µm nylon membrane (Chrom Tech, Inc., Apple Valley, MN), followed by degassing in a sonication bath (Bransonic Ultrasonic cleaner, Model 5200, Bransonic corporation, Danbury, CT). Methyl and ethyl esters were detected at 285 nm while the propyl and butyl esters were detected at 282 nm. The flow rate was set to 0.2 ml/min. Injection volumes of 5 µl were used for samples and standards.

For acetaminophen, the concentrations were determined by eluting (isocratic) samples through an RP C<sub>18</sub> column (300 x 1.5 mm, Waters™ µBondpack, Milford, MA) fitted to the HPLC system described above. The mobile phase consisted of 1:4 (v/v) methanol:water mixture and a flow rate of 1.5 ml/min. All samples were detected at 243 nm (2 µl injection volume)

Standards for all the analytes were prepared over a concentration range of 0.001 to 0.2 mg/ml and the methods validated by analyzing standards at three different times over a 24 hour period.

Total protein assay:

The concentrations of bovine serum albumin (BSA) and lysozyme chloride (LZY) were determined using the assay method provided in the Micro BCA™ kit (Thermo Fisher Scientific Inc., Marietta, OH). Briefly, 1 ml samples of protein and 1 ml of working reagent were mixed in a 2 ml sealed glass vial and shaken in a thermostatic shaker at 60°C (C-24, New Brunswick Scientific, Edison, NJ) for 1 hour. The working reagent consisted of 25 parts of proprietary alkaline tartarate-carbonate buffer, 24 parts of proprietary bicinchonic acid solution and 1 part proprietary copper sulfate solution. The standards for BSA and LZY were prepared in the range of 0.3 to 2.5 µg/ml using the same method. All protein concentrations were analyzed using Hewlett-Packard 8450-A diode array UV spectrophotometer (Hewlett-Packard Corporation, Palo Alto, CA) at 590 nm after allowing the samples to equilibrate to room temperature, following shaking and incubation.

## **Results**

### Preparation of depolymerized cotton linters

Cotton linters were depolymerized using the mineral acid hydrolysis method [77]. Figure 6 shows the average degree of polymerization of cellulose in cotton linter samples from three separate reaction flasks, using the same reaction conditions (2 N HCl, 40 °C), as a function of time. All measurements were obtained using the ‘single-point’ method. The de-polymerization of cellulose was erratic between 2 – 24 hours. This could be due

to the uneven mixing and penetration of the acid in cotton linter fibers in the reaction flask. However, by the end of 72 hours, the degree of polymerization of cotton linters in the three reaction flasks was nearly similar, indicating 'leveling of depolymerization'. Battista attributed this outcome to hydrolysis of cellulose in the amorphous regions while the crystalline regions remain intact and resist any further depolymerization due to lack of solvent penetration in the highly ordered cellulose network [77]. Hence, the 72 hour depolymerized product was used in the fabrication of low molecular weight (4.4 % w/w) cellulose solution (MC-DP) and the resulting film prepared referred to as RC-DP.

#### Cellulose yield from precipitation of MC solution in various non-solvents

The amount of cellulose retrieved from MC solution in various non-solvents was estimated by measuring the amount of dry mass retrieved after precipitation of the solution in excess water, acetone, methanol, ethanol, 1-propanol and 1-butanol. Table 3 lists the percentage of cellulose retrieved from 4.4% w/w MC solution in various non-solvents. These results indicate that complete retrieval of cellulose is observed from all the non-solvent media utilized for precipitation of RC membranes and these membranes do not contain any solvents or non-solvents.

#### Polymer stability during film formation

The polymer stability during film formation process was investigated by analyzing the degree of polymerization of cellulose in cotton linters prior to dissolution in DMSO/ PF, and after thermal annealing of RC films. The degree of polymerization of

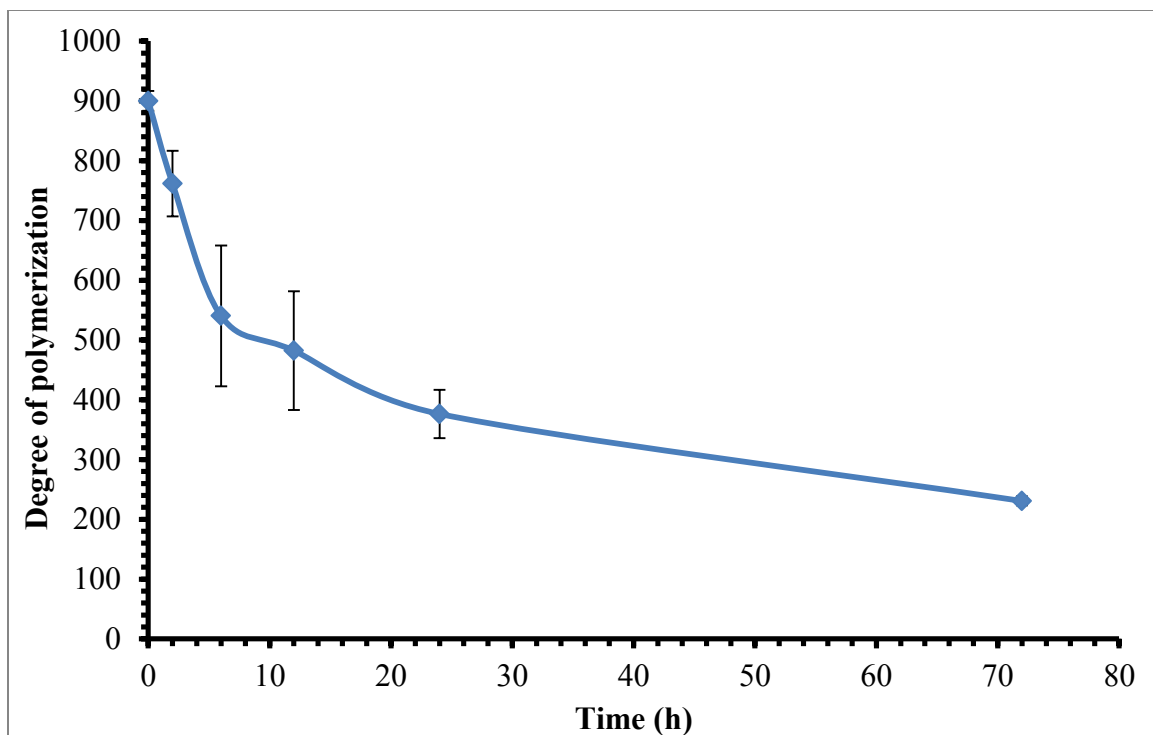


Figure 6: Degree of polymerization vs. reaction time for cotton linters at 40°C in 2 N HCl. Error bars shows standard deviation of three samples. The degree of polymerization was determined by single point method.

Table 3: Cellulose yield from MC-4 solution in various non-solvents

| Non-solvent utilized for cellulose precipitation | Weight of MC starting solution | Weight of dry mass retrieved | Percentage Cellulose yield <sup>a</sup> | Average $\pm$ S.D.<br>(%, n=3) |
|--------------------------------------------------|--------------------------------|------------------------------|-----------------------------------------|--------------------------------|
|                                                  | (g)                            | (g)                          | (%)                                     |                                |
| Acetone                                          | 50.24                          | 2.21                         | 99.97                                   | 100.46 $\pm$ 0.42              |
|                                                  | 51.66                          | 2.29                         | 100.75                                  |                                |
|                                                  | 53.96                          | 2.39                         | 100.66                                  |                                |
| Methanol                                         | 53.23                          | 2.33                         | 99.48                                   | 99.66 $\pm$ 0.93               |
|                                                  | 49.67                          | 2.16                         | 98.83                                   |                                |
|                                                  | 48.76                          | 2.16                         | 100.68                                  |                                |
| Ethanol                                          | 51.23                          | 2.26                         | 100.26                                  | 100.76 $\pm$ 0.71              |
|                                                  | 52.58                          | 2.35                         | 101.58                                  |                                |
|                                                  | 49.78                          | 2.20                         | 100.44                                  |                                |
| Water                                            | 48.65                          | 2.16                         | 100.90                                  | 101.25 $\pm$ 1.81              |
|                                                  | 50.87                          | 2.31                         | 103.20                                  |                                |
|                                                  | 52.24                          | 2.29                         | 99.63                                   |                                |
| 1-Propanol                                       | 51.33                          | 2.28                         | 100.95                                  | 99.88 $\pm$ 0.92               |
|                                                  | 50.56                          | 2.21                         | 99.34                                   |                                |
|                                                  | 49.64                          | 2.17                         | 99.36                                   |                                |
| 1-Butanol                                        | 54.53                          | 2.41                         | 100.45                                  | 100.90 $\pm$ 0.48              |
|                                                  | 53.79                          | 2.40                         | 101.40                                  |                                |
|                                                  | 52.05                          | 2.31                         | 100.86                                  |                                |

<sup>a</sup> Based on 4.4 % (w/w) cellulose content in the solution

cotton linters and RC films was calculated according the 'multi-point method'. Figure 7 shows the relation between reduced viscosity ( $\log\{(\eta_{rel}-1)/C\}$ ) and the concentration of cellulose sample in the cuen solution for cotton linters, depolymerized cotton linters, RC-W, RC-A, RC-M, RC-E, RC-P, RC-B and RC-DP films. The linear fitting functions (obtained using regression package in Microsoft® Office Excel™), intrinsic viscosity, degree of polymerization and viscosity average molecular weight of cellulose from cotton linter sources and RC films are listed in Table 4. The degree of polymerization of the cotton linters, used as the starting material, was approximately 894 while, the degree of polymerization of RC-W film was approximately 837. The degree of polymerization of cellulose from acid hydrolyzed cotton linters was approximately 251, and that of RC-DP films was approximately 225. The degree of polymerization of RC films prepared in different non-solvents (using MC solution) was similar to the degree of polymerization of cellulose in RC-W film. These results indicate that the polymer chain length was not significantly altered during cellulose precipitation and thermal annealing, irrespective of the non-solvent utilized.

Changes in cellulose structure were also monitored using FT-IR. Figure 8 shows the absorbance FT-IR spectra of cotton linter, RC-W and RC-DP films. Figure 9 shows the FT-IR spectra of thermally annealed RC-A, RC-M, RC-E, RC-P and RC-B films. All spectra display strong absorbance bands of hydroxyl groups in the range of 3100 to 3600  $\text{cm}^{-1}$ . Peak absorption of the hydroxyl groups in cotton linters was 3350  $\text{cm}^{-1}$  while that in the RC films shifted towards 3450  $\text{cm}^{-1}$ . The broadening of the -OH band in RC films can be associated with the disruption of the hydrogen bonding pattern involving the hydroxyl groups within and with neighboring cellulose chains in comparison to cellulose in cotton



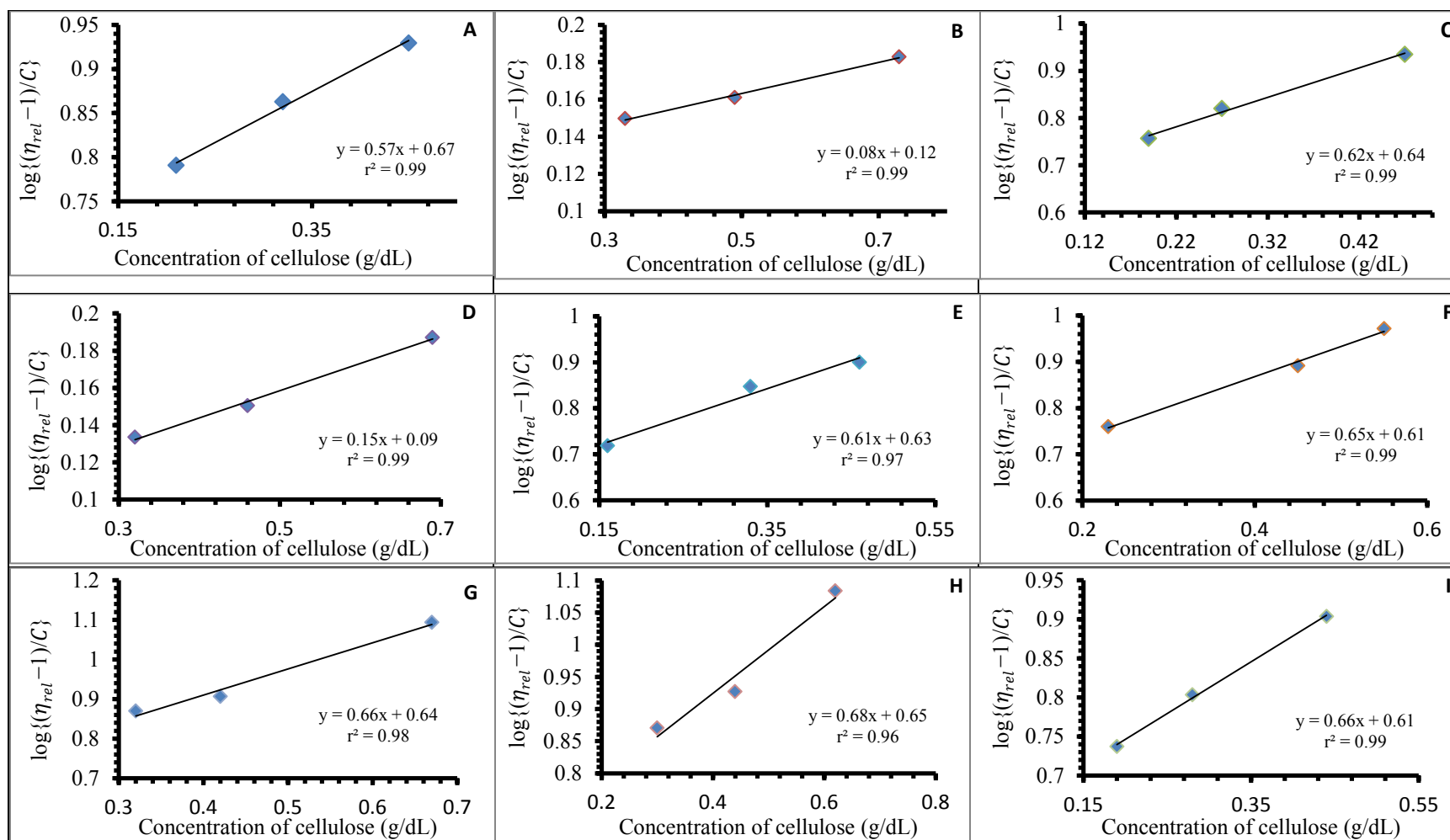


Figure 7: Relationship between  $\log\{(\eta_{rel}-1)/C\}$  and the concentration of cellulose in 0.5 M cuen solution for (A) cotton linter, (B) depolymerized cotton linter, (C) RC-W, (D) RC-DP, (E) RC-A, (F) RC-M, (G) RC-E, (H) RC-P and (I) RC-B films in 0.5M cuen solution, at 25 °C.

Table 4: Summary of degree of polymerization of cellulose and viscosity average molecular weight of cellulose of cotton linter, depolymerized cotton linters and RC films from the linear fitting parameters of  $\log\{(\eta_{rel}-1)/C\}$  vs. concentration plots.

| Sample                              | Intercept <sup>a</sup> | Intrinsic viscosity <sup>b</sup> | Degree of polymerization <sup>c</sup> | Viscosity average molecular weight <sup>d</sup> |
|-------------------------------------|------------------------|----------------------------------|---------------------------------------|-------------------------------------------------|
|                                     |                        | (dL/g)                           |                                       | (g/mole)                                        |
| <b>Cotton linters</b>               | 0.67                   | 4.70                             | 894                                   | 144,833                                         |
| <b>Depolymerized cotton linters</b> | 0.12                   | 1.32                             | 251                                   | 40,725                                          |
| <b>RC-W</b>                         | 0.64                   | 4.41                             | 837                                   | 135,602                                         |
| <b>RC-DP</b>                        | 0.09                   | 1.22                             | 231                                   | 37,468                                          |
| <b>RC-A</b>                         | 0.63                   | 4.25                             | 807                                   | 130,788                                         |
| <b>RC-M</b>                         | 0.61                   | 4.05                             | 769                                   | 124,614                                         |
| <b>RC-E</b>                         | 0.64                   | 4.42                             | 840                                   | 136,228                                         |
| <b>RC-P</b>                         | 0.65                   | 4.51                             | 856                                   | 138,729                                         |
| <b>RC-B</b>                         | 0.61                   | 4.12                             | 781                                   | 126,551                                         |

<sup>a</sup> Intercept of linear fitting functions as displayed in Figure 7

<sup>b</sup>  $[\eta] = 10$  (intercept of fitting function)

<sup>c</sup> Degree of polymerization =  $[\eta] \times 190$  [78,79]

<sup>d</sup> Viscosity average molecular weight = (Degree of polymerization) x 162, where 162 is the molecular weight of glucose monomer in cellulose

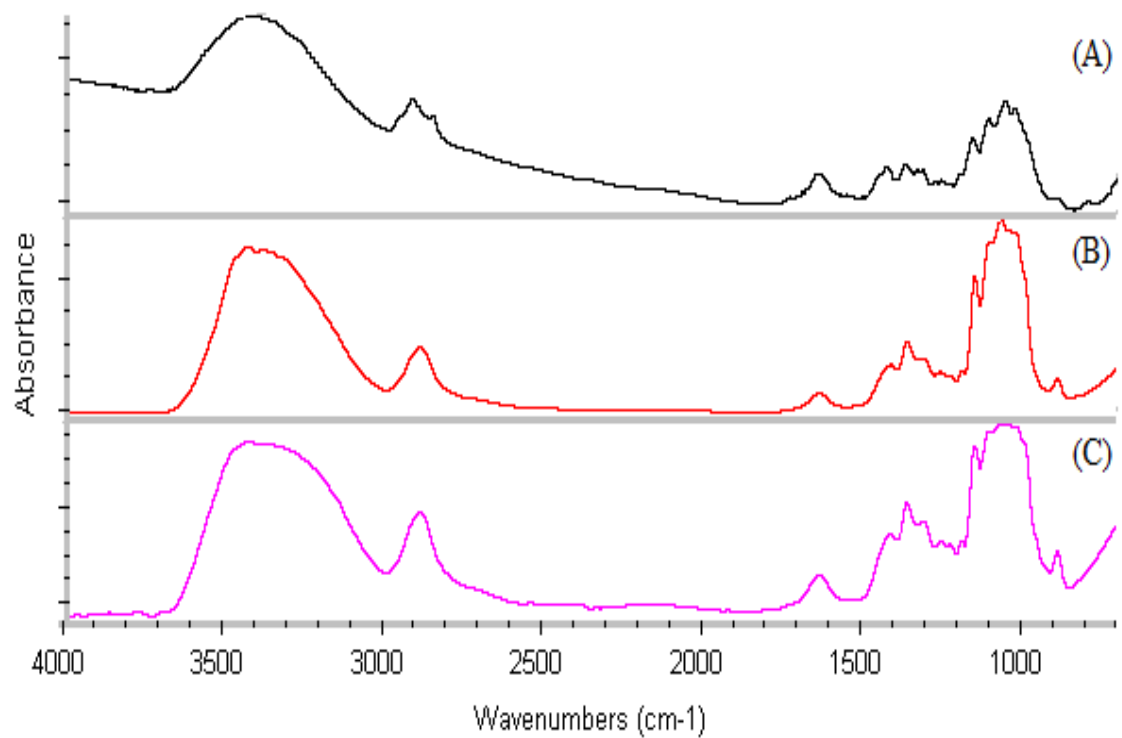


Figure 8: Fourier transformed infrared absorbance spectrum of (A) cotton linter, (B) RC-W film and (C) RC-DP film. The RC film samples were thermally annealed at 120°C for 24 hours after precipitation in water.

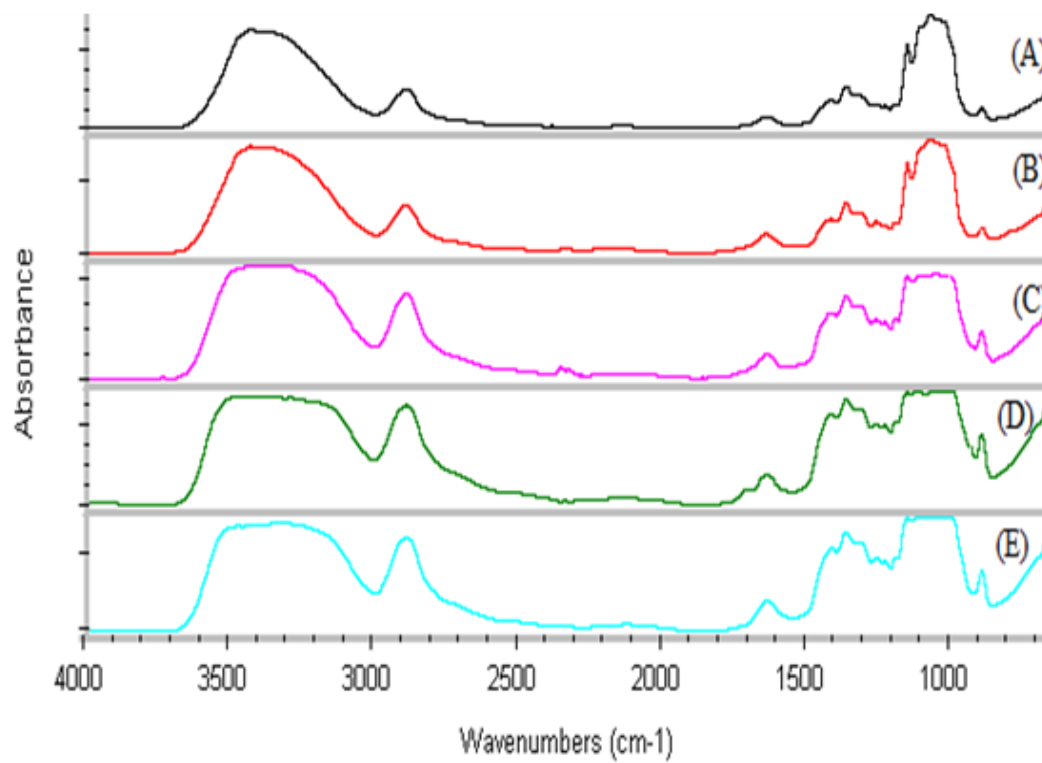


Figure 9: Fourier transformed infrared spectra of (A) RC-A, (B) RC-M, (C) RC-E, (D) RC-P, and (E) RC-B films. The RC film samples were thermally annealed in an oven at 120°C for 24 hours after precipitation in their respective non-solvents

linters, there by implying changes in the polymorphic form associated with hydrogen bonding pattern[83]. The absorption band at  $1640\text{ cm}^{-1}$  for RC films is attributed to strongly bound water within the cellulose polymer network which could not be removed even after overnight curing. The intensities of the bands in the  $1450\text{ cm}^{-1}$  (-OH wagging) and  $1320\text{ cm}^{-1}$  (-CH<sub>2</sub>- bending at C<sub>6</sub> position) region are similar in cotton linter while the intensity of the same bands in the RC films changed indicating that inter- and intra-molecular hydrogen bonding was altered at the C<sub>6</sub> position[84]. A unique shoulder appears for RC films in the  $900\text{ cm}^{-1}$  region which is attributed to the -CH- bending in the glucopyranose ring or -CH<sub>2</sub>- stretching at C<sub>6</sub> due to either the amorphous nature of cellulose or conversion to cellulose II polymorphic form [85]. To verify this conversion, X-ray diffractograms were obtained for RC films and compared to cotton linters as well as a cellulose II crystalline standard.

#### X-Ray diffractograms of RC films

Figure 10 shows the X-ray diffractograms between  $2\theta = 10^\circ$  and  $30^\circ$  for cotton linter, cellulose II standard, RC-W and RC-DP films. Figure 11 shows the X-ray diffractograms of RC-A, RC-M, RC-E, RC-P and RC-B films between  $2\theta = 5^\circ$  and  $30^\circ$ . No peaks were observed in the  $5^\circ$ -  $10^\circ$   $2\theta$  and above  $30^\circ$   $2\theta$ . Cotton linters exhibit cellulose I polymorphism with  $2\theta$  peaks at  $14.8^\circ$ ,  $16.3^\circ$  and  $22.6^\circ$ , while cellulose II, that was prepared by alkali treatment and hydrolysis of cotton linters, displayed peaks at  $2\theta = 11.5^\circ$ ,  $19.8^\circ$  and  $21.9^\circ$ . In contrast, all the RC films display a diffuse halo over the  $16^\circ$  to  $22^\circ$   $2\theta$  range. The weak peak observed in RC-DP, RC-W RC-M, RC-E, RC-P and RC-B films at  $12^\circ$   $2\theta$  is attributed to  $1\bar{1}0$  crystal lattice plane which corresponds to the stacking of glucopyranose ring structures brought together by hydrogen bonding at the C<sub>6</sub> position

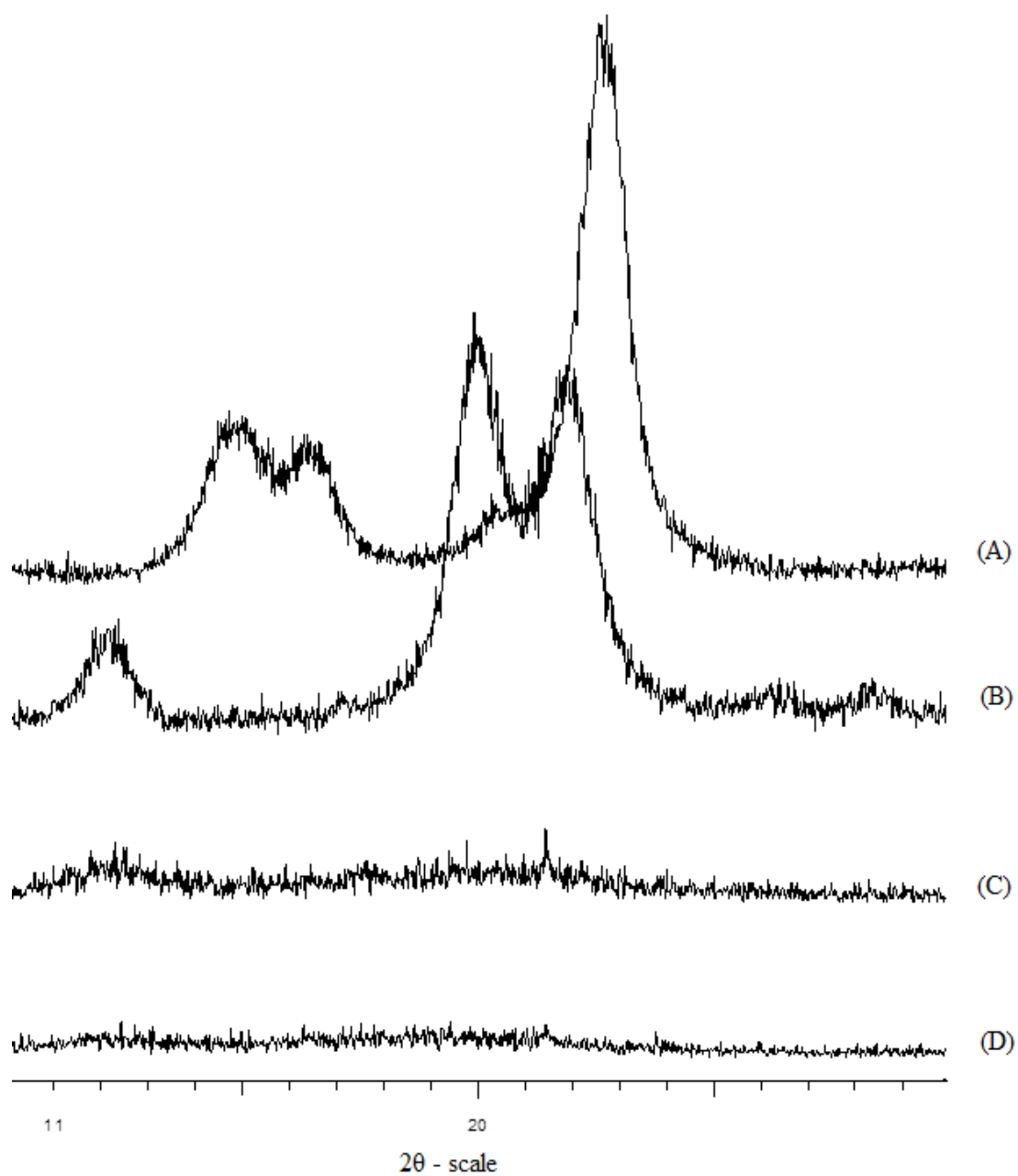


Figure 10: X-ray diffractograms of (A) cotton linter sheets, (B) cellulose-II crystalline standard, (C) RC-DP and (D) RC-W films. The RC film samples were thermally annealed in an oven at 120°C for 24 hours, after precipitation in water.

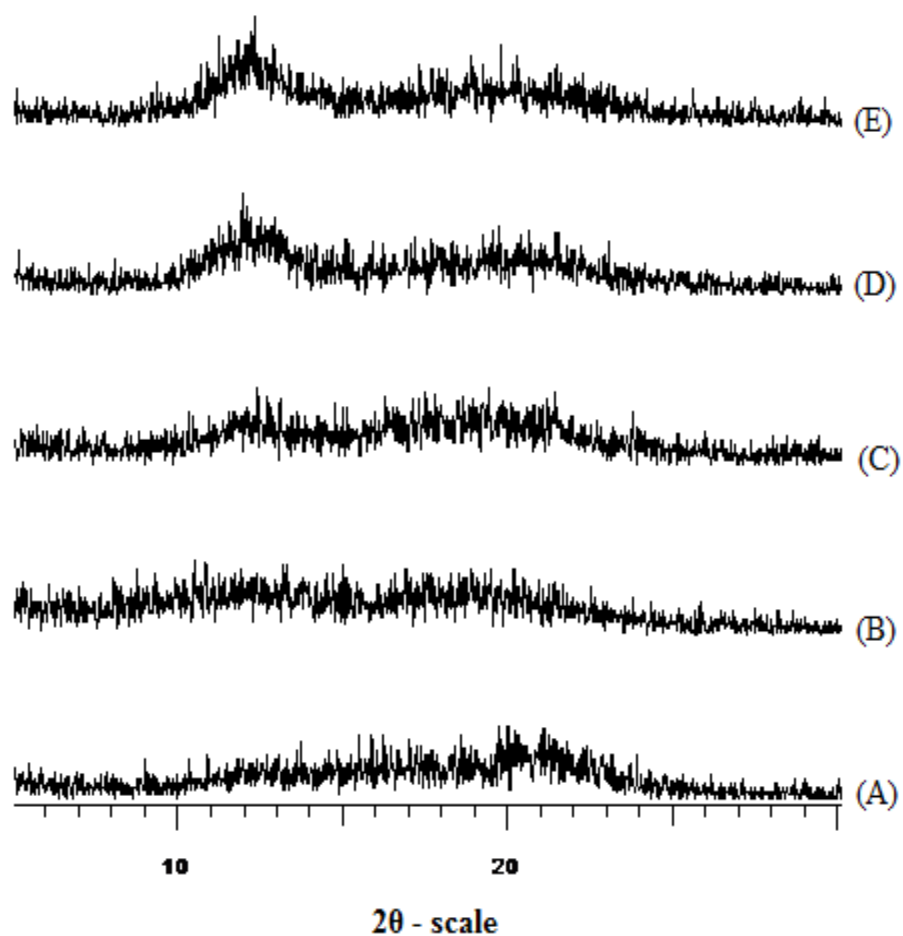


Figure 11: X-ray diffractograms of (A) RC-4A, (B) RC-4M, (C) RC-4E, (D) RC-4P and (E) RC-4B. The RC film samples were thermally annealed in an oven at 120°C for 24 hours after precipitation in their respective non-solvents.

as well as hydrophobic interactions between the glucopyranose rings [83]. Moreover, a small but discernible increase in the  $12^\circ 2\theta$  peak is observed among RC films precipitated in acetone and 1-alkanols of increasing carbon chain length. The increase in  $12^\circ 2\theta$  intensity is an indication of increased glucopyranose-ring stacking. The presence of a diffuse halo for all RC films in the  $16^\circ$  to  $22^\circ 2\theta$  range indicates that the hydrogen bonding of cellulose polymer is largely heterogeneous possibly due to rapid precipitation in all the non-solvents examined. These results demonstrate that RC films prepared by thermal curing are largely amorphous irrespective of the degree of polymerization of the starting cellulose source or the type of non-solvent utilized for precipitation/phase inversion.

#### Visual examination of cellulose film formation

The formation of RC films by the precipitation of MC solution in water was visually examined using a scanning electron microscope. Figure 12 shows the SEM images of a solvent/ non-solvent exchange interface, cross-section and the test tube facing interface of the RC-W film that was formed after precipitation in excess water. Figure 13 shows the SEM images of a solvent/ non-solvent exchange interface, cross-section and the test tube facing interface of the RC-W films which were thermally annealed after precipitation in water. These images indicate that after the immersion precipitation process, the RC-W films contain surface pores that possibly act as pathways for removal of DMSO/ formaldehyde from the internal sections of the film. Upon thermal treatment, the wet films coalesce to form a near monolithic surface and cross-section. This observation indicates that thermal curing possibly imparts mobility to the wet polymer during heating which tends to associate with neighboring units. Since water



interacts with cellulose via hydrogen bonding, it can be deduced that its removal is led by inter-polymer association by hydrogen bonding [47]. Moreover, the glucopyranose rings from neighboring chains, which consists of hydrophobic  $-CH_2-$  groups, can stack together by hydrophobic interactions [86], [3].

The presence of porous cavities in the cross-section indicates that the film forms regions of empty pockets that represent an overall honeycomb like internal structure. The lack of ‘finger like’ projections in the cross-section, extending from solvent/non-solvent facing interface to the test tube facing surface of the film, commonly observed with cellulose acetate immersion precipitation membranes [87], indicates that precipitation of cellulose possibly occurs by progression from the solvent non-solvent exchange interface towards the test tube facing interface. Comparison of the solvent non-solvent exchange interface and the test tube facing surface of the RC-W film, freeze dried after precipitation, shows that the two surfaces are visually different, indicating that the film is possibly asymmetric with larger pores appearing on the precipitation front and denser polymer arrangement towards the inner surface. This is commonly observed during the phase inversion process owing to slower diffusion of the solvent from the internal sections of the film in to the non-solvent medium.

Figure 14 shows the SEM micrographs of rehydrated RC-W film solvent/non-solvent exchange interface, cross section and test tube facing interface. These films were rehydrated in excess water after thermal curing for 24 hours at 105°C. Although these films lose their porous structure when dehydrated, the porous cavities re-appear after re-exposure to water. These observations indicate that the film consists of possibly two regions; (i) loosely hydrogen bonded regions that can take up water and swell to form

porous cavities, and (ii) non-swelling domains that are possibly held to-gather by inter and intra-molecular hydrogen bonding, and hydrophobic interaction [86] [3].

#### Influence of degree of polymerization of cellulose

Figure 15 shows the SEM images of a thermally annealed and rehydrated RC-DP film's solvent/ non-solvent exchange surface. These films were prepared from MC-DP solution in excess water as non-solvent. Visually, the pore sizes on RC-DP film surface (observed at higher magnification than RC-W film) were significantly smaller than the pore sizes observed on RC-W films (Figure 14). The formation of smaller pore sizes can be explained based on the freedom of polymeric rearrangement during the precipitation process. The depolymerized cellulose chain in MC-DP solution is approximately 1/5<sup>th</sup> as long as the native cellulose in MC solution and hence, has relatively more freedom of movement and the ability to reorganize into denser larger non-swelling domains which are not accessible to intruding water. Comparatively, the larger molecular weight cellulose forms a more disorganized internal structure with fewer non-swelling domain due to the more limited freedom of movement of the bulky regenerated polymer. When the thermally annealed films are exposed to water, the larger molecular weight cellulose swells to a greater extent due to increased penetration of water into the loosely held domains, which leads to the formation of larger pores. Kleinebudde et al. have demonstrated this phenomenon in micro beads of varying degree of polymerization of cellulose which displayed a porous sponge like structure when powdered cellulose (degree of polymerization of approximately 1300) was used as starting material, while a gel like bead formed when they were manufactured from microcrystalline cellulose (degree of polymerization approximately 200) [88].

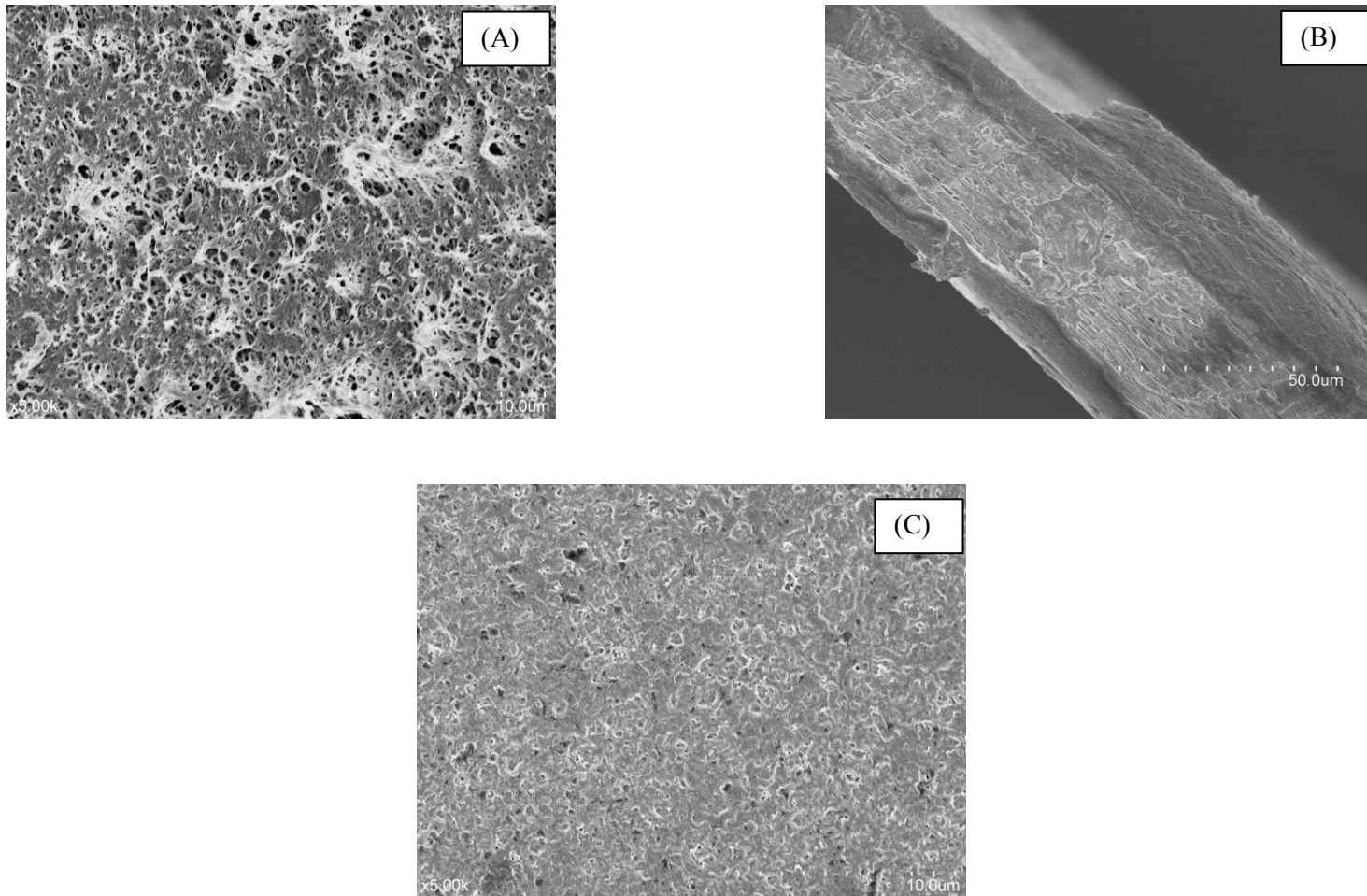


Figure 12: Scanning electron micrographs of RC-W films freeze dried immediately after precipitation in water: (A) Solvent/ non-solvent exchange interface, (B) cross section and, (C) test tube support facing interface.

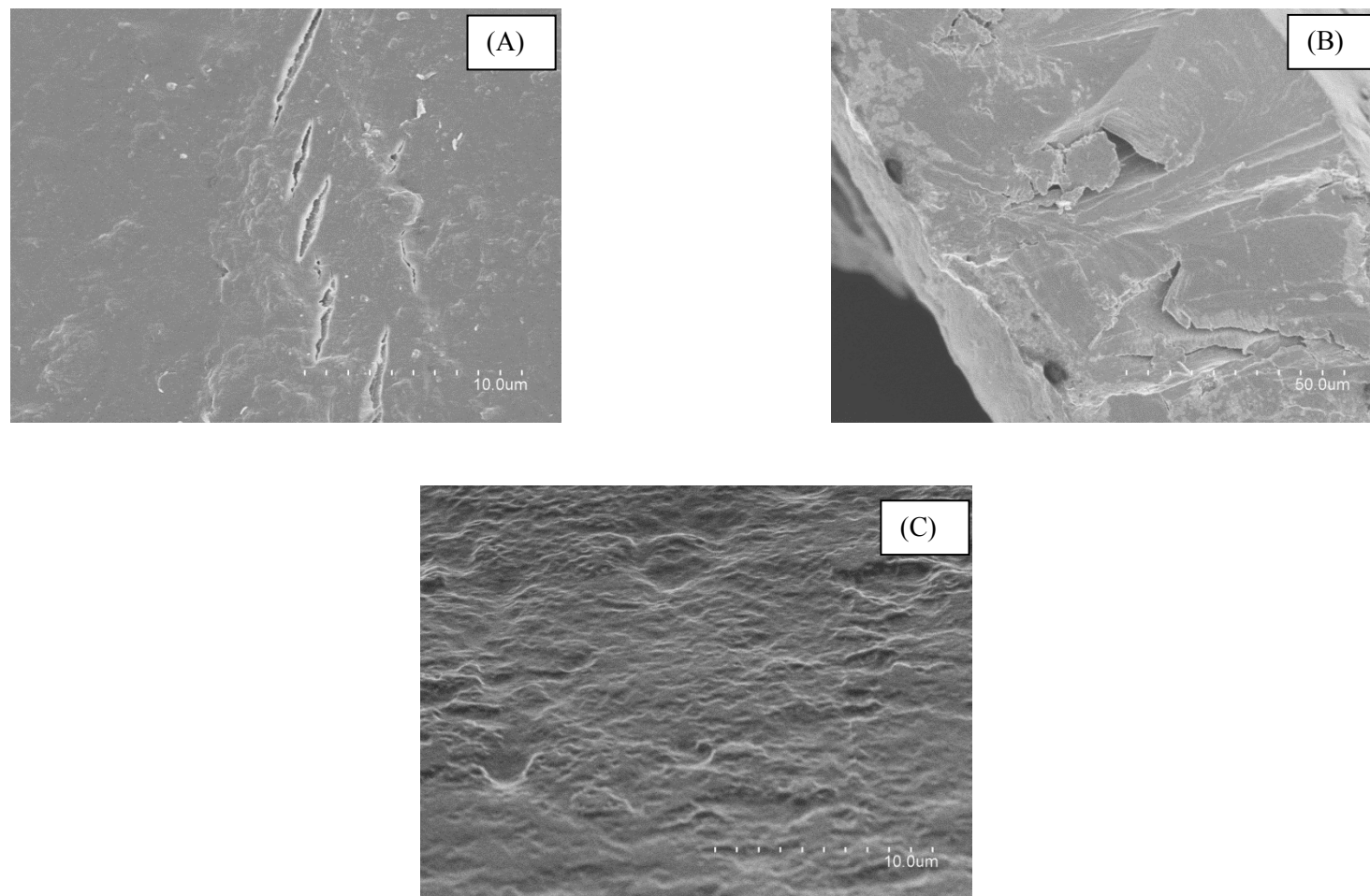


Figure 13: Scanning electron micrographs of RC-W films thermally annealed at 105°C for 24 hours: (A) Solvent/ non-solvent exchange interface, (B) cross section and, (C) test tube support facing interface.

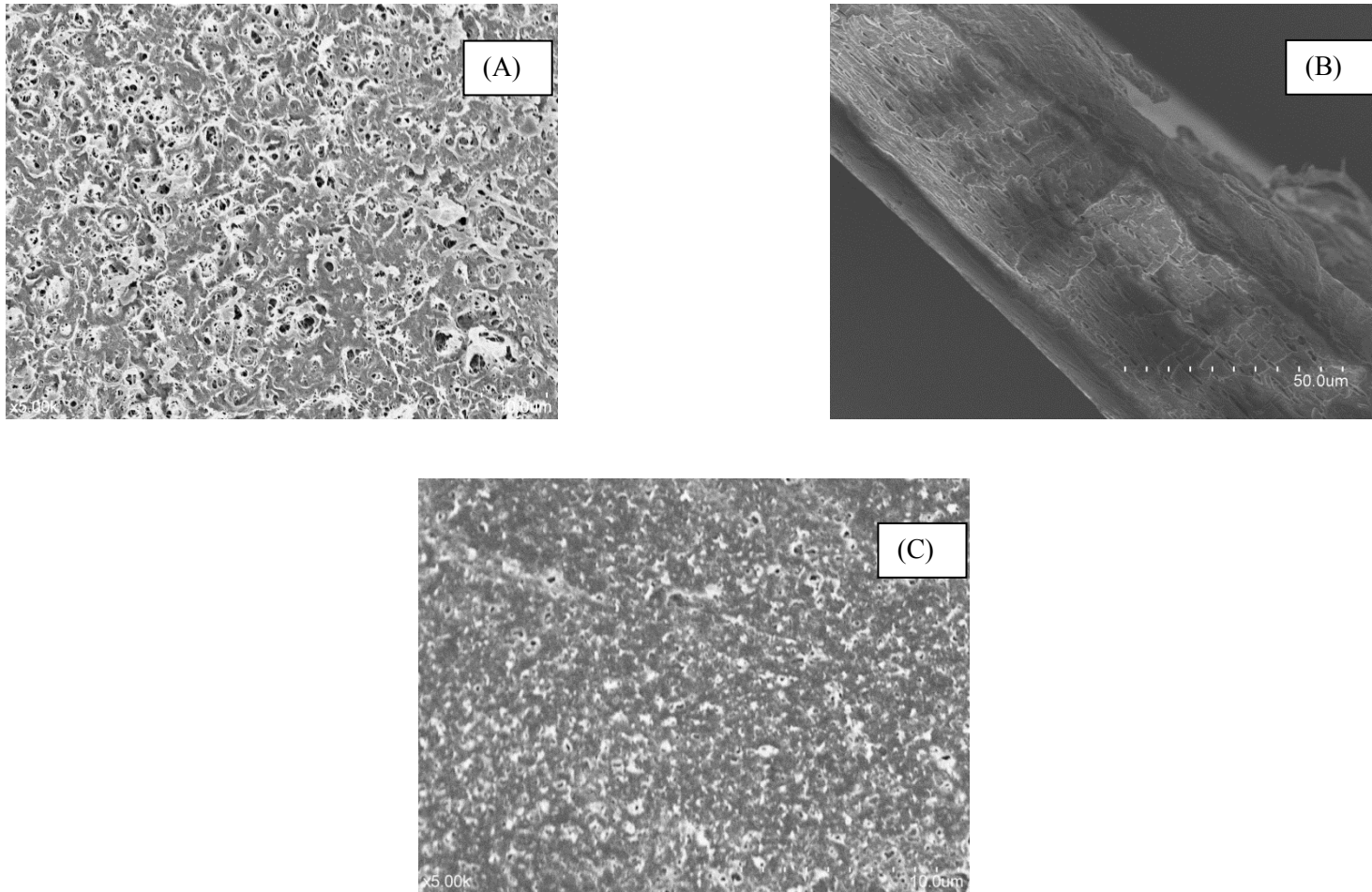


Figure 14: Scanning electron micrographs of RC-W films rehydrated after thermal curing: (A) Solvent/ non-solvent exchange interface, (B) cross section and, (C) test tube support facing interface.

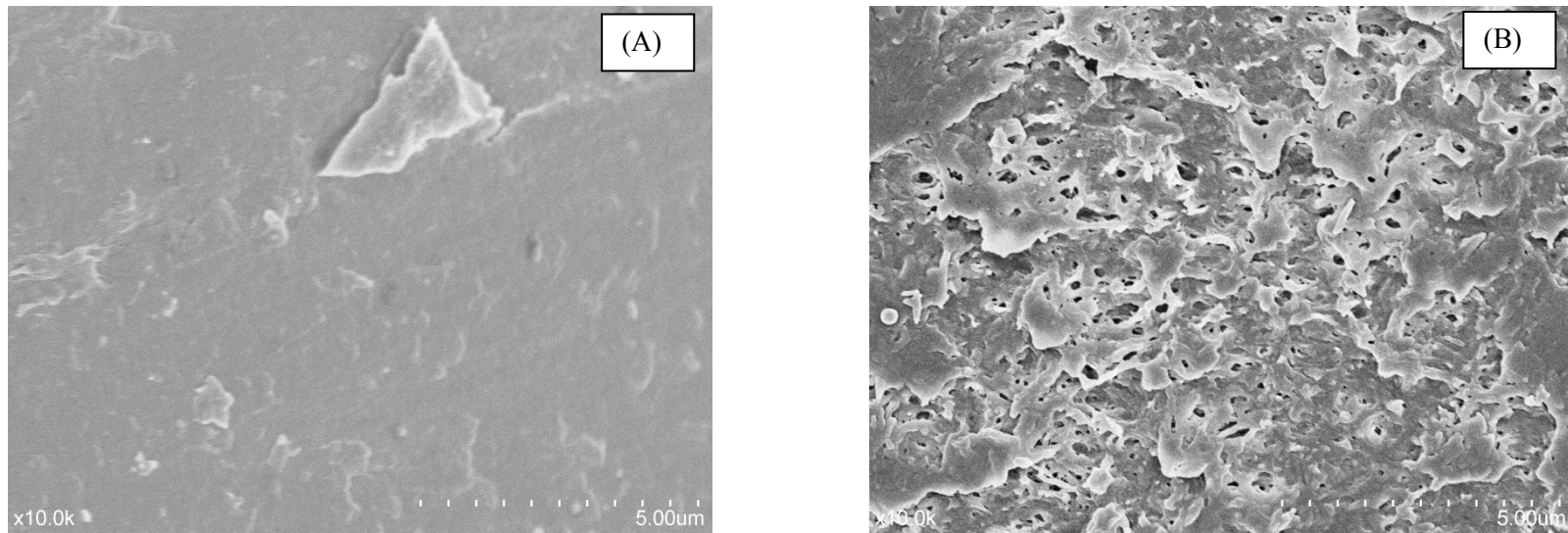


Figure 15: Scanning electron micrographs of (A) thermally annealed and (B) rehydrated RC-DP film solvent/ non-solvent exchange interface

### Hydration and its influence on solute flux through thermally annealed RC films

Morphological studies on RC-W and RC-DP films showed that they were nearly monolithic when the wet films were annealed after precipitation. However, a marked difference was observed in the porous structure upon hydration of these films. It is likely that the extent of hydration and formation of pores in these films would have significant impact on the transport of solutes through them. Although cellulose is an inert polymer, its hydration and swelling capability can be influenced by the presence of a non-aqueous solvents in the swelling medium, such as ethanol. Figure 16 shows the equilibrium solvent uptake by thermally annealed RC-W and RC-DP films exposed to ethanol-water binary mixtures at 37°C, after exposure for 24 hours. The solvent uptake by RC-W and RC-DP films decreased as the amount of ethanol in the binary solvent mixture was increased. Since cellulose swells in water by disruption of inter- and intra-polymer hydrogen bonds and formation of water-cellulose hydrogen bonds, the presence of ethanol possibly reduces the hydrogen bonding capability of the binary solvent and thereby reduces the solvent uptake by RC films [89]. The alteration in the swelling of RC films in the presence of ethanol can be presented by the following relation:

Equation 17

$$\varphi = \frac{V_f^*}{V_f^0}$$

where, ' $\varphi$ ' is the relative swelling, ' $V_f^*$ ' is the volume fraction of the ethanol-water binary mixtures in the film and ' $V_f^0$ ' is the volume fraction of pure water in absence of ethanol, in the swollen film. The relative swelling (analogous to porosity) describes the fraction of volume occupied by the solvent (s) in the swollen film. At  $\varphi = 1$ , the RC film swells to its maximum capability, while at  $\varphi = 0$ , no swelling is observed. Table 5 summarizes the solvent uptake (SU), volume fraction of solvent ( $V_f^*$ ) in swollen film and the relative

swelling ( $\varphi$ ) of RC-W and RC-DP films when exposed to water-ethanol binary mixtures at 37°C for 24 hrs.

Acetaminophen was utilized as model solute to analyze the changes in transport behavior under the controlled hydration conditions. Figure 17 shows the flux profiles of acetaminophen in varying ethanol-water binary mixtures through RC-W and RC-DP films, at 37°C. Since the solubility of acetaminophen increases from 21.41 mg/ml in pure water, to 241.62 mg/ml in pure ethanol, at 37°C, the flux values were normalized with their respective donor side concentrations (saturated donor side acetaminophen concentration equivalent to its solubility). Using the fluxes from saturated acetaminophen solutions and the saturation concentration, a flux alteration factor ' $\Omega$ ', defined as the ratio of the maximum flux in a given vehicle composition ( $J_*$ ) to that in pure water ( $J_o$ ), was calculated using the following relationship:

Equation 18

$$\Omega = \frac{\left\{ \frac{J}{C} \right\}_*}{\left\{ \frac{J}{C} \right\}_o} = \frac{J_*}{J_o}$$

where, "J" is the flux of acetaminophen with donor side concentration "C". Table 6 summarizes the flux, solubility and flux alteration factor of acetaminophen through RC-W and RC -DP films in ethanol-water binary mixtures.

Figure 18 compares the flux alteration factor ( $\Omega$ ) of RC-W and RC-DP films with the relative solvent volume fraction ( $\varphi$ ) of the hydrated film. As  $\varphi$  reduces, a decline in  $\Omega$  indicates that the reduction in hydration leads to a reduction in the transport of acetaminophen across the film. The solute flux rate was approximately two times higher through RC-W film (3.69 mg/cm<sup>2</sup>-h) than it was through RC-DP film (1.35 mg/cm<sup>2</sup>-h), in purified water as the medium. These results imply that the formation of pores, due to



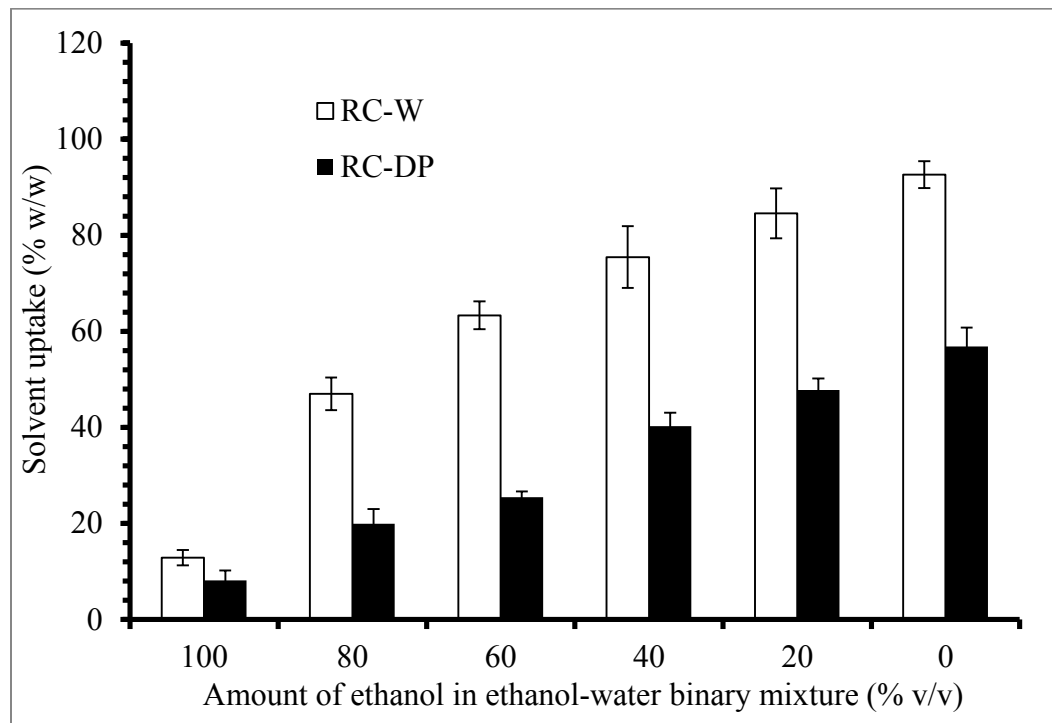


Figure 16: Equilibrium ethanol-water binary solvent uptake by RC-W and RC-DP films from ethanol-water mixtures with varying amounts of ethanol (% v/v), at 37°C, determined gravimetrically after 24 hours.

Table 5: Summary of solvent uptake (SU), volume fraction of solvent ( $V_f^*$ ), solvent density and relative solvent volume ( $\varphi$ ) in swollen RC-W and RC-DP films at 37°C, calculated using solvent uptake data

| Conc. of ethanol | Solvent density at 37°C ( $\rho_s$ ) | RC-W film           |                                                  |                                                             | RC-DP film          |                                                  |                                                             |
|------------------|--------------------------------------|---------------------|--------------------------------------------------|-------------------------------------------------------------|---------------------|--------------------------------------------------|-------------------------------------------------------------|
|                  |                                      | Solvent uptake (SU) | Solvent volume fraction ( $V_f^*$ ) <sup>a</sup> | Relative solvent volume fraction ( $\varphi$ ) <sup>b</sup> | Solvent uptake (SU) | Solvent volume fraction ( $V_f^*$ ) <sup>a</sup> | Relative solvent volume fraction ( $\varphi$ ) <sup>b</sup> |
| (%)              | (g/cm <sup>3</sup> )                 | (% w/w) n=3         | (%)                                              |                                                             | (% w/w) n=3         | (%)                                              |                                                             |
| 100              | 0.77                                 | 6.95 ± 0.66         | 11.14                                            | 0.11                                                        | 4.91 ± 2.00         | 9.20                                             | 0.16                                                        |
| 80               | 0.84                                 | 18.43 ± 4.21        | 28.32                                            | 0.29                                                        | 11.86 ± 3.26        | 19.50                                            | 0.34                                                        |
| 60               | 0.89                                 | 32.85 ± 1.97        | 44.41                                            | 0.46                                                        | 16.40 ± 2.62        | 24.98                                            | 0.44                                                        |
| 40               | 0.94                                 | 52.16 ± 3.21        | 63.90                                            | 0.67                                                        | 28.81 ± 7.15        | 39.64                                            | 0.70                                                        |
| 20               | 0.96                                 | 72.13 ± 6.52        | 80.28                                            | 0.85                                                        | 36.19 ± 3.63        | 47.14                                            | 0.84                                                        |
| 0                | 0.99                                 | 92.17 ± 3.64        | 94.75                                            | 1 <sup>c</sup>                                              | 45.56 ± 2.75        | 56.21                                            | 1 <sup>c</sup>                                              |

$$^a V_f = \frac{\frac{SU}{100} \rho_c}{\rho_s \left\{ 1 - \frac{SU}{100} \right\} + \frac{SU}{100} \rho_c}, \rho_c = 1.5 \text{ g/cm}^3$$

$$^b \varphi = \frac{V_f^*}{V_f^0}$$

<sup>c</sup>  $V_f^* = V_f^0$ , where  $V_f^0$  is solvent volume fraction in swollen film when exposed to pure water.

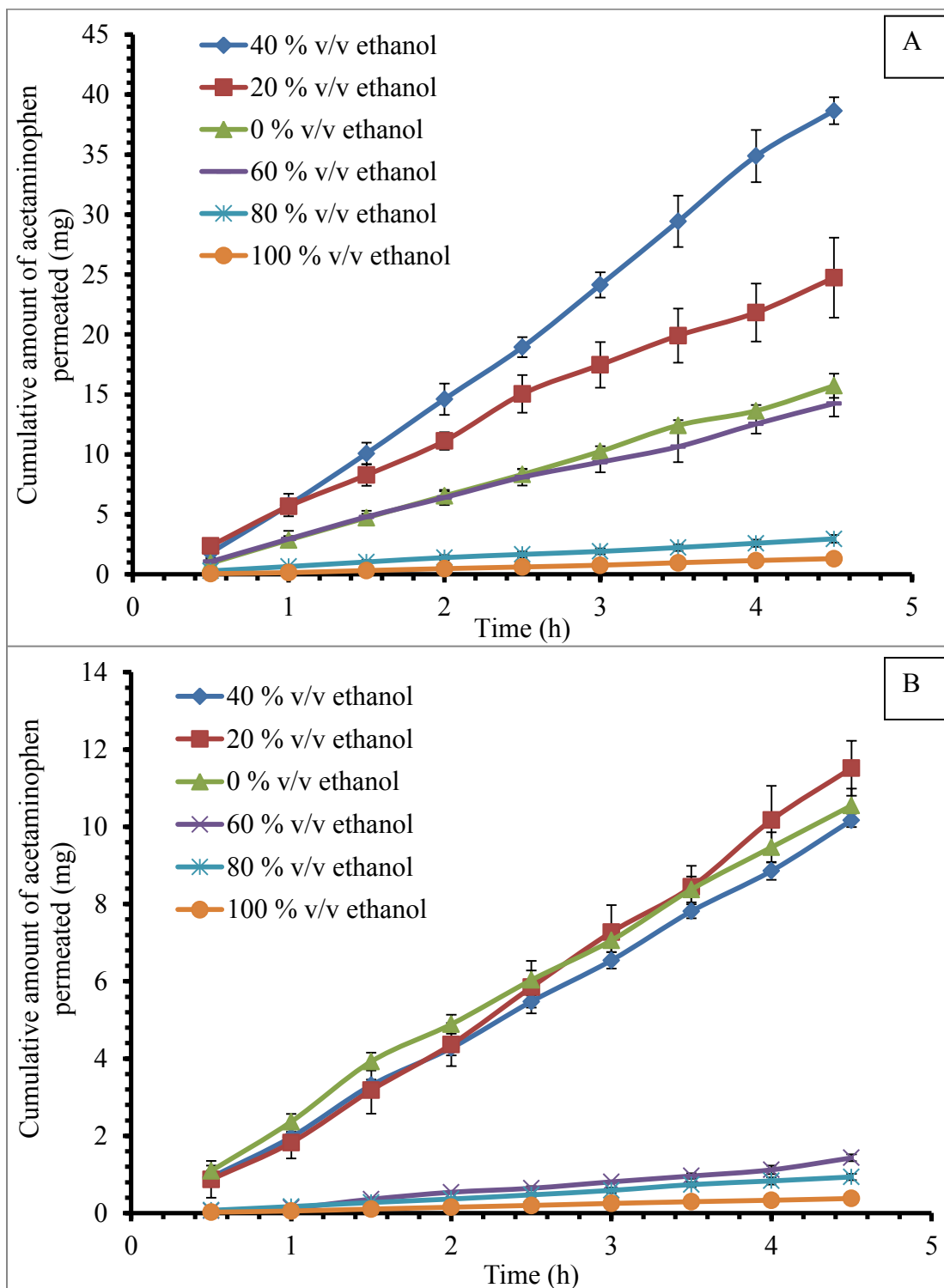


Figure 17: Flux profiles of acetaminophen through (A) RC-W and (B) RC-DP films, in Side-by-Side® diffusion cells containing varying amounts of ethanol in ethanol-water binary mixtures with saturated acetaminophen on the donor side, at 37°C.

Table 6: Summary of mass transfer rate, flux, solubility normalized flux and flux alteration factor of acetaminophen through RC-W and RC-DP films using Side-by-Side<sup>®</sup> diffusion cells in ethanol-water binary solvent systems with varying ethanol concentrations, at 37°C

| Ethanol Concentration in solvent medium | Saturated concentration of acetaminophen in the vehicle on the donor side (C) | RC-W                       |                         |                                  |                            | RC-DP                      |                         |                                  |                            |
|-----------------------------------------|-------------------------------------------------------------------------------|----------------------------|-------------------------|----------------------------------|----------------------------|----------------------------|-------------------------|----------------------------------|----------------------------|
|                                         |                                                                               | Mass transfer rate (dM/dt) | Flux (J) <sup>a</sup>   | Solubility normalized flux (J/C) | Flux alteration factor (Ω) | Mass transfer rate (dM/dt) | Flux (J) <sup>a</sup>   | Solubility normalized flux (J/C) | Flux alteration factor (Ω) |
| (v/v, %)                                | (mg/cm <sup>3</sup> )                                                         | (mg/h)                     | (mg/cm <sup>2</sup> -h) | (cm/h, x 10 <sup>-3</sup> )      |                            | (mg/h)                     | (mg/cm <sup>2</sup> -h) | (cm/h, x 10 <sup>-3</sup> )      |                            |
| 0                                       | 21.41 ± 0.96                                                                  | 3.69                       | 2.17                    | 99.94                            | 1                          | 2.33                       | 1.35                    | 62.22                            | 1                          |
| 20                                      | 54.94 ± 1.67                                                                  | 5.58                       | 3.28                    | 59.77                            | 0.59                       | 2.71                       | 1.59                    | 28.94                            | 0.46                       |
| 40                                      | 132.79 ± 3.68                                                                 | 9.41                       | 5.55                    | 41.76                            | 0.41                       | 2.29                       | 0.80                    | 6.02                             | 0.10                       |
| 60                                      | 180.13 ± 2.11                                                                 | 3.20                       | 1.88                    | 10.46                            | 0.10                       | 0.31                       | 0.18                    | 0.99                             | 0.02                       |
| 80                                      | 219.33 ± 3.87                                                                 | 0.65                       | 0.38                    | 1.73                             | 0.02                       | 0.27                       | 0.16                    | 0.72                             | 0.01                       |
| 100                                     | 241.62 ± 7.79                                                                 | 0.31                       | 0.18                    | 0.75                             | 0.01                       | 0.26                       | 0.15                    | 0.63                             | 0.01                       |

<sup>a</sup>  $J = \frac{dM}{dt} / A$ , where A = 1.7 cm<sup>2</sup>

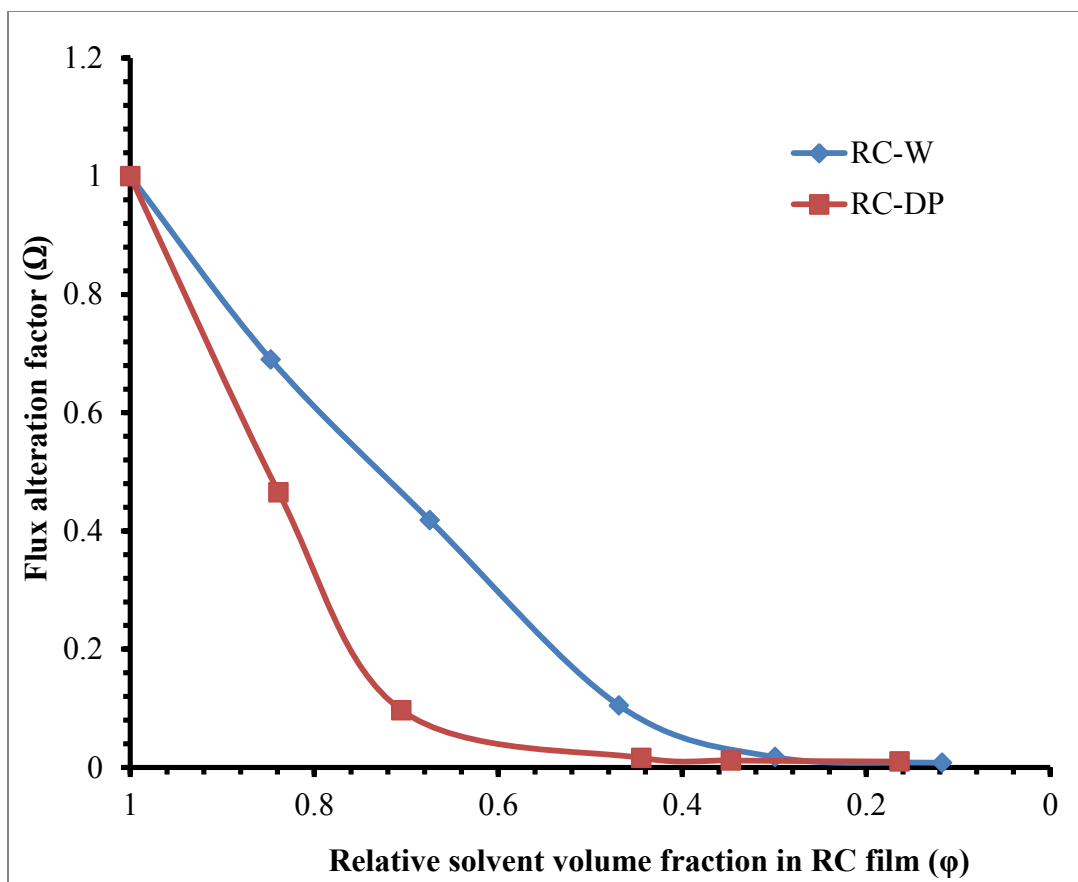


Figure 18: Comparison of flux alteration factor ( $\Omega$ ) and relative solvent volume ( $\phi$ ) in swollen RC-W and RC-DP films, using acetaminophen as model solute.

hydration, leads to transport of acetaminophen across these films. The flux through RC-W films is higher owing to the larger and/or greater number of pores formed in comparison to RC-DP film, as observed in the SEM images. In 100 % ethanol as solvent medium, the flux rate acetaminophen through RC-W and RC-DP films was nearly equal ( $0.18 \text{ mg/cm}^2\text{-h}$  and  $0.15 \text{ mg/cm}^2\text{-h}$ , respectively). Since both films are monolithic in the dry/ non-hydrated state, after thermal curing, the influence of polymer chain length has no impact on the flux of acetaminophen as the results suggests that it may be traversing the films by partition mechanism. In both films, an inflection point is observed where reduction in  $\phi$  had very little influence on  $\Omega$ . For RC-W film, this inflection point was at  $\phi = 0.29$ , while for RC-DP film, the inflection point was  $\phi = 0.70$ . These values indicate that a minimum of 29% hydration of RC-W and 70% hydration of RC-DP film is required in order for the pore-mediated transport of solute to occur. A higher degree of hydration required for RC-DP film indicates fewer porous routes connecting the two surfaces of the film as well as smaller sizes of these pores.

#### Transient effect of RC film hydration

The transient effect of ethanol on cellulose hydration was analyzed on thermally annealed RC-W films by observing acetaminophen flux in pure water, followed by flux in pure ethanol and finally again in pure water. The donor side concentration in both solvents was maintained at  $15 \text{ mg/cm}^3$ . The films in the diffusion cells were never removed or pretreated with diffusion medium during the transition points and the time to exchange the solutions in the diffusion cells was never more than 5 minutes. Figure 19 shows the cumulative acetaminophen transported into the receiver cell as the solvent medium was changed from 100% water to 100% ethanol, and followed by 100 % water

again, at 37°C over a period of 13 hours. The transition points for change in solvent medium are marked with dashed lines. The slopes of the cumulative amount of acetaminophen permeated vs time indicates the mass transfer rates of acetaminophen through the RC-W film. During the first phase, the mass transfer rate was 1.31 mg/h in purified water, followed by 0.10 mg/h in 100% ethanol during the second phase, and finally 1.29 mg/h in purified water in the third phase. The presence of ethanol after the first transition caused a drastic change in the mass transfer rate across the film. Ethanol being a strong de-hydrant caused rapid removal of water from the film and since the hydration and swelling of the film is essential to formation of transport pathways, its absence leads to coalescence of these channels and hence leads to loss of accessible pathways for solute transport. When the ethanol content was replaced again with water after 10 hours, the film regained its permeability characteristic and the mass transfer rate was equivalent to the original mass transfer rate. Hence the reduction of acetaminophen flux through RC film in presence of ethanol can be considered as transient and can be easily be reversed in the presence of water.

#### Blending of MC and MC-DP solutions

The robustness of any film coating technology can be attributed to the ability to modify the permeability characteristics to suit desired drug release characteristics. The ability to modify regenerated cellulose film properties was investigated by blending native cotton linters and depolymerized cotton linter solutions in the following ratios 4:1, 3:2, 2:3 and 1:4, and the resulting films prepared by the precipitation process in water and followed by thermal curing. These films will be herein referred to as RC-4/1, RC-3/2, RC-2/3 and RC-1/4, respectively. Figure 20 shows the SEM micrographs of the RC

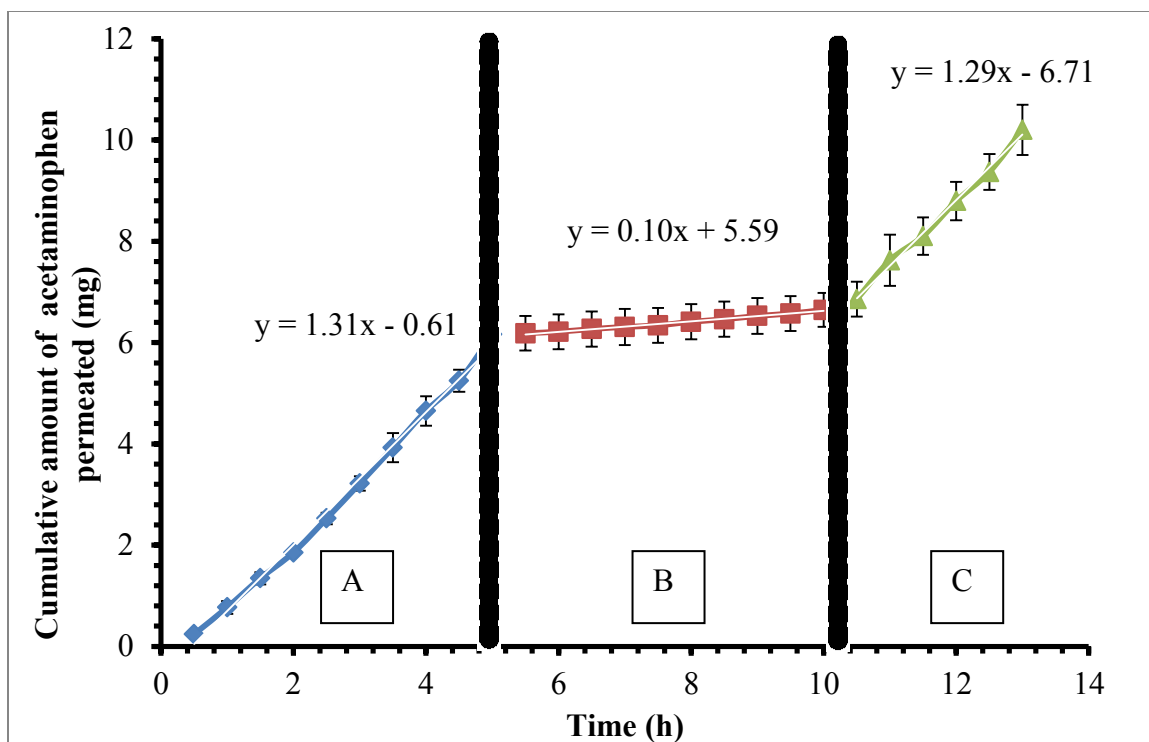


Figure 19: Analysis of transient effect of ethanol acetaminophen flux through RC-W film in (A) 100 % water, (B) 100% ethanol, and (C) 100% water as solvent medium. The flux was measured through same set of films and the transition points for solvent exchange are marked by dashed lines. The donor cell concentration was maintained at  $15 \text{ mg/cm}^3$  by periodically replacing the medium with fresh solution. Transport studies were conducted at  $37^\circ\text{C}$ .



blended film solvent/non-solvent exchange interface. Visually, the pore sizes appeared smaller as the fraction of depolymerized cellulose increased in the film. Figure 21 shows the water uptake profiles of RC-W, RC-DP, and RC blended films. These films absorb water quickly and the maximum water uptake reduces as the fraction of depolymerized cellulose increased in the films. Table 7 summarizes the dry and hydrated state porosities as well as the maximum water uptake capacity and average pore sizes observed via SEMs of RC-W, RC-DP and RC blend films. The dry state porosities were similar for all films while the hydrated state porosity decreased as the fraction of depolymerized cellulose increased in the films. These results indicate that as the fraction of depolymerized cellulose increases in the films, the swelling of RC films reduces as well as surface pore sizes.

The tortuosity of the RC-W, RC-DP and RC blended films were compared in order to assess changes in film internal structure as the fraction of depolymerized cellulose is increased in the RC films. Potassium chloride was used as a model permeant due to its lack of partitioning into the cellulose polymer phase [90]. Figure 22 shows the thickness normalized flux profiles of KCl through RC-W, RC-4/1, RC-3/2, RC-2/3, RC-1/4 and RC-DP in purified water, at 37°C. The slopes of the steady state portion of the flux profiles were utilized to calculate the permeability coefficient using the following relationship [68]:

Equation 19

$$P = \frac{\frac{dM}{dt} h}{A \Delta C}$$

where, 'dM/dt\*h' is the steady-state solute transfer rate obtained from the slope of the cumulative amount permeated vs. time profile, 'h' is the thickness of the swollen RC

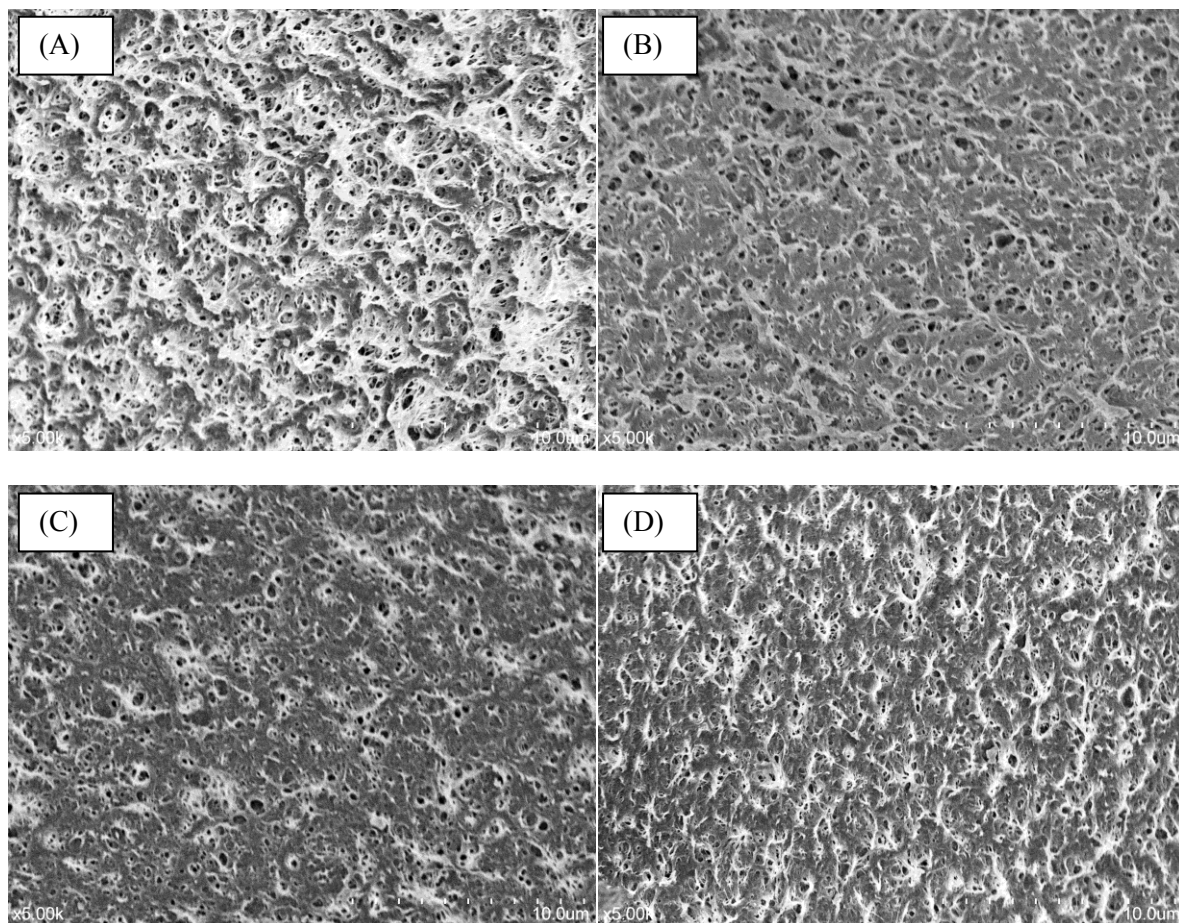


Figure 20: Scanning electron micrographs of rehydrated solvent/ non-solvent exchange interfaces of (A) RC-4/1, (B) RC-3/2, (C) RC-2/3 and (D) RC-1/4 films

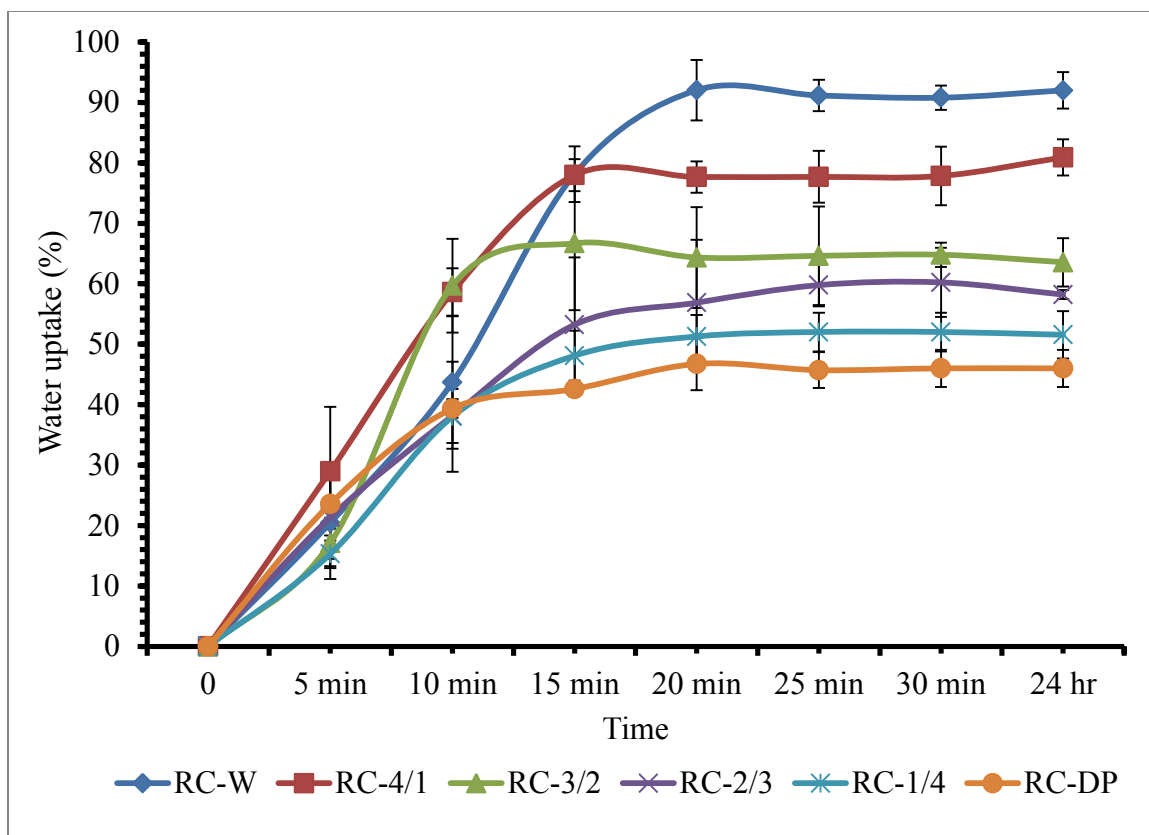


Figure 21: Water uptake by RC-W, RC-DP and blend films. Water uptake was analyzed gravimetrically in 37°C purified water on thermally annealed RC films that were precipitated in water.

Table 7: True density, porosity, degree of swelling and average pore size of RC-W, RC-4/1, RC-3/2, RC-2/3, RC-1/4 and RC-DP films

| RC film type   | True density <sup>a</sup> | Dry state porosity <sup>b</sup> | Hydrated state porosity <sup>c</sup> | Maximum water uptake capacity | Average pore diameter <sup>d</sup> |
|----------------|---------------------------|---------------------------------|--------------------------------------|-------------------------------|------------------------------------|
|                | (g/cm <sup>3</sup> ), n=6 | (%), n=6                        |                                      | (%), n=3                      | ( $\mu$ m) n= 450 - 550            |
| <b>RC-W</b>    | 1.53 $\pm$ 0.04           | 0.03 $\pm$ 0.01                 | 0.69 $\pm$ 0.02                      | 91.74 $\pm$ 2.99              | 2.87 $\pm$ 0.84                    |
| <b>RC-4/1</b>  | 1.51 $\pm$ 0.06           | 0.05 $\pm$ 0.04                 | 0.63 $\pm$ 0.02                      | 80.92 $\pm$ 7.28              | 2.64 $\pm$ 0.73                    |
| <b>RC-3/2</b>  | 1.52 $\pm$ 0.05           | 0.04 $\pm$ 0.03                 | 0.58 $\pm$ 0.02                      | 63.56 $\pm$ 4.64              | 2.33 $\pm$ 0.75                    |
| <b>RC-2/3</b>  | 1.52 $\pm$ 0.07           | 0.04 $\pm$ 0.04                 | 0.55 $\pm$ 0.02                      | 58.21 $\pm$ 0.74              | 2.10 $\pm$ 0.63                    |
| <b>RC-1/4</b>  | 1.49 $\pm$ 0.03           | 0.05 $\pm$ 0.04                 | 0.49 $\pm$ 0.02                      | 51.55 $\pm$ 3.92              | 1.91 $\pm$ 0.42                    |
| <b>RC/DP-4</b> | 1.51 $\pm$ 0.02           | 0.03 $\pm$ 0.03                 | 0.43 $\pm$ 0.03                      | 46.01 $\pm$ 3.08              | 1.32 $\pm$ 0.41                    |

<sup>a</sup> Determined from freeze dried films after exposure of thermally annealed films to water for 24 hrs

<sup>b</sup> Dry state porosity measured on RC film discs thermally annealed after precipitation in excess water.

<sup>c</sup> Hydrated state porosity measured after exposure to water (at 37 °C) for 24hs, on water swollen RC film discs that were annealed thermally after precipitation in water

<sup>d</sup> Pores were measured on SEM images from 3 different samples of each film type

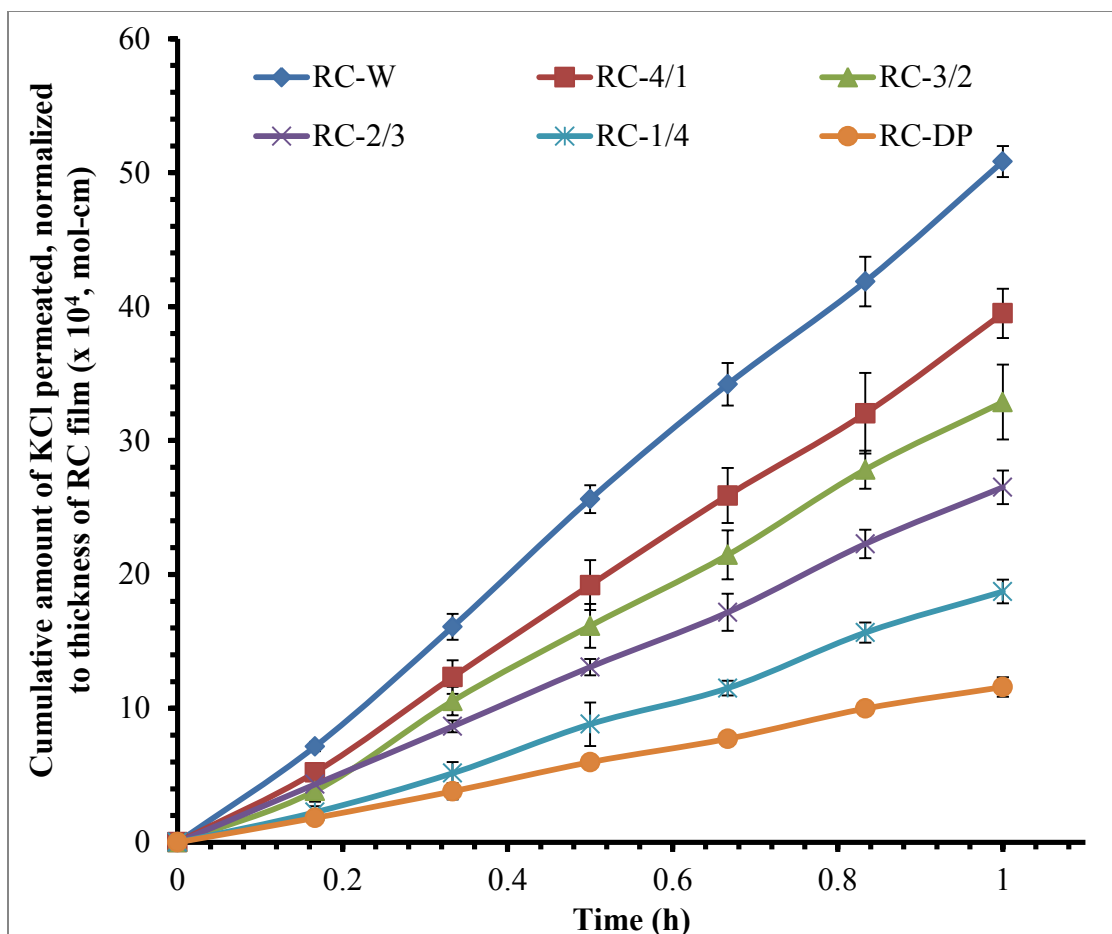


Figure 22: Thickness normalized flux profiles of KCl through RC-W, RC-DP and blended films in purified water at 37°C. Films were placed in purified water for 24 h prior to transport studies.

film, 'A' is the area of the film exposed in the diffusion cell and  $\Delta C$  is the concentration gradient across the film. Since sink conditions were maintained in the receiver cell,  $\Delta C$  is equivalent to the donor cell concentration. The permeability coefficient is the sum of the diffusion occurring through the polymer phase and through the porous aqueous channels. When solute partitioning into the polymer phase is negligible, the permeability coefficient is related to the aqueous diffusion coefficient of the solute by the following relationship [91] [69]:

Equation 20 
$$P = \frac{\varepsilon}{\tau} D_w$$

where ' $\varepsilon$ ' is the porosity of the film, ' $\tau$ ' is the tortuosity factor, and ' $D_w$ ' is the aqueous diffusion coefficient of the solute in the solvent. The ratio of ' $\varepsilon/\tau$ ', which is equivalent to ' $P/D_w$ ' in the absence of partitioning, describes the hindrance behavior of a film compared to solute diffusion in the pure solvent [91]. This ratio can be utilized in elucidating the influence of various fabrication parameters that can alter the final performance of the porous film [69]. Moreover, knowing the values of ' $D_w$ ', ' $\varepsilon$ ' and calculating ' $P$ ' from the flux data, the ' $\tau$ ' value can be estimated, which describes the effective path length of the channels. Table 8 lists the KCl flux parameters, calculated permeability coefficient, hindrance factor, porosity and estimated tortuosity factor of RC blended films using  $D_w = 2.28 \times 10^{-5} \text{ cm}^2/\text{sec}$  for KCl at 37°C [92]. Figure 23 compares the tortuosity factor vs. the fraction of depolymerized cellulose in RC films. The tortuosity factor of RC-W was 1.92 while that of RC-DP was nearly three times higher, at 5.51. The significant increase in tortuosity factor of the RC-DP films indicates that the pathways for solute transport are longer than those in RC-W films. Scanning electron micrographs of RC-W and RC-DP films have shown that the shorter chain length

Table 8: Flux parameters and calculated permeability coefficient as well as hindrance factors and tortuosity estimated from KCl flux through RC-W, RC-4/1, RC-3/2, RC-2/3, RC-1/4 and RC-DP films in Side-by-Side<sup>®</sup> diffusion cells, using purified water as solvent at 37°C

| Film   | Thickness<br>normalized mass<br>transfer rate<br>$(\frac{dM}{dt} h)$ | Permeability<br>coefficient<br>(P)             | Hindrance<br>factor<br>$(\frac{P}{D_w})^a$ | Porosity<br>( $\epsilon$ ) <sup>b</sup> | Tortuosity<br>( $\tau$ ) <sup>c</sup> |
|--------|----------------------------------------------------------------------|------------------------------------------------|--------------------------------------------|-----------------------------------------|---------------------------------------|
|        | (x 10 <sup>-4</sup> , mol-<br>cm/h)                                  | (x 10 <sup>-6</sup> ,<br>cm <sup>2</sup> /sec) |                                            |                                         |                                       |
| RC-W   | 192.85                                                               | 7.93                                           | 0.34                                       | 0.69                                    | 1.92                                  |
| RC-4/1 | 148.95                                                               | 6.25                                           | 0.27                                       | 0.62                                    | 2.26                                  |
| RC-3/2 | 125.88                                                               | 5.43                                           | 0.24                                       | 0.59                                    | 2.48                                  |
| RC-2/3 | 99.07                                                                | 4.23                                           | 0.19                                       | 0.55                                    | 2.91                                  |
| RC-1/4 | 71.41                                                                | 3.11                                           | 0.14                                       | 0.49                                    | 3.59                                  |
| RC-DP  | 43.98                                                                | 1.82                                           | 0.08                                       | 0.44                                    | 5.51                                  |

<sup>a</sup>  $D_w = 2.28 \times 10^{-5} \text{ cm}^2/\text{sec}$  for 0.1 M KCl at 37°C [92]

<sup>b</sup> hydrated state porosity

$$^c \tau = \frac{D_w}{P} \epsilon,$$

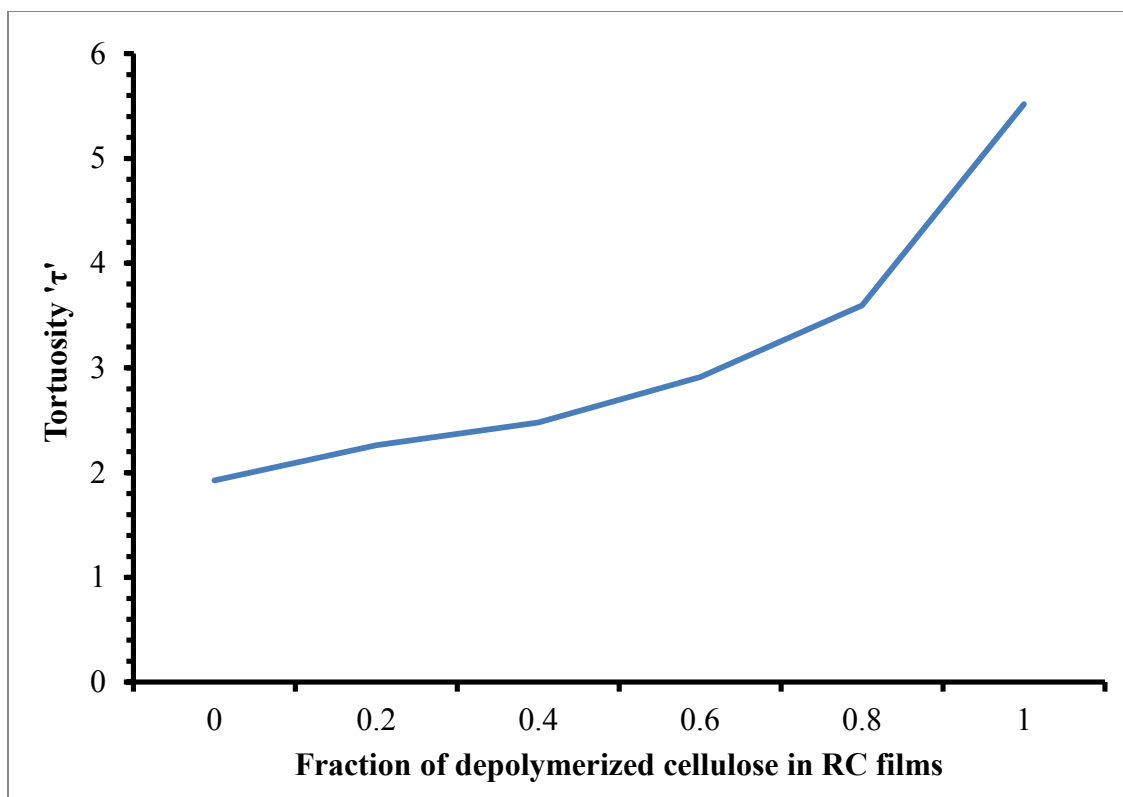


Figure 23: Comparison of tortuosity observed by KCl through RC films with varying fractions of depolymerized cellulose in RC films



cellulose causes reduction in void volume and hence the traversing solute has fewer immediate pathways to travel across the film surfaces. In blended films, the tortuosity factor increases from 2.26 to 3.59 as the fraction of depolymerized cellulose in the film increases from 20% to 80% w/w. These results indicate that longer chain length celluloses causes branching of transport channels and hence shorter path lengths for solute transport.

Cellulose polymers contain significant hydrophobic regions in the form of  $-CH_2-$  groups. Blending of depolymerized cellulose with native celluloses caused significant reduction in porosity as well as water uptake by these films. In order to determine whether these films transformed the mechanism of solute transport from porous to partition route, four alkyl *p*-aminobenzoate esters of increasing *n*-alkyl chain length were evaluated for their transport behavior through the blended films. Figure 24 shows the thickness normalized flux profiles of methyl-, ethyl-, propyl- and butyl-*p*-aminobenzoates through RC blended films in purified water at 37°C. Table 9 lists the flux parameters of the alkyl-*p*-aminobenzoates as well as calculated permeability coefficients and hindrance factors. The hindrance factors for the alkyl-*p*-aminobenzoate esters were estimated using the aqueous diffusion coefficients obtained from literature [93]. Figure 25 compares the hindrance factors of potassium chloride and the four alkyl-*p*-aminobenzoates. These results indicate that ionic as well as hydrophobic solutes travel through the same aqueous channels that are formed upon hydration of the thermally annealed RC films. Irrespective of the content of depolymerized cellulose in these RC films, they are not suited as partitioning type membranes for controlled release but instead rely primarily on the aqueous diffusion through the pores.

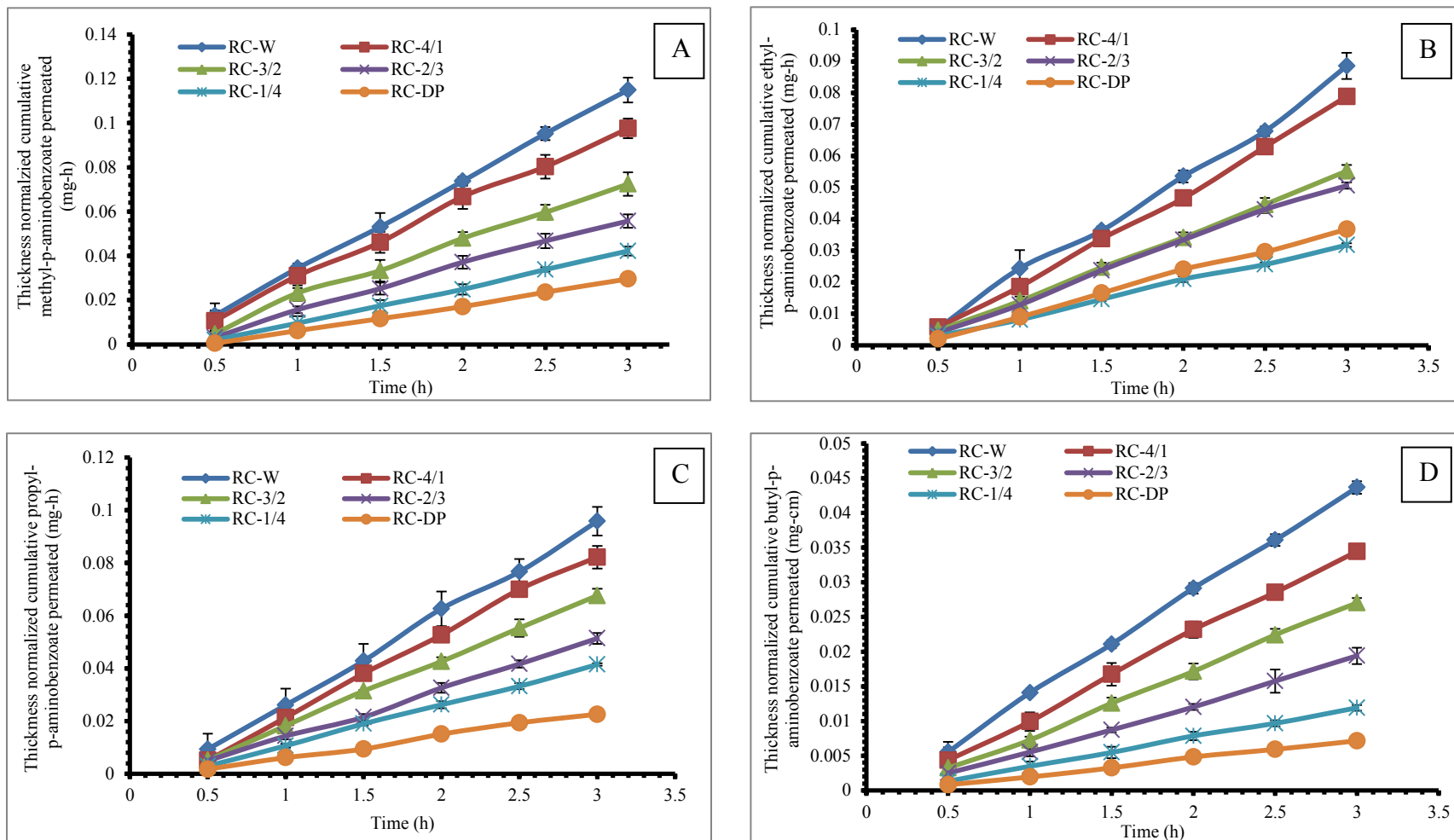


Figure 24: Thickness normalized flux profiles of (A) methyl-, (B) ethyl-, (C) propyl-, and (D) butyl-p-aminobenzoate in purified water at 37°C through RC-W, RC-4/1, RC-3/2, RC-2/3, RC-1/4 and RC-DP films, using Side-by-Side® diffusion cells.

Table 9: Flux, permeability and hindrance factors of methyl-, ethyl-, propyl- and butyl-p-aminobenzoates through RC-W, RC-4/1, RC-3/2, RC-2/3, RC-1/4 and RC-DP films in water at 37°C, using Side-by-Side® diffusion cells.

|                                                                                     | <b>Methyl-p-aminobenzoate</b> |                                             |                     | <b>Ethyl-p-aminobenzoate</b> |                                             |                     | <b>Propyl-p-aminobenzoate</b> |                                             |                     | <b>Butyl-p-aminobenzoate</b> |                                             |                     |
|-------------------------------------------------------------------------------------|-------------------------------|---------------------------------------------|---------------------|------------------------------|---------------------------------------------|---------------------|-------------------------------|---------------------------------------------|---------------------|------------------------------|---------------------------------------------|---------------------|
| Donor cell concentration (n=3, mg/cm <sup>3</sup> ) <sup>a</sup>                    | 2.83 ± 0.08                   |                                             |                     | 1.64 ± 0.10                  |                                             |                     | 0.76 ± 0.09                   |                                             |                     | 0.25 ± 0.06                  |                                             |                     |
| Aqueous diffusion coefficient (D <sub>w</sub> ) (cm <sup>2</sup> /sec) <sup>b</sup> | 7.06 x 10 <sup>-6</sup>       |                                             |                     | 6.40 x 10 <sup>-6</sup>      |                                             |                     | 6.20 x 10 <sup>-6</sup>       |                                             |                     | 5.70 x 10 <sup>-6</sup>      |                                             |                     |
| <b>Film type</b>                                                                    | $(\frac{dm}{dt}h)^c$          | (P) <sup>d</sup>                            | $(\frac{P}{D_w})^e$ | $(\frac{dm}{dt}h)^c$         | (P) <sup>d</sup>                            | $(\frac{P}{D_w})^e$ | $(\frac{dm}{dt}h)^c$          | (P) <sup>d</sup>                            | $(\frac{P}{D_w})^e$ | $(\frac{dm}{dt}h)^c$         | (P) <sup>d</sup>                            | $(\frac{P}{D_w})^e$ |
|                                                                                     | (mg/h)                        | (x 10 <sup>-6</sup> , cm <sup>2</sup> /sec) |                     | (mg/h)                       | (x 10 <sup>-6</sup> , cm <sup>2</sup> /sec) |                     | (mg/h)                        | (x 10 <sup>-6</sup> , cm <sup>2</sup> /sec) |                     | (mg/h)                       | (x 10 <sup>-6</sup> , cm <sup>2</sup> /sec) |                     |
| <b>RC-W</b>                                                                         | 1.17                          | 2.35                                        | 0.33                | 0.65                         | 2.31                                        | 0.36                | 0.26                          | 2.06                                        | 0.35                | 0.091                        | 2.11                                        | 0.37                |
| <b>RC-4/1</b>                                                                       | 1.47                          | 2.09                                        | 0.29                | 0.99                         | 1.78                                        | 0.28                | 0.40                          | 1.49                                        | 0.25                | 0.14                         | 1.69                                        | 0.30                |
| <b>RC-3/2</b>                                                                       | 2.20                          | 1.53                                        | 0.21                | 1.21                         | 1.45                                        | 0.23                | 0.43                          | 1.18                                        | 0.18                | 0.14                         | 1.34                                        | 0.23                |
| <b>RC-2/3</b>                                                                       | 1.75                          | 1.21                                        | 0.17                | 1.14                         | 1.37                                        | 0.21                | 0.41                          | 0.88                                        | 0.15                | 0.16                         | 0.92                                        | 0.16                |
| <b>RC-1/4</b>                                                                       | 2.29                          | 0.93                                        | 0.14                | 1.29                         | 0.70                                        | 0.11                | 0.57                          | 0.73                                        | 0.11                | 0.18                         | 0.58                                        | 0.10                |
| <b>RC-DP</b>                                                                        | 2.32                          | 0.67                                        | 0.09                | 1.27                         | 0.56                                        | 0.09                | 0.34                          | 0.32                                        | 0.05                | 0.17                         | 0.54                                        | 0.09                |

<sup>a</sup> Determined from the solubility of the solute in purified water at 37 °C

<sup>b</sup> Taken from reference [93]

<sup>c</sup> Thickness normalized mass transfer rate

<sup>d</sup> Permeability coefficient

<sup>e</sup> Hindrance factor

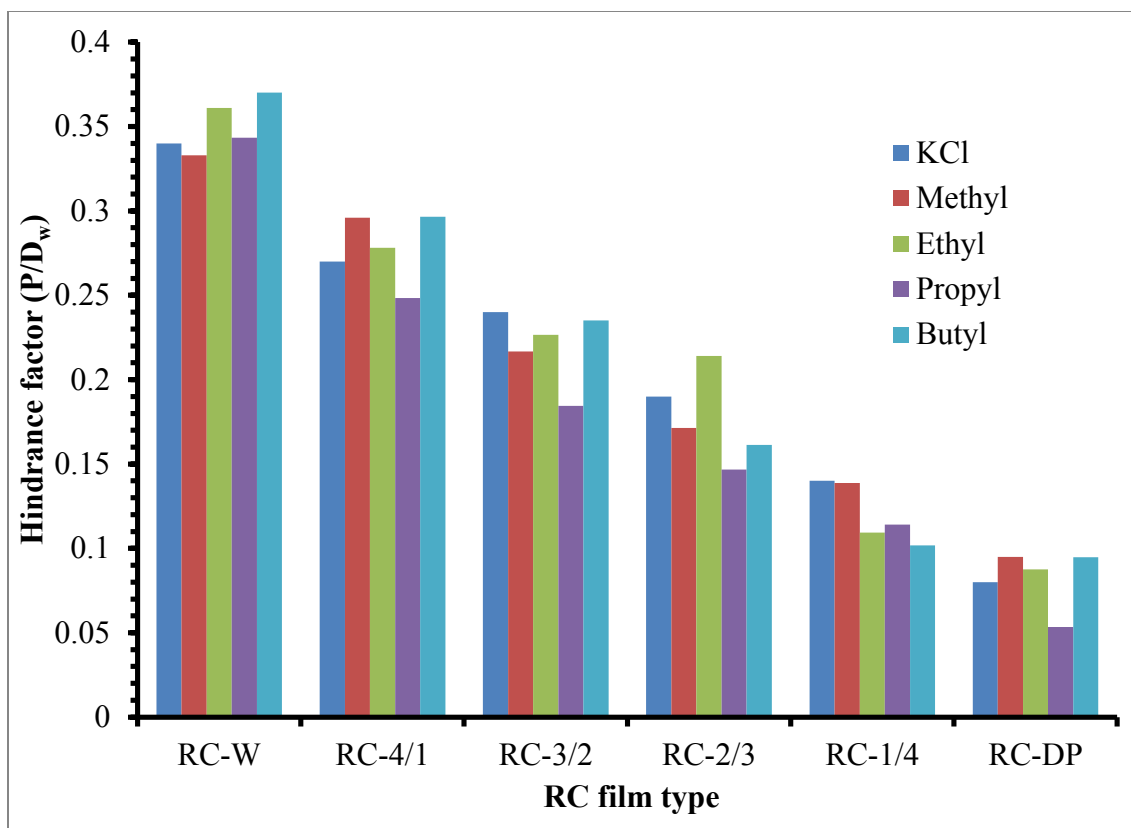


Figure 25: Comparison of hindrance factors ( $P/D_w$ ) of KCl, methyl-, ethyl-, propyl- and butyl-p-aminobenzoate through RC-W, RC-4/1, RC-3/2, RC-2/3, RC-1/4 and RC-DP films in purified water, at 37°C.

To analyze the changes in channel sizes with increasing content of depolymerized cellulose, the permeabilities of lysozyme chloride (LZY, 2.5 nm hydrodynamic radius [96]) and bovine serum albumin (BSA, 5 nm hydrodynamic radius [90]) were examined and compared with KCl. Figure 26 shows the flux profiles of LZY (pH 4.5 acetate buffer medium) and BSA (pH 7.4 phosphate buffer medium) through RC-W, RC-DP and blended films at 37 °C. The diffusion coefficient for LZY at 37°C in pH 4.5 buffer has been reported to be  $5.60 \times 10^{-6} \text{ cm}^2/\text{sec}$  [94], while the aqueous diffusion coefficient of BSA at 37°C in pH 7.4 buffer has been reported to be  $8.83 \times 10^{-7} \text{ cm}^2/\text{sec}$  [95]. The protein partitioning as well as immobilization into the polymer phase is considered negligible since LZY at pH 4.5 has a net positive charge (isoelectric point 11) and BSA at pH 7.4 has a net negative charge (isoelectric point 4.7) [96],[90]. Based on these diffusion coefficients and the permeability coefficients obtained from the protein flux data, the hindrance factors were estimated and listed in Table 10. The transport reduction factor of the protein, ' $\partial_{Protein}$ ', owing to its size limitation was calculated by the following relation:

$$\text{Equation 21} \quad \partial_{Protein} = \frac{\left\{ \frac{P}{D_w} \right\}_{Protein}}{\left\{ \frac{P}{D_w} \right\}_{KCl}}$$

Since the hindrance factors of the solutes are related to the porosity of the RC films, the above ratio describes the fraction of channel sizes that are available for protein flux in comparison to KCl, i.e.  $\{(P/D_w)_{LZY}/(P/D_w)_{KCl}\}$  would represent the fraction of pores whose diameters are greater than 5 nm, while the  $\{(P/D_w)_{BSA}/(P/D_w)_{KCl}\}$  ratio would represent the fraction of pores whose pore diameters are greater than 10 nm. [97]. Figure 27 compares the transport reduction factors of proteins  $\{(P/D_w)_{protein}/(P/D_w)_{KCl}\}$

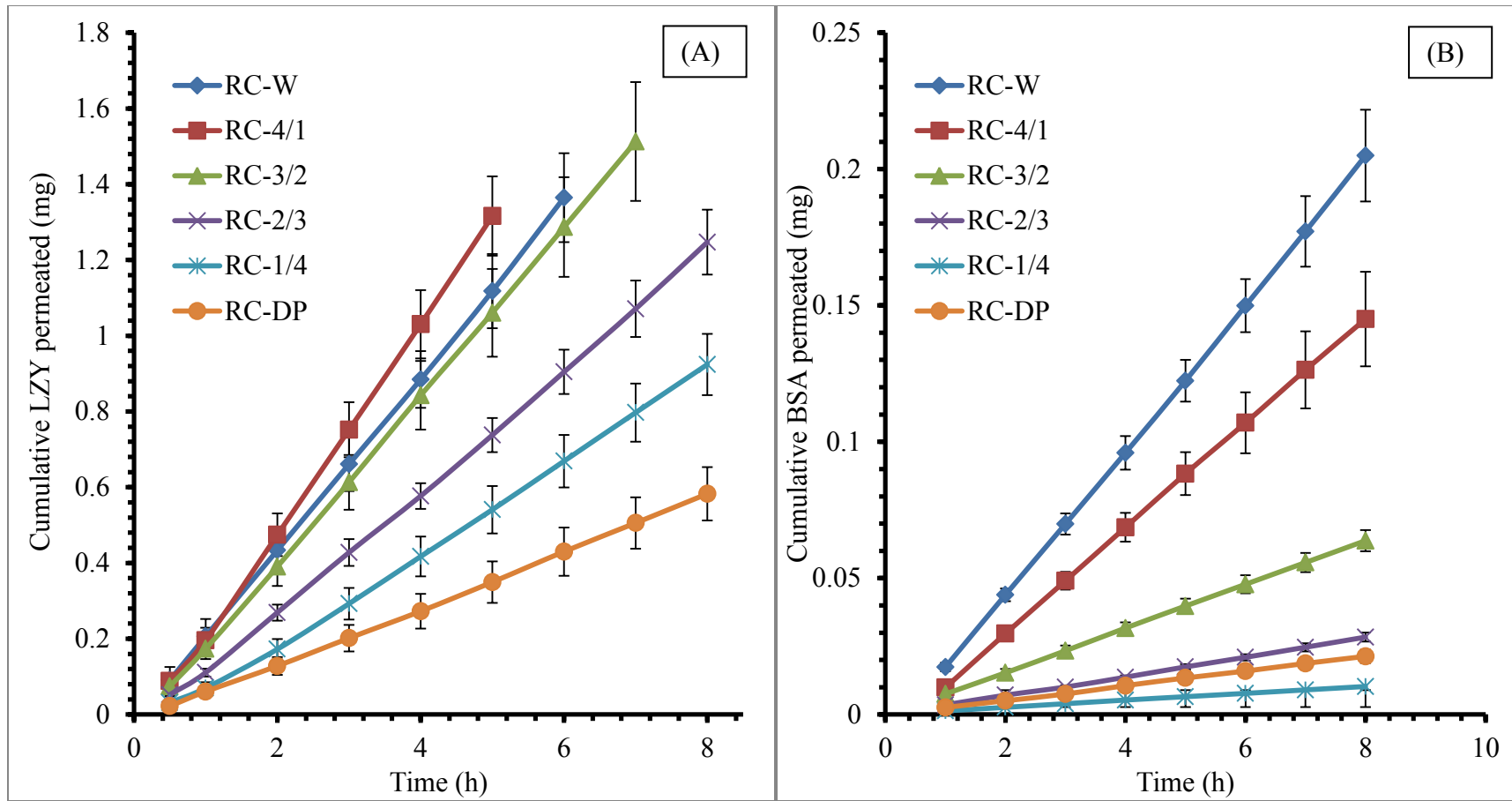


Figure 26: Flux profiles of (A) lysozyme chloride (LZY) in pH 4.5, and (B) bovine serum albumin (BSA) in pH 7.4, through RC-W, RC-DP and blended films at 37°C.

Table 10: Flux parameters and calculated permeability coefficient as well as hindrance factors for lysozyme chloride (LZY) in pH 4.5 buffer ( $\mu \approx 0.15$ ) and bovine serum albumin (BSA) in pH 7.4 buffer ( $\mu \approx 0.15$ ) through RC-W, RC-DP and blend films, at 37°C.

|                                                      | <b>Lysozyme Chloride</b>                     |                  |                         |                     | <b>Bovine Serum Albumin</b>                  |                  |                         |                     |
|------------------------------------------------------|----------------------------------------------|------------------|-------------------------|---------------------|----------------------------------------------|------------------|-------------------------|---------------------|
| Aqueous diffusion coefficient ( $D_w$ ) <sup>a</sup> | 5.60 x 10 <sup>-6</sup> cm <sup>2</sup> /sec |                  |                         |                     | 8.83 x 10 <sup>-7</sup> cm <sup>2</sup> /sec |                  |                         |                     |
| Donor cell concentration                             | 1.0 mg/cm <sup>3</sup>                       |                  |                         |                     |                                              |                  |                         |                     |
| Film type                                            | $(\frac{dm}{dt})^b$                          | (h) <sup>c</sup> | (P) <sup>d</sup>        | $(\frac{P}{D_w})^e$ | $(\frac{dm}{dt})^b$                          | (h) <sup>c</sup> | (P) <sup>d</sup>        | $(\frac{P}{D_w})^e$ |
|                                                      | (mg/h)                                       | (cm)             | (cm <sup>2</sup> /sec)  |                     | (mg/h)                                       | (cm)             | (cm <sup>2</sup> /sec)  |                     |
| <b>RC-W</b>                                          | 0.251                                        | 0.037            | 1.55 x 10 <sup>-6</sup> | 0.28                | 0.034                                        | 0.036            | 1.57 x 10 <sup>-7</sup> | 0.18                |
| <b>RC-4/1</b>                                        | 0.286                                        | 0.026            | 1.22 x 10 <sup>-6</sup> | 0.22                | 0.023                                        | 0.025            | 7.88 x 10 <sup>-8</sup> | 0.089               |
| <b>RC-3/2</b>                                        | 0.234                                        | 0.021            | 7.59 x 10 <sup>-7</sup> | 0.14                | 0.008                                        | 0.019            | 2.51 x 10 <sup>-8</sup> | 0.028               |
| <b>RC-2/3</b>                                        | 0.165                                        | 0.013            | 3.43 x 10 <sup>-7</sup> | 0.061               | 0.004                                        | 0.015            | 8.82 x 10 <sup>-9</sup> | 0.0099              |
| <b>RC-1/4</b>                                        | 0.137                                        | 0.011            | 2.41 x 10 <sup>-7</sup> | 0.043               | 0.001                                        | 0.013            | 2.76 x 10 <sup>-9</sup> | 0.0031              |
| <b>RC-DP</b>                                         | 0.083                                        | 0.090            | 1.10 x 10 <sup>-7</sup> | 0.020               | 0.002                                        | 0.091            | 1.86 x 10 <sup>-9</sup> | 0.0021              |

<sup>a</sup> Obtained from references [94] and [95]

<sup>b</sup> Mass transfer rate

<sup>c</sup> Hydrated film thickness

<sup>d</sup> Permeability coefficient

<sup>e</sup> Hindrance factor

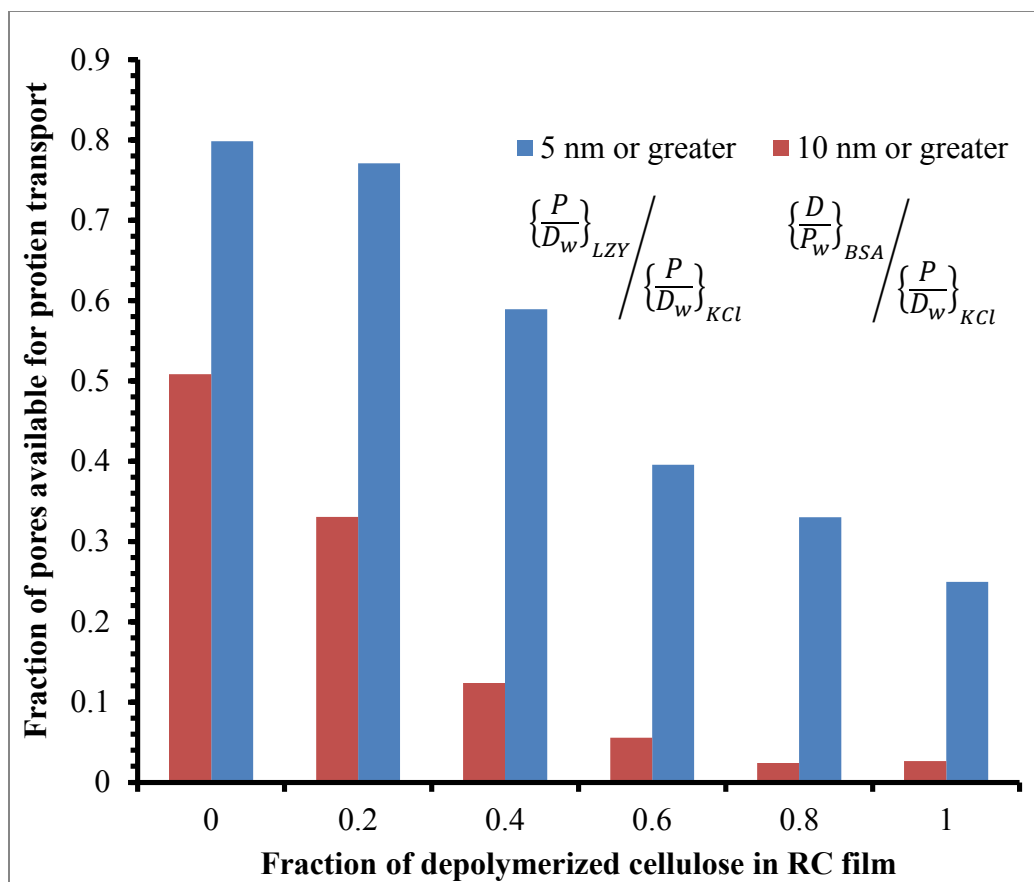


Figure 27: Fraction of pores greater than 5 nm and 10 nm as a function of fraction of depolymerized cellulose in RC films.



through blended RC films. Films formed from native cotton linters (RC-W) exhibit a LZY transport reduction factor of 0.8, indicating that 80% of the channels available for KCl transport are greater than or equal to 5 nm. For the same RC film, the BSA transport reduction factor was 0.5 of KCl, indicating that only 50% of these channel diameters are greater than or equal to 10 nm. Films formed from only depolymerized cellulose (RC-DP) show nearly 75 % reduction in the LZY hindrance factor indicating that only 25 % of the channels available for transport are larger than or equal to 5 nm. At the same time, a 99 % reduction of BSA hindrance factor indicates that almost all the channels available for KCl are less than or equal to 10 nm. In blended films, a systematic decline in LZY and BSA hindrance factor is observed when the fraction of depolymerized cellulose increases within the RC films. These results indicate that channel sizes formed upon hydration of the thermally annealed films are smaller in size than those observed on SEM micrographs. Moreover, the pore sizes are not constant in each film type, i.e. the films consist of transport pathways of varying sizes. As the fraction of depolymerized cellulose increases in the blended films, the both size and number of transport pathways tend to decrease.

#### Influence of non-solvents on RC film formation and solute flux

The use of organic non-solvents on cellulose precipitation has a varied impact on the properties of RC membranes based on the non-solvent utilized for precipitation of membranes. Gavillion et al have shown that cellulose membranes prepared from cellulose N-methylmorpholine-N-oxide monohydrate hydrogels show a reduction of water uptake capacity of cellulose membranes as the Hildebrand solubility parameter difference between cellulose and the non-solvent bath increased when alcohols of increasing carbon

chain length as were used non-solvents [98]. Isobe et al have reported that cellulose regenerated from cellulose-NaOH-urea solution revealed very little change in porosity and pore size when precipitation was carried out in methanol, ethanol, acetone and aqueous solutions of Na<sub>2</sub>SO<sub>4</sub> and H<sub>2</sub>SO<sub>4</sub> [99]. Moreover, cellulose pulps and cotton fabrics are also known to form consolidated non-swelling domains (hornification) when they undergo thermal treatment for the removal of solvents\ non solvents [45].

To evaluate whether the use of organic non-solvents impacted the RC film formation during precipitation and/or during thermal annealing, the adsorption of methylene blue dye on RC membranes that were either freeze dried immediately after precipitation in their respective non-solvents, or thermally annealed after precipitation. Methylene blue adsorption on cellulose products (cotton fibers) has been shown to occur via hydrogen bonding of the amine groups of the dye molecules with the axial hydroxyl groups on the glucopyranose rings [100], [101]. The comparison of dye absorptivity from aqueous solutions, between freeze dried and thermally annealed membranes would hence be an indication of the extent of polymer consolidation during regeneration as well as following thermal annealing. Figure 28 shows the methylene blue adsorption isotherms from pH 8.5 NaOH solution on to RC-A, RC-M, RC-E, RC-W, RC-P, RC-W and RC-B membranes, prepared by either freeze drying or thermally annealing after precipitation in their respective non-solvents. The dye adsorption data were fitted to the Langmuir-like equation as shown below:

Equation 22

$$\frac{N}{N_g} = \frac{\beta C_\beta}{1 + \beta C_\beta}$$

where, 'N' is the amount of dye adsorbed on cellulose membranes, 'N<sub>g</sub>' is the maximum capacity of the dye for the cellulose membranes, 'β' is the affinity constant between the

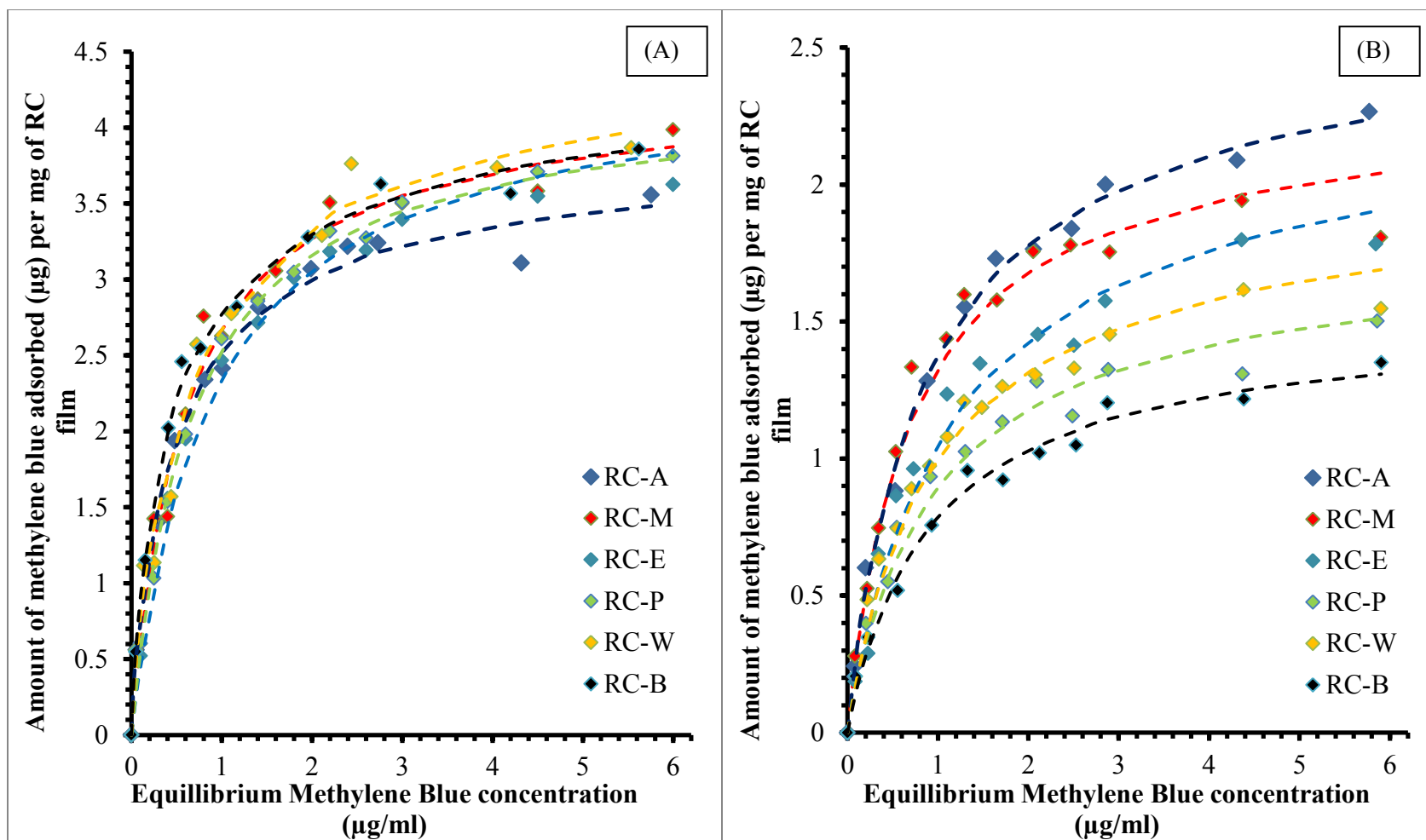


Figure 28: Adsorption isotherms of methylene blue dye from pH 8.0 solution on (A) freeze dried and (B) thermally annealed RC-A, RCM, RC-E, RC-P, RC-W and RC-B films, after precipitation in respective non-solvents. Dashed lines represent curve fitting to Langmuir-like equation.

dye molecule and the cellulose membranes, and ' $C_{\beta}$ ' is the equilibrium concentration of the dye in bulk solution. Table 11 summarizes these parameters obtained by data fitting using the 'least squares' method in Microsoft Excel Solver<sup>®</sup>. The maximum dye adsorption capacity ( $N_g$ ) of methylene blue was similar for the freeze dried membranes. Visually, these films formed instantly when methylolcellulose was immersed non-solvents. The rapid inversion is related to the high miscibility/ solubility of DMSO and formaldehyde with the non-solvents. Hence, the internal structure of the film formed in the non-solvent medium during phase inversion was not reliant on non-solvent used for phase inversion.

The maximum dye adsorption capacity of thermally annealed RC membranes decreases when compared to the dye adsorption capacity of freeze dried films. This reduction is maybe due to the irreversible collapse of the capillary voids between regenerated cellulose aggregates during non-solvent removal by thermal curing, which are now not accessible to the newly intruding water carrying the dye molecules [43]. The maximum adsorption capacity of the thermally annealed RC films decreases in the following order: RC-A > RC-M > RC-E > RC-W > RC-P > RC-B. Since the maximum dye adsorption capacity is related to the available surface area for dye interaction, the extent of polymer consolidation during thermal treatment observed in each film type can be estimated by the following relation:

$$\text{Equation 22} \quad \begin{aligned} & \text{Extent of polymer consolidation (\%)} \\ & = \left\{ \frac{N_{g(\text{freeze dried})} - N_{g(\text{thermally annealed})}}{N_{g(\text{freeze dried})}} \right\} 100 \end{aligned}$$

where, ' $N_{g(\text{freeze dried})}$ ' is the maximum dye adsorption capacity of the freeze dried film

and ' $N_{g(\text{thermally annealed})}$ ' is the maximum dye adsorption capacity of the thermally annealed membrane. The extent of polymer consolidation due to thermal curing for each RC membranes are summarized in Table 11. Figure 29 compares the extent of polymer consolidation in the RC membrane vs. the boiling point of the non-solvents utilized for phase inversion\ precipitation of cellulose. The extent of polymer consolidation increases as the boiling point of the non-solvent increases. It is likely that the higher boiling point non-solvents reside within the precipitated membrane for a longer period of time during thermal curing and owing to their extended presence in the wet membrane they aid in formation of greater non-swelling domains which in turn do not allow newly intruding water to penetrate these regions.

To evaluate whether the irreversible polymer consolidation influenced solute permeability, the flux of ethyl-p-aminobenzoate was examined through RC-A, RC-M, RC-E, RC-W, RC-P, RC-W and RC-B films freeze dried immediately after precipitation in their respective solvents, and through same set of films that were thermally annealed after precipitation. Figure 30 shows the thickness normalized flux profiles of ethyl-p-aminobenzoate through these RC films. Prior to thermal curing, the thickness normalized flux profiles were nearly identical for all the films that were immediately freeze dried after precipitation of MC-4 solution, in their respective non-solvents. However, the flux of ethyl-p-aminobenzoate decreased in the thermally annealed RC films in the following order: RC-A > RC-M > RC-E > RC-P > RC-B. The order of decreasing flux is similar to the trend observed in analysis of dye adsorption on thermally annealed RC membranes, indicating that the thermal curing of RC films caused reduction in transport pathways connecting the two surfaces.

Table 11: Methylene blue adsorption parameters determined by fitting Langmuir like equation to adsorption isotherms shown in Figure 28 for RC-A, RC-M, RC-E, RC-P, RC-W and RC-B freeze dried and thermally annealed films.

| Membrane type | Langmuir like equation regression parameters |                       |                |                                                     |                       |                | Extent of polymer consolidation <sup>a</sup> |
|---------------|----------------------------------------------|-----------------------|----------------|-----------------------------------------------------|-----------------------|----------------|----------------------------------------------|
|               | RC films freeze dried after precipitation    |                       |                | Wet RC films thermally annealed after precipitation |                       |                |                                              |
|               | Adsorption capacity (N <sub>g</sub> )        | Affinity constant (β) | r <sup>2</sup> | Adsorption capacity (N <sub>g</sub> )               | Affinity constant (β) | r <sup>2</sup> |                                              |
|               | (μg/mg)                                      | (cm <sup>3</sup> /μg) |                | (μg/mg)                                             | (cm <sup>3</sup> /μg) |                |                                              |
| RC-A          | 3.85                                         | 1.46                  | 0.96           | 2.61                                                | 0.98                  | 0.92           | 33                                           |
| RC-M          | 4.25                                         | 1.06                  | 0.92           | 2.32                                                | 1.21                  | 0.89           | 45                                           |
| RC-E          | 4.40                                         | 1.48                  | 0.93           | 1.96                                                | 0.75                  | 0.93           | 56                                           |
| RC-P          | 4.22                                         | 1.12                  | 0.98           | 1.73                                                | 0.93                  | 0.94           | 59                                           |
| RC-W          | 4.39                                         | 1.67                  | 0.96           | 1.59                                                | 0.90                  | 0.96           | 64                                           |
| RC-B          | 4.32                                         | 1.58                  | 0.97           | 1.42                                                | 0.68                  | 0.97           | 68                                           |

$$^a \text{Extent of polymer consolidation (\%)} = \left\{ \frac{N_{g(\text{freeze dried})} - N_{g(\text{thermally annealed})}}{N_{g(\text{freeze dried})}} \right\} 100$$

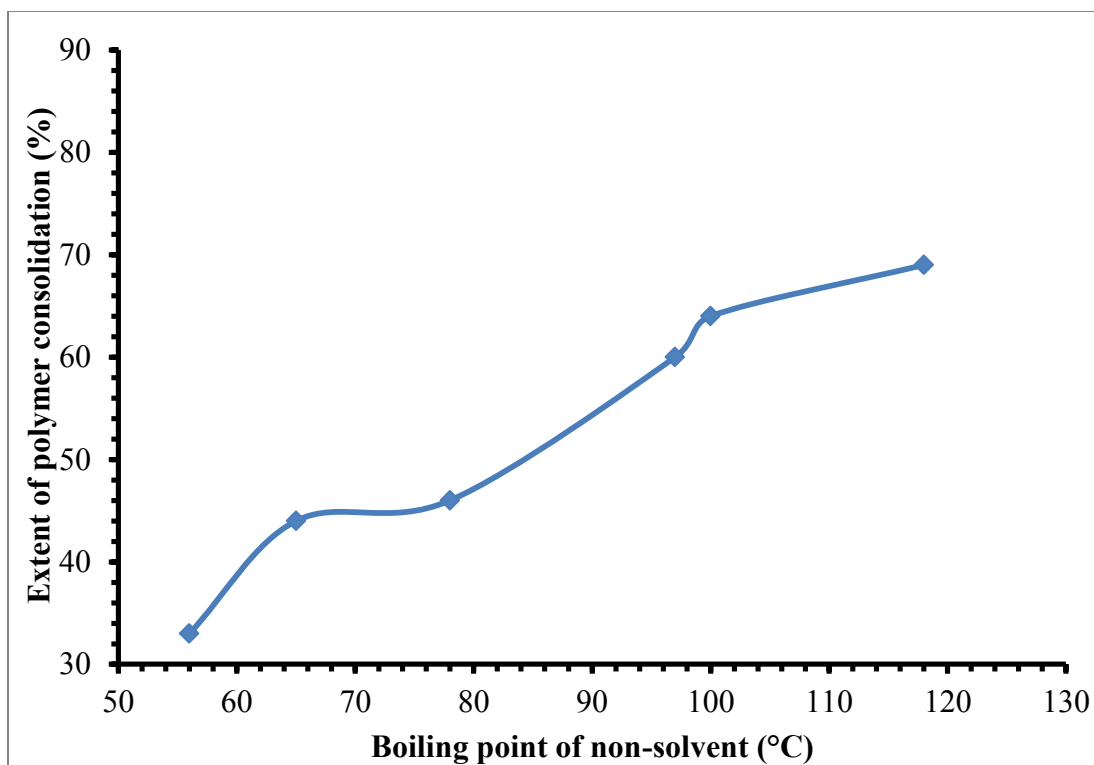


Figure 29: Comparison of extent of polymer consolidation of RC films following thermal annealing vs. the boiling of non-solvent utilized for phase inversion/ precipitation of cellulose from MC-4 solution.

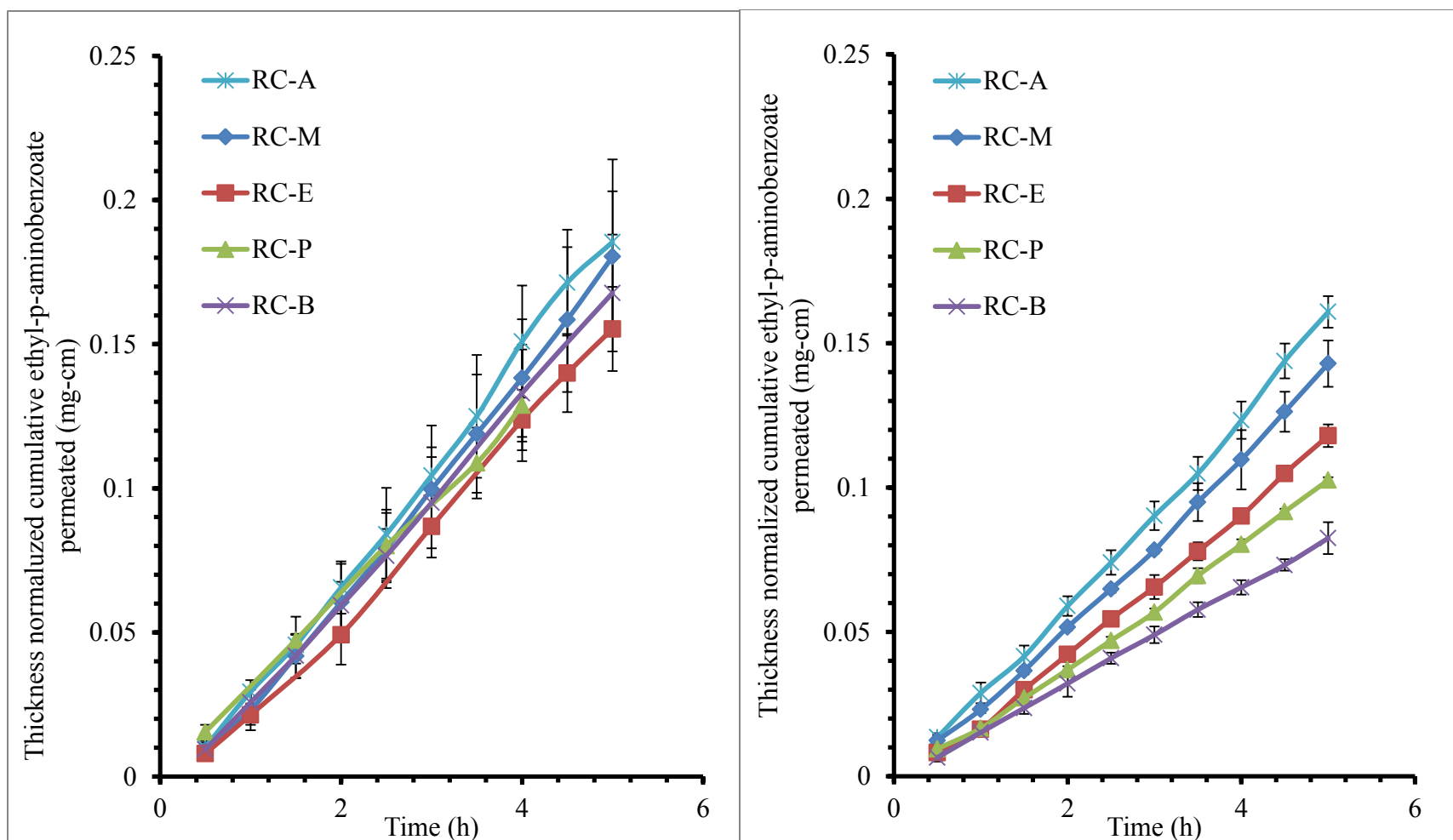


Figure 30: Thickness normalized flux profiles of ethyl-p-aminobenzoate in purified water at 37 °C through RC-A, RC-M, RC-E, RC-P and RC-B films (A) freeze dried immediately after phase inversion in their respective non-solvents and (B) after thermal treatment of wet films regenerated in their respective non-solvents.



### Modulation of RC film thickness and its impact on solute permeability

Modulation of film thickness is a common method utilized in to alter drug release in controlled release dosage forms. Since RC films investigated in this research were fabricated by dip coating method, a procedure utilized in manufacturing two-piece capsule shells, the thickness of RC films was altered by multiple dip coating/ lamination method. Acetone was utilized as an intermediary non-solvent between applications of subsequent coatings. The reason for using acetone as an intermediate non-solvent medium was: (i) acetone has a low boiling point and can be evaporated at room temperature, and (ii) similar to precipitation in water, regeneration of cellulose in acetone was instantaneous and had no influence on the RC film, prior to thermal annealing (Figure 28). Regenerated cellulose films prepared by 2, 3, 4 and 5 applications of MC solution are herein referred to as RC-2T, RC-3T, RC-4T and RC-5T, respectively. The changes permeability of the film with multiple applications of MC solution was analyzed using ethyl-p-aminobenzoate as a model solute. Figure 31 shows the thickness normalized flux profiles of ethyl-p-aminobenzoate through RC-2T, RC-3T, RC-4T and RC-5T. Table 12 lists the calculated flux, permeability coefficient, hindrance factors of ethyl-p-aminobenzoate through these films as well as calculated porosity and tortuosity. The ethyl-p-aminobenzoate flux rates through these films decreased with increasing coating level of RC films. The porosities of these films were nearly constant indicating that water is able to penetrate into these films and induce swelling as it were penetrating a single coat film. The decrease in permeability coefficient of ethyl-p-aminobenzoate through these films indicates that lamination method of increasing film thickness caused partial or complete closure of some of the transport pathway channels. Moreover, an

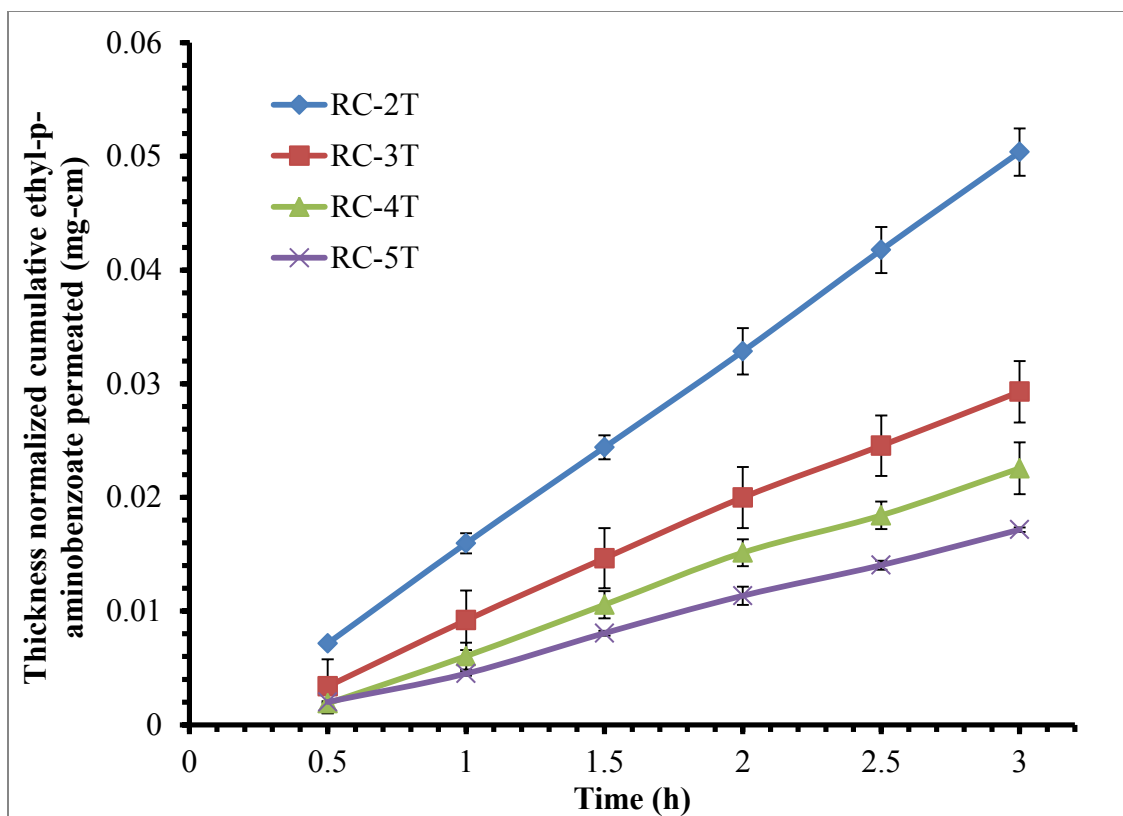


Figure 31: Thickness normalized flux profiles of ethyl-p-aminobenzoate through RC-2T, RC-3T, RC-4T and RC-5T films in purified water at 37°C, using Side-by-Side<sup>®</sup> diffusion cells.

Table 12: Flux parameters of ethyl-p-aminobenzoate through RC -2T, RC-3T, RC-4T and RC-5T films, in purified water at 37°C.

| Film type    | Hydrated thickness | Thickness normalized mass transfer rate $\left(\frac{dm}{dt} h\right)$ | Permeability coefficient (P)               | Hindrance factor $\left(\frac{P}{D_w}\right)^a$ | Hydrated Porosity ( $\epsilon$ ) | Tortuosity ( $\tau$ ) |
|--------------|--------------------|------------------------------------------------------------------------|--------------------------------------------|-------------------------------------------------|----------------------------------|-----------------------|
|              | (mm)               | (mg/h-cm)                                                              | ( $\times 10^{-6}$ , cm <sup>2</sup> /sec) |                                                 | (n = 6)                          |                       |
| <b>RC-2T</b> | 0.39               | 0.017                                                                  | 1.70                                       | 0.26                                            | 0.68 ± 0.01                      | 2.56                  |
| <b>RC-3T</b> | 0.45               | 0.010                                                                  | 1.04                                       | 0.16                                            | 0.68 ± 0.02                      | 4.15                  |
| <b>RC-4T</b> | 0.49               | 0.009                                                                  | 0.83                                       | 0.13                                            | 0.66 ± 0.01                      | 5.11                  |
| <b>RC-5T</b> | 0.57               | 0.006                                                                  | 0.61                                       | 0.09                                            | 0.65 ± 0.03                      | 6.85                  |

<sup>a</sup>  $D_w = 6.40 \times 10^{-6}$  cm<sup>2</sup>/sec, taken from reference [93]

increase in tortuosity indicates that the transport pathways are extended possibly due to increased blocking and branching of the pores from overlapping of multiple cellulose layers.

### **Conclusions**

Regenerated cellulose films were readily prepared from DMSO/PF solvent system by immersion precipitation, followed by thermal curing. The physiochemical as well as solute transport evaluation of these films in this research led to the following conclusions:

- 1) Irrespective of the type of non-solvent utilized or the degree of polymerization of cellulose polymer, these films are porous when precipitated from the DMSO/PF solvent system. These films lose their porous structure when thermally annealed after precipitation. The porous structure is regained as soon these films are re-exposed to water.
- 2) Physiochemical evaluation of these films revealed that the polymer chain length was not significantly altered during cellulose dissolution, precipitation and thermal curing. Cellulose primarily existed in amorphous state in the thermally annealed films irrespective of the non-solvent utilized for precipitation or the degree of polymerization of the starting cellulose source. Scanning electron micrographs revealed that the pore sizes were smaller in the rehydrated RC film prepared from depolymerized cotton linters when compared to RC films prepared from native cotton linters.
- 3) Re-hydration of RC films in ethanol-water binary mixtures indicated that the

solvent uptake capability of these films was diminished in the presence of an organic solvent component in the solvent uptake medium. The diminished solvent uptake in turn affected the solute transport through these films. It was also discovered that a minimum level of hydration/solvent uptake was required in order to facilitate the flux of acetaminophen through the porous routes formed when the films are hydrated. The minimum hydration required to initiate solute flux through pores was lower for films prepared from native cotton linters than for films prepared from depolymerized cotton linters.

- 4) Blending of methylolcellulose solutions containing depolymerized and native cotton linters led to alteration of the porosity and water uptake of the re-hydrated RC films. Both water uptake and porosity was reduced as the fraction of depolymerized cellulose increased in the RC films. Evaluation of KCl transport through blended films indicated that the reduction in porosity was responsible for reduced KCl flux and tortuosity of RC-W and the blended films was not significantly altered, while RC-DP film showed a significant increase in tortuosity. Evaluation of transport behavior of four alkyl-p-aminobenzoates indicated that even through the porosity decreased in RC blended and RC-DP films, the mechanism of solute transport occurred through the porous routes. Comparison of flux parameters of LZY and BSA to that of KCl, through blended films also indicated that as the fraction of depolymerized cellulose increases in the RC films, the pore sizes also decreased.
- 5) Dye adsorption studies on RC films precipitated in organic non-solvents indicated that the polymer organization and formation of porous structures was not

dependent on the type of non-solvent utilized during the precipitation process.

However, the irreversible polymer consolidation (hornification) and formation of non-water swelling domains was directly related to the presence of these non-solvents during the thermal curing stage. Higher boiling point non-solvents caused greater consolidation and hence led to a reduction in solute flux through the films owing to irreversible closure of some of the porous pathways.

- 6) Increasing the RC film thickness by multiple dip coating method led to a reduction in the permeability coefficient of the model solute, ethyl-p-aminobenzoate. The reduction in the permeability coefficient was attributed to an increase in the tortuosity of the porous pathways owing to lamination/ over-laying of subsequent layers of precipitated cellulose.

## CHAPTER IV

### PREPARATION AND IN-VITRO PERFORMANCE OF TWO-PIECE HARD SHELL REGENERATED CELLULOSE CAPSULES

#### **Introduction**

Capsules represent about 10% of the dosage forms used in oral drug delivery. Gelatin, and to some extent hydroxypropylmethyl cellulose, are the most common starting materials employed in fabrication of two piece telescoping capsules. In addition to possessing the advantages of elegance, ease of use, and portability, capsules are a popular dosage form because they provide a smooth, slippery, easily swallow-able and tasteless shell for drugs; the last advantage is particularly beneficial for drugs having unpleasant tastes and/or odors [102]. However, capsules, especially the telescoping – two piece hard shell variant, are rarely utilized in controlled drug delivery. Theoretically, as a controlled release dosage form, capsules would provide a universal system for screening of multiple drug:excipient combinations during early phase trials. The feasibility for controlled release could be determined in a relatively short time with small quantities of bulk drug, especially when dealing with early drug candidates [65]. Moreover, since the capsule properties could be independently modulated without interacting with the core formulation, these dosage forms are suitable for drug molecules that are difficult and expensive to obtain, and sensitive to aqueous/ organic environments and/or elevated temperatures typically encountered during tablet coating for controlled release [103].

For these reasons, several researchers have looked at modifying gelatin capsule properties to for use in controlled drug delivery systems. Crosslinking was investigated by Digenis et al [51] and Bussermer et al [104] to extend gelatin dissolution times in the gastro-intestinal tract, thereby improving gelatin capsule feasibility for delayed and extended drug delivery. However, the presence of pepsin and pancreatin in the stomach and intestinal fluids were shown to dissolve even the cross-linked gelatin which can lead to device failures early in the gastro-intestinal tract [105]. Several investigators have placed additional coating over hard gelatin capsules in order to achieve controlled, delayed and or sustained release from capsules [106], [58], [107]. However, the additional processing steps involved with these techniques increases overhead costs and manufacturing times.

To overcome the biochemical stability of gelatin and to reduce development times in dosage form manufacturing, the use of regenerated cellulose is proposed for the fabricating of capsule-based controlled drug delivery system. Cellulose is a biologically and chemically inert and stable polymer and hence is an ideal candidate for capsule based controlled drug delivery. The purpose of this study was to investigate the drug release performance from regenerated cellulose capsules *in vitro*. To assess the feasibility of these capsules in controlled delivery, drug release studies were evaluated on a selection of solutes exhibiting a wide range of solubilities. The objective was to identify the mechanisms involved in drug release as the solubility of the enclosed solute was varied. The influence of varying agitation conditions and pH of the external medium was also investigated in order to study changes in environmental conditions influencing drug release.



## **Experimental**

### Materials

Cellulose in the form of cotton linter sheets was obtained from Southern Cellulose Products Inc. (Grade R270; Chattanooga, TN). Paraformaldehyde and dimethyl sulfoxide were obtained from Fischer Chemicals (Fair Lawn, NJ). Potassium chloride and diphenhydramine HCl were purchased from Fisher Chemicals (Fair Lawn, NJ) and Arcos Organics (Geel, Belgium), respectively. Tramadol HCl and acetaminophen were purchased from Sigma Life Sciences (St. Louis, MO). Niacinamide and ketoprofen were obtained from Professional Compounding Centers of America (Houston, TX). Glacial acetic acid (A.C.S grade, 99.7%) was obtained from Research Products International Corp. (Mt. Prospect, IL), methanol and acetonitrile from Fisher Chemicals (Fair Lawn, NJ) and triethylamine from Mallinckrodt (St. Louis, MO).

### Preparation of methylolcellulose solutions

Methylolcellulose (MC) solutions containing 4.4, 3.3 and 2.2 % w/w cellulose were prepared from cotton linter sheets in a manner similar to that described in Chapter III (Preparation of Methylolcellulose solution. The exact compositions of the solutions are listed in Table 13.

### General method for preparing capsule halves

Two piece hard shell capsules are generally prepared by dip coating process. In case of gelatin capsules, they are usually prepared by dip coating stainless steel mold pins in molten gelatin solution. Following coating, these pins are spun to allow even distribution of the molten solution on the surface prior to the thermally induced phase

Table 13: Composition of methylolcellulose solutions utilized in fabrication of capsules

| <b>Amount of cotton<br/>linters added in<br/>solution</b> | <b>Paraformaldehyde</b> | <b>Dimethyl sulfoxide</b> | <b>Concentration of<br/>cellulose in<br/>solution</b> |
|-----------------------------------------------------------|-------------------------|---------------------------|-------------------------------------------------------|
| (g)                                                       | (g)                     | (g)                       | (% w/w)                                               |
| 12                                                        | 30                      | 500                       | 2.2                                                   |
| 19                                                        | 47.5                    |                           | 3.3                                                   |
| 26                                                        | 65                      |                           | 4.4                                                   |

inversion of gelatin after which the solidified shells are trimmed to the desired length and ejected from the pins. Cellulose capsule halves were fabricated in a similar manner by dip coating polytetrafluoroethylene (Teflon) mold pins (Department of Physics machine shop, University of Iowa, Iowa City, IA) in methylolcellulose solution. All solutions, contained in 25 ml glass scintillation vials and sealed with screw caps, were degassed and conditioned to 25°C in a water sonication bath (Bransonic Ultrasonic Cleaner, Model 5200, Bransonic Corporation, Danbury, CT) for 30 minutes. Mold pins were immersed in methylolcellulose solution containing vials for 1 to 2 minutes and then held inverted to remove any excess solution from the pins for a few more minutes. These pins were then placed on electric motors (GKH model GT-21, G. K. Keller Corp, Floral Park, N.Y.) attached to an electrical voltage regulator (GKH model GR-45, G. K. Keller Corp, Floral Park, N.Y.) and rotated at 75 rpm at a 45° angle to the horizontal. It was discovered by trial and error method that the 45° angle allowed for a more homogenous distribution of the solution along the surface of the mold pin. After spinning, the mold pins were placed in a water bath (> 5 L) for 24 hours to regenerate cellulose. Water was replaced in the bath periodically. Following regeneration, the pins were placed in a thermostatic oven for 24 hours at 105°C and the capsule shell were then ejected and trimmed using a surgical blade. The general fabrication procedure is schematically summarized in Figure 31.

#### Improving reproducibility of capsules

The general capsule fabrication procedure described above led to the formation of very thin shells that collapsed during the ejection process. This collapse occurs due to the formation of void volume in-situ between the mold pin and the thermally annealed capsule shell as the shell is ejected from the mold pin. In general, two types of failures

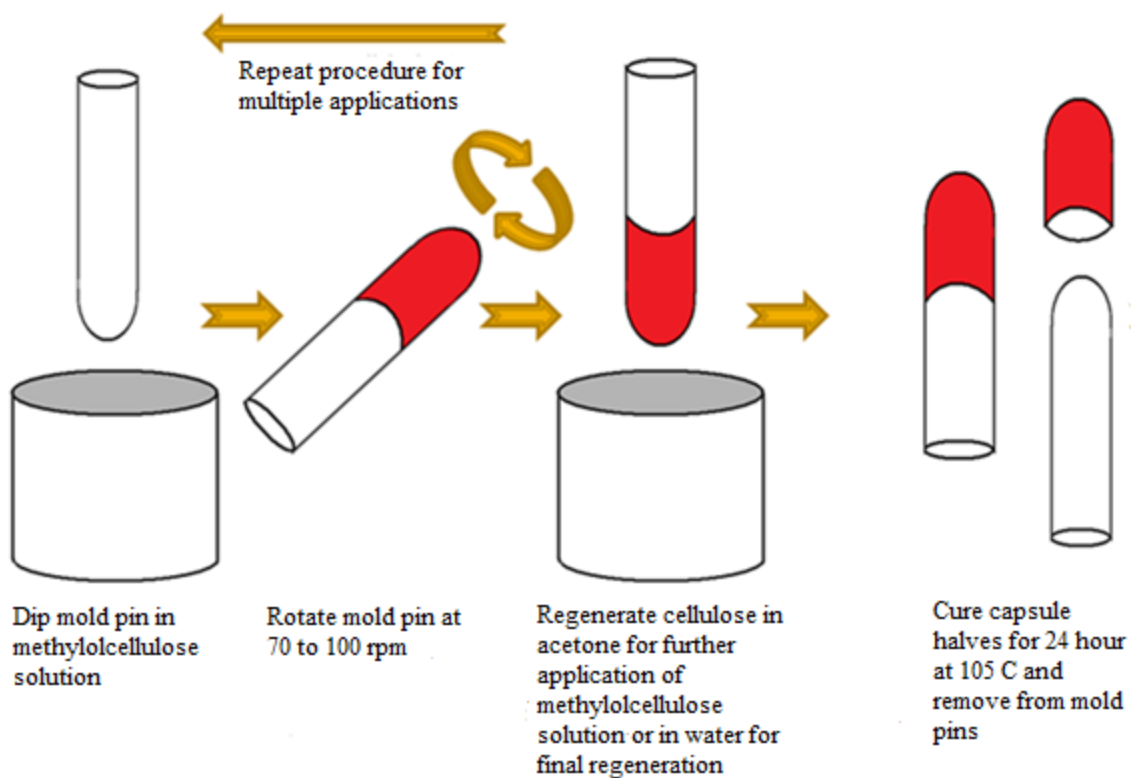


Figure 32: Schematic representation of capsule fabrication methodology employed for preparing two piece telescoping capsule. Dimensions of the pin were 8 mm x 35 mm.

were observed because of this void volume formation; (i) Failure type A (FTA) where the capsule walls shredded into multiple pieces, and, (ii) Failure type B (FTB) where the capsule shell integrity would remain intact but still collapsed under the pressure difference between the empty volume formed and the external environment. In case of FTA, the capsule shells were not thick enough to withstand the pressure difference during the ejection process, while FTB occurred due to variability in the thickness across the shell diameter, i.e. the shell would collapse in the region with the thinner walls.

Additionally, the variability occurs due to un-even distribution of methylolcellulose solution during the coating/spinning stage. Since increasing the thickness of the capsule wall would impart mechanical stability and increasing the rotation time would reduce variability in capsule wall thickness, the influence of multiple coatings and rotation time were investigated to reduce both failure types. The objective of these investigations was to repeatedly fabricate capsule shells with a reproducible thickness and sufficient mechanical strength to withstand the ejection process, in the shortest time possible.

Rotation time was the preliminary variable investigated. Capsule shells were fabricated using the general fabrication method described above with mold pin spinning times of 3, 5, 8, 10, 15, 20, 25 and 30 minutes prior to placing them in regeneration medium. Capsule shell integrity was visually monitored for FTA and FTB during the ejection process and shell thickness measured using digital calipers.

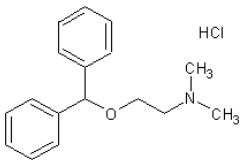
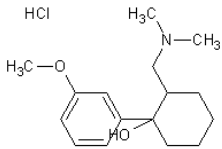
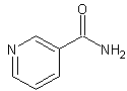
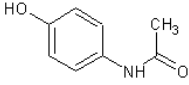
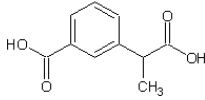
In the multiple dip coating approach, following determination of minimum rotation time required to achieve even coating along the mold pin surface after single application of methylolcellulose solution, the mold pins were immersed in acetone for 15 minutes followed by air drying for another 15 minutes. After air drying, these pins were

re-immersed in methylolcellulose solution and the process repeated until desired number of coatings were applied, then regenerated in water and annealed in the thermostated oven at 105°C for 24 hours, trimmed to desired length and visually monitored for FTA and FTB during the ejection process. Shell thickness was measured using digital calipers. Capsules with up to seven coatings were prepared to investigate reduction in FTA, FTB and variability in capsule wall thickness.

#### Preparation of one component formulations for capsule filling

The active pharmaceutical ingredients (APIs) utilized in filling the capsules were in the form of dry powders. The APIs were ground into a fine powder-like consistency using a roll mill (operating in oscillation mode) attached to a 250 micron stainless steel screen (Erweka AR400, Ottostraße, Germany). The dry API granules and powders (as obtained) were fed in to the mill using a hopper in 50 g batches and the resulting milled powder was then collected over a sieve stack with 250 and 180 µm opening (USP 60 and 80, respectively) placed on an electrical shaker (Geoscience Instrument Corp., Mt. Vernon, NY). The sieves were shaken for 10 minutes at a constant rate (250 rpm) and the fraction of powder collected between the two sieves was stored in a vacuum desiccator over P<sub>2</sub>O<sub>5</sub> at 25 °C until further use. Table 14 shows the API chemical structure, molecular weight and reported approximate water solubility (in 25°C purified water) used in assessment of *in-vitro* capsule performance and maximum powder fill achieved with one component formulations. A one component formulation is defined as powder composition consisting of only one chemical entity.

Table 14: List of APIs, their molecular weight, literature reported water solubility, and maximum powder fill achieved in cellulose capsule filling.

| Chemical structure                                                                  | Molecular weight<br>(g/mole) | Water solubility at<br>25°C<br>(mg/ml) <sup>a</sup> | Maximum powder fill<br>achieved with<br>API (mg) |
|-------------------------------------------------------------------------------------|------------------------------|-----------------------------------------------------|--------------------------------------------------|
| KCl<br>Potassium Chloride                                                           | 74.18                        | > 250                                               | 800                                              |
|    | 292.63                       | ≈ 500                                               | 700                                              |
| Diphenhydramine HCl                                                                 |                              |                                                     |                                                  |
|   | 298.44                       | ≈ 500                                               | 650                                              |
| Tramadol HCl                                                                        |                              |                                                     |                                                  |
|  | 122.12                       | > 100                                               | 550                                              |
| Niacinamide                                                                         |                              |                                                     |                                                  |
|  | 151.17                       | ≈ 10                                                | 450                                              |
| Acetaminophen                                                                       |                              |                                                     |                                                  |
|  | 254.38                       | < 1                                                 | 450                                              |
| Ketoprofen                                                                          |                              |                                                     |                                                  |

<sup>a</sup> Taken from references [108] [109]

### Capsule filling and sealing

Dry milled powders were filled into the capsule body manually using a spatula and the API was compacted using a stainless steel metal plunger (8 mm in diameter) in order to achieve maximum fill. The cap was then fit on to the powder filled body and sealed using a light application of methylolcellulose solution around the region where the cap and body came in contact. All powder filled capsules were stored in vacuum desiccators at room temperature prior to use.

### Determination of water solubility of the APIs

The water solubility of all the APIs utilized in capsule performance was determined by loading excess solid API into 20 ml scintillation vials containing 10 – 15 ml deionized water. The scintillation vials were placed in 37 °C water bath and shaken for 72 hrs. The vials were then removed and placed in a sonication bath (operating at 37 °C) until the solid and liquid phase separated and the liquid phase was extracted through a 0.22 µm filter and subsequently diluted in purified water. The API concentrations were determined by the analytical method listed in the proceeding section. All measurements were carried out in triplicate.

### *In-vitro* release studies from capsules

All *in-vitro* API release studies from capsules were performed in a Hansen Research™ SR8 6 station dissolution system (Hansen Research™ Corp., Chatsworth,



CA), attached to an automated temperature controller and a rotor employing a USP paddle apparatus [110]. The capsules were placed in 2 x 6 cm cylindrical mesh baskets. The purpose of the basket was to provide an effective means to submerge the capsule (sinker) in the medium for the duration of the experiment. All dissolution vessels contained 900 to 1000 ml dissolution medium and were equilibrated to 37°C in an external water bath prior to each experiment. At predetermined time intervals 0.1 to 0.5 ml aliquots were withdrawn from the medium and replaced with fresh stock medium. The samples were diluted subsequently with either purified water (for potassium chloride assay) or with the respective mobile phase utilized in the analytical procedure mentioned in the next section, for each API. All samples were withdrawn using a syringe attached to a 0.45 µm filter. All drug release studies were conducted in triplicates.

To analyze the influence of drug aqueous solubility on its release from release from cellulose capsules, the release of dry powder fill capsules was examined in the dissolution apparatus described above. Release of KCl, diphenhydramine HCl, tramadol HCl, niacinamide, acetaminophen and ketoprofen was examined from cellulose capsules in 900 ml purified water at a paddle speed of 100 rpm.

To investigate the process of drug release from cellulose capsules in the gastrointestinal tract, additional release studies were conducted with the capsules filled with dry powders, suspensions and solutions of API. These studies were performed using potassium chloride and acetaminophen filled capsules. The dry powder capsules were prepared as described above, while suspension fill was achieved by first adding 300 mg of dry powder and then 1 ml of the drug solution. Solution fills was achieved by only filling the capsule body with solution of the API. Solution of KCl was prepared by

dissolving 7 grams in 20 ml purified water while the solution of acetaminophen was prepared by dissolving 0.3 grams in 20 ml purified water. The solutions were prepared in 20 ml glass scintillation vials held in a sonication bath operating at 37 °C. These solutions were equilibrated at 37 °C for 24 hours prior to filling. The caps were immediately placed over the capsules body after adding solution and then sealed using a light application of methylcellulose. Drug release from these capsules was immediately examined in order to minimize solvent leaching.

To verify the effect of osmotic pressure as a mediator for drug release from cellulose capsules, the release of water soluble APIs was examined in a release medium with variable urea concentrations. Potassium chloride release was examined in 1.25, 2.51, 3.75 and 4.55 M urea media. Diphenhydramine release was examined in 1.25, 2.51 and 3.75 M urea media. Tramadol HCl release was examined in 0.67, 1.65 and 2.51 M urea medium. Niacinamide release was examined in 0.25, 0.75 and 1.25 M urea media. All release studies were performed with a paddle speed of 100 rpm at 37 °C.

To analyze the effect of pH changes in the gastro-intestinal tract on the release of API from cellulose capsules, release studies with capsules containing dry ketoprofen were performed in 1000 ml 0.2 M pH 2.2 HCl/KCl buffer and in 0.2 M pH 7.4 phosphate buffer release medium, at 37°C. The agitation speed of the paddles was set at 100 rpm. Ketoprofen exhibits pH dependent solubility where solubilities of 0.28 mg/ml in pH 4.0 and 40.00 mg/ml in pH 6.8 media are reported [111].

To assess the influence of *in vivo* agitation conditions, release of potassium chloride and acetaminophen was measured in purified water at 37°C with paddle speed settings of 50, 100 and 150 rpm. The amount of KCl and acetaminophen filled into the

capsules was held constant.

#### Osmotic pressure of urea and saturated API solutions

The osmotic pressure can be estimated indirectly by measuring other colligative properties such as vapor pressure [70]. Vapor pressure of purified water and aqueous saturated solutions of API as well as known concentrations of aqueous urea solutions was determined in a sealed round bottom flask attached to a vacuum machine (Labconco Freezone 4.5, Labconco Corp, Kansas City, MO) and a digital pressure gauge (Vernier Gas Membrane Pressure Sensor GPS-BTA, Vernier Software and Technology, Beaverton, OR) via a 3-way glass tube with end valves. All solutions were prepared in 100 ml volumetric flasks and loaded in to the round bottom flask, prior to sealing it. The entire experimental setup was placed in a freezer (Amana Model ESU17D, Benton Harbor, MI) at  $-25^{\circ}\text{C}$  with the vacuum line disconnected and the respective valve closed. Upon freezing the samples for 6 hours, setup was removed from the freezer and the vacuum line was connected and the respective valve opened till the vacuum system displayed a stable 0.2 mBar reading. The samples in the round bottom flask were then thawed in a  $37^{\circ}\text{C}$  self-contained heating water bath (RM6 Lauda Brinkman, Lauda Brinkmann Corp., Delran, NJ) while disconnected from the vacuum line. Each sample was thawed for 3 hours. The whole setup was then placed in a thermostatic oven (Precision Model STM 80, Precision Instruments, Des Plaines, IL) operating at  $37^{\circ}\text{C}$  with the pressure gauge turned on. The vapor pressure of water was recorded once the pressure gauge displayed a stable value. The whole process was repeated three times and an average of three runs utilized to calculate the osmotic pressure. Vapor pressure of purified water was measured to be  $46.99 \pm 0.02$  mmHg which was close to the literature

reported value of 47.07 mmHg, at 37°C [112]. The osmotic pressure ‘ $\pi$ ’ of the saturated API solutions and known concentrations of aqueous urea solutions were determined using the following relationship [70]:

Equation 24 
$$\pi = \frac{R T}{V^0} \ln \left\{ \frac{p^0}{p} \right\}$$

where, ‘R’ is the universal gas constant (82.09 cm<sup>3</sup> atm K<sup>-1</sup> mol<sup>-1</sup>), ‘T’ is the absolute temperature of the system (310.15 K), ‘V<sup>0</sup>’ is the molar volume of water (18.17 cm<sup>3</sup>/mole) at 310.15 K, ‘p<sup>0</sup>’ is the vapor pressure of purified water at 310.15 K and ‘p’ is the vapor pressure of water vapor from saturated API solution or known concentrations of urea solution at 310.15K. The entire process is schematically presented in Figure 33.

#### Permeability of APIs through RC films

Permeability of the APIs from capsules was compared with the permeabilities of the APIs through RC films. The RC films were prepared using glass test tube molds (25 mm x 15 cm) in order to obtain films that were large enough to cover the orifice opening of Side-by-Side glass diffusion cells. Transport studies of APIs through RC films were conducted using dual chambered ‘Side-Bi-Side’ horizontal glass diffusion cells (Figure 5, PermeGear Inc., Hellertown, PA) with an orifice opening of 1.7 cm<sup>2</sup> and a cell volume of 8 ml. The temperature in each cell was maintained at 37 ± 0.5°C using circulating water bath attached to a water heater (RM 6 Lauda, Lauda Brinkmann L.L.C, Delran, NJ). The stirring rate within the diffusion cells was maintained at approximately 600 rpm using magnetic stir bars. The concentration of KCl, diphenhydramine HCl, tramadol HCl and niacinamide in the donor cell were maintained at 0.1 M by periodic replacement with

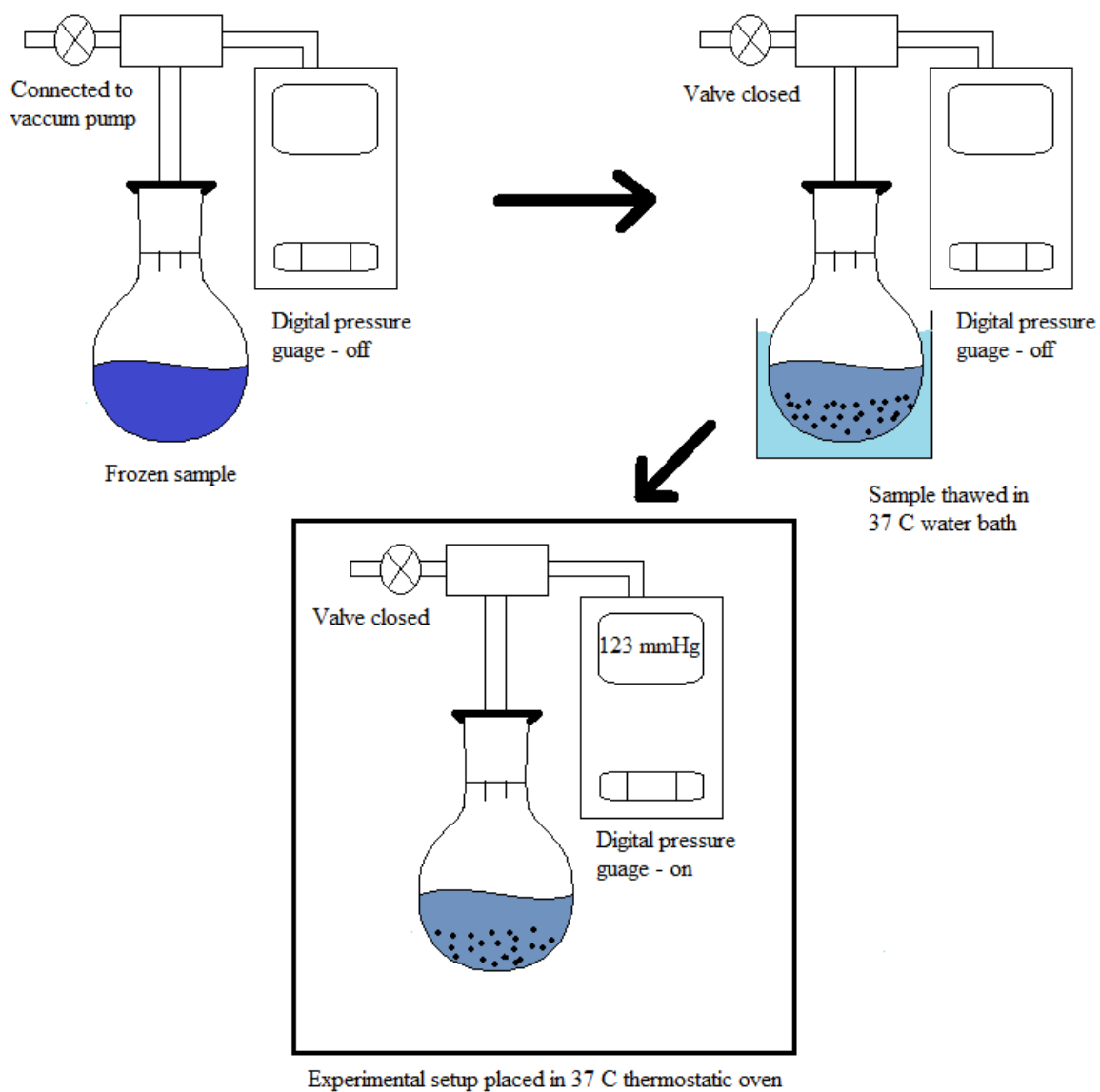


Figure 33: Schematic representation of method utilized in determining vapor pressure of water vapor above liquid gas interface of purified water, saturated API solutions and known concentrations of aqueous urea solutions.

fresh stock solution, while the receiver cell was emptied at predetermined time intervals and replaced with purified water. For acetaminophen and ketoprofen, saturated solutions were utilized in the donor cell.

### Analytical methods

Potassium chloride concentrations were determined using a potassium-ion selective electrode (Cole Parmer, Vernon Hills, IL) attached to a pH meter (Orion™ Model 420A, Cole Parmer, Vernon Hills, IL) operating in potential difference measurement mode (mV). All samples were pre-conditioned to room temperature prior to analysis. Calibration curves were prepared using potassium ion concentrations in the range of 10 to 0.001 M in purified water as well as in aqueous urea solutions up to 5 M. Concentrations of diphenhydramine HCl, tramadol HCl, niacinamide, acetaminophen, and ketoprofen were determined using reversed phase high pressure liquid chromatographic (HPLC) method provided in USP 23 [81]. Two different Shimadzu (Shimadzu Corporation, Kyoto, Japan) HPLC systems were employed for the analysis of solute concentrations. The 6 series HPLC system consisted of a system controller (LC-6A), a pump (SIL-6A), an automated sample injector (SIL-9B), an ultraviolet-visible spectrophotometric detector (SPD -6A) and an analog data processor/ recorder (CR-5A). The 10 series Shimadzu HPLC system consisted of a system controller (LC-10A), a pump (SIL-10A), an automated sample injector (SIL-10A), an ultraviolet-visible spectrophotometric detector (SPD -10AV) and an analog data processor/ recorder (CR-501). All samples were eluted in isocratic mode. The types of columns, mobile phase compositions and HPLC settings employed for each analyte are listed in Table 15. All

Table 15: Summary of HPLC settings and column specifications utilized in analysis of API concentrations

| Analyte             | Mobile phase composition                                            | Flow rate | Column                                                                                   | Injection volume | UV wavelength | HPLC system        |
|---------------------|---------------------------------------------------------------------|-----------|------------------------------------------------------------------------------------------|------------------|---------------|--------------------|
|                     | (v/v)                                                               | (ml/min)  |                                                                                          | ( $\mu$ l)       | (nm)          |                    |
| Diphenhydramine HCl | Acetonitrile: water: triethylamine: glacial acetic acid (48:48:1:3) | 1.50      | C <sub>8</sub> (5 $\mu$ , 15 x 4.6 mm) Supelco <sup>®</sup> , Bellefonte, PA             | 2.5              | 229           | Shimadzu 6 series  |
| Tramadol HCl        | Methanol: water: glacial acetic acid: triethylamine (25:70:5:0.1)   | 0.25      | C <sub>8</sub> (3 $\mu$ , 50 x 3 mm) Phenomenex <sup>®</sup> Gemini, Torrance, CA        | 2                | 274           | Shimadzu 10 series |
| Acetaminophen       | Methanol: water (20:80)                                             | 1.50      | C <sub>18</sub> (5 $\mu$ , 300 x 1.5 mm) Waters <sup>™</sup> $\mu$ Bondpack, Milford, MA | 2                | 243           |                    |
| Niacinamide         | Methanol: 0.005 M aqueous sodium 1-heptanesulfonate (35:65)         | 2.00      |                                                                                          |                  | 254           |                    |
| Ketoprofen          | Acetonitrile: water: glacial acetic acid (42:55:3)                  | 1.00      | C <sub>18</sub> (5 $\mu$ , 250 x 4.6 mm) Zorbax Rx, Mac-Mod Analytical, Chadds Ford, PA  | 1                | 233           | Shimadzu 6 series  |

components of the mobile phase were thoroughly mixed for 10 minutes and filtered through a 0.45  $\mu\text{m}$  nylon membrane (Chrom Tech, Inc., Apple Valley, MN), followed by degassing in a sonication bath (Bransonic Ultrasonic cleaner, Model 5200, Bransonic Corporation, Danbury, CT) for 30 minutes. Standards for all the APIs were prepared in the ranges of 0.005 to 0.1 mg/ml. Standards were analyzed in triplicates and the relative standard deviation of the slopes of the calibration curve were never more than 1 %. Analysis of all samples was carried out at room temperature.

## **Results and Discussion**

### Fabrication of capsules

The preliminary objective of this section was to develop a method to repeatedly fabricate mechanically stable/intact capsule halves with high precision in terms of the dry capsule wall thickness. Mold pin rotation time and cellulose concentration were the two variables initially investigated. Three cellulose concentrations were utilized for improving the reproducibility of capsule shells; 2.2%, 3.3% and 4.4% w/w cellulose in methylcellulose solution. Figure 34A shows the thickness of capsule shells fabricated following one application of methylcellulose solution after 3, 5, 8, 10, 15, 20, 25 and 30 minutes of pin rotation using 2.2, 3.3 and 4.4 % w/w methylcellulose solution. The orange and yellow bars indicate FTA and FTB, respectively, while the green bar represents capsules with intact shell integrity following capsule shell ejection from mold pins. The relative standard deviation of dry capsule wall was used to monitor the precision of the capsule fabrication process in terms of dry shell thickness. Figure 34B shows the relative standard deviation of capsule shell thickness as a function of mold pin rotation time using 2.2, 3.3 and 4.4 % w/w methylcellulose solution. As the rotation



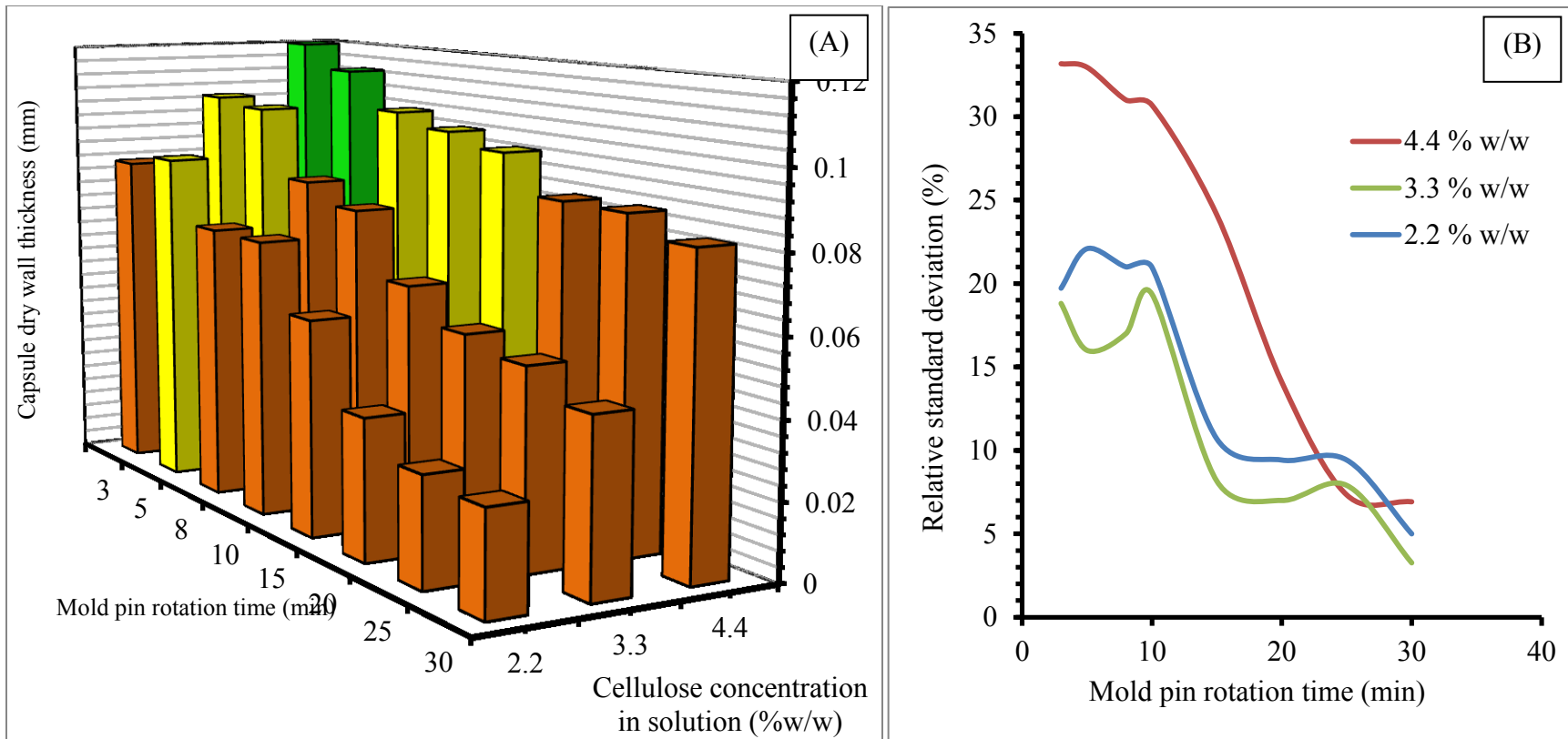


Figure 34: (A) Influence of mold pin rotation time and cellulose concentration, on the capsule dry wall thickness, (B) Relative standard deviation (n=6) of capsule wall thickness as a function of mold pin rotation time using MC solution with 4.4, 3.3 and 2.2 % w/w cellulose. Green bars represent formation of intact capsule shell, yellow bars represent FTB and orange bars represent FTB

|                        |                                                          |
|------------------------|----------------------------------------------------------|
| ■ Failure type A (FTA) | : Capsule wall tearing                                   |
| ■ Failure type B (FTB) | : Capsule collapsing leaving behind a distinctive crease |
| ■ Intact capsules      |                                                          |
| n = 6                  |                                                          |

time of the mold pins increased, the capsule shell thickness decreased. The variability in shell thickness also decreased with increasing rotation time. The large variability observed in thickness of the capsule walls prepared from 4.4 % w/w solution can be attributed to the viscous nature of methylolcellulose solution and uneven coating along the mold pin surface. Although intact capsule shells were fabricated using 4.4% w/w solution with short mold pin rotation times (< 5 minutes), these capsules could not be utilized for release studies owing to high variability in the shell thickness. Increasing the rotation time using 4.4% w/w solution also led to increased FTA and FTB. It was discovered that rotating the mold pins for 30 minutes lead to the fabrication of shell walls with relatively high precision (thickness relative standard deviation  $\leq 6\%$ ). Based on these results, the application of multiple dip coatings was investigated with mold pin rotation time of 30 minutes after each coating of 4.4% methylolcellulose solution in order to improve the mechanical stability of the dry capsule shells.

Figure 35A shows the thickness of capsules shells with up to seven applications of methylolcellulose coatings, using 2.2, 3.3 and 4.4% w/w methylolcellulose solution, with mold pin rotation time of 30 minutes after each coating application. Figure 35B shows the relative standard deviation in shell thickness as a function of number of applications of methylolcellulose solution. The capsule shell thickness increased as the number of applications increased while the relative standard deviation decreased from 12% to 5%, irrespective of the concentration of cellulose utilized. Both FTA and FTB were observed using 2.2% and 3.3% w/w methylolcellulose solutions, however, using 4.4% w/w methylolcellulose solution with three coatings and higher, led to the fabrication of mechanically stable and intact capsules. It was discovered that

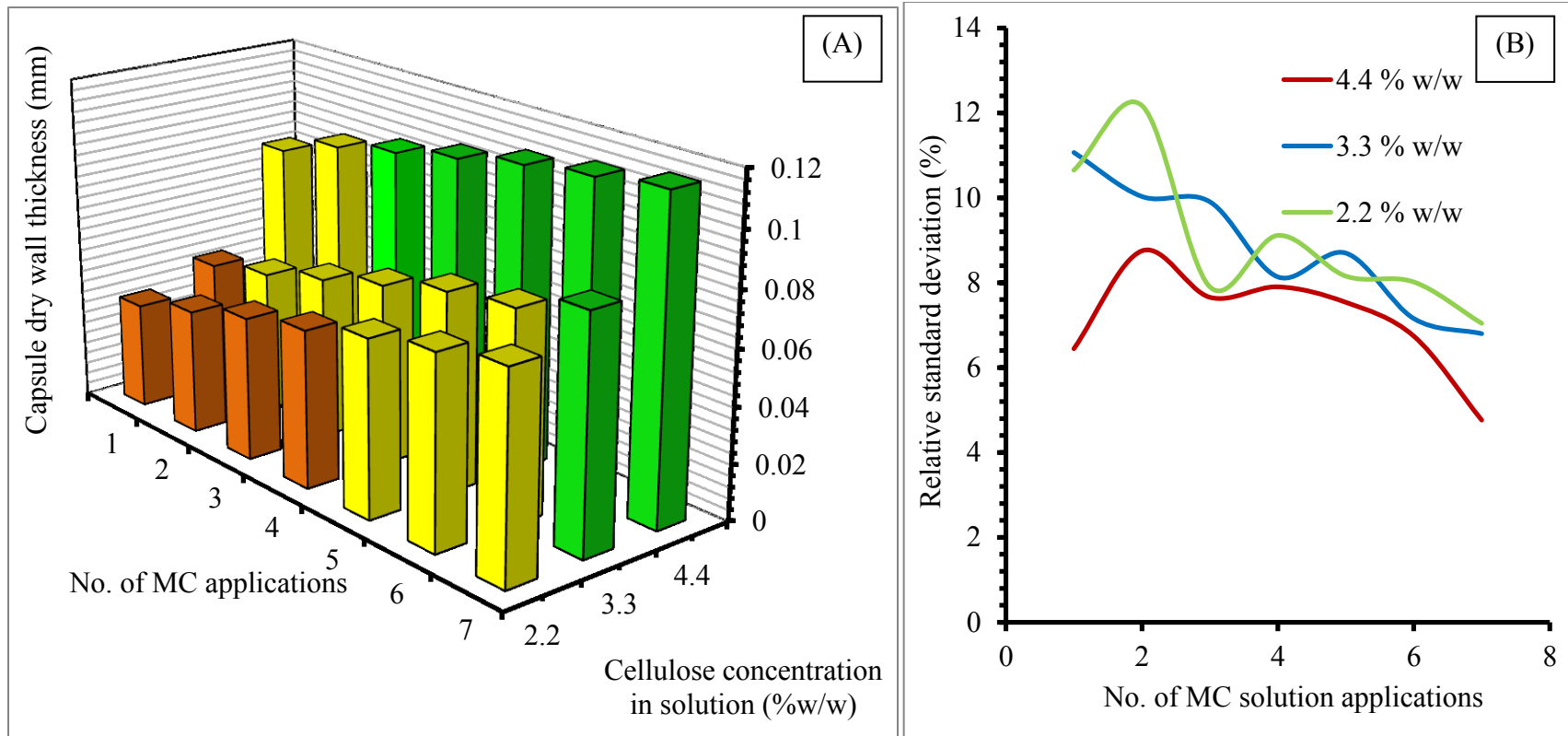


Figure 35: (A) Influence of number of applications and cellulose concentration, on the capsule dry wall thickness, (B) Relative standard deviation (n=6) of capsule wall thickness as a function of no. of coating applications, using MC solutions with 4.4, 3.3 and 2.2% w/w cellulose. Green bars represent formation of intact capsule shell, yellow bars represent FTB and orange bars represent FTA

|                        |                                                          |
|------------------------|----------------------------------------------------------|
| ■ Failure type A (FTA) | : Capsule wall tearing                                   |
| ■ Failure type B (FTB) | : Capsule collapsing leaving behind a distinctive crease |
| ■ Intact capsules      |                                                          |
| n = 6                  |                                                          |

minimum thickness of 0.10 mm was required in order to achieve mechanically stable capsule shells that can withstand the ejection process.

Figure 36A shows a photograph of a typical capsule body and cap fabricated using the described reproducible procedure. Both capsule halves appeared nearly transparent. The typical dimensions of the capsule, when fit together, are shown in Figure 36B and summarized in Table 16. The powder fill volume within the cellulose capsule, when assembled, ( $1.20 \text{ cm}^3$ ) was similar to the fill volume in most commonly utilized hard shell gelatin capsules of size 000 ( $1.37 \text{ cm}^3$ ) [50].

#### Drug release and its dependence on enclosed API solubility

Figure 37 shows the release profiles of potassium chloride (KCl), diphenhydramine HCl, tramadol HCl, niacinamide, acetaminophen and ketoprofen from cellulose capsules in purified water at  $37^\circ\text{C}$ . Each capsule consisted of API powder alone and no attempt was made to modulate its release from the core. These APIs were selected to study the performance of the capsule for contents with water solubilities encompassing a wide range of values. Release of water soluble KCl, diphenhydramine HCl and tramadol HCl showed a sigmoidal pattern with nearly 75 % of the enclosed API was released within 6-8 hours, while niacinamide, acetaminophen and ketoprofen were released from the capsules at slower rates. All APIs show zero order release profiles for a large fraction of the amount enclosed, however, some of the water soluble APIs do show a lag phase prior to reaching zero order state. Table 17 lists the zero order release rates of the APIs and their measured solubility in purified water, at  $37^\circ\text{C}$ . The zero order release rates were determined by performing linear regression on the linear portion of the cumulative release vs. time data using Microsoft Excel. The zero order release rates of

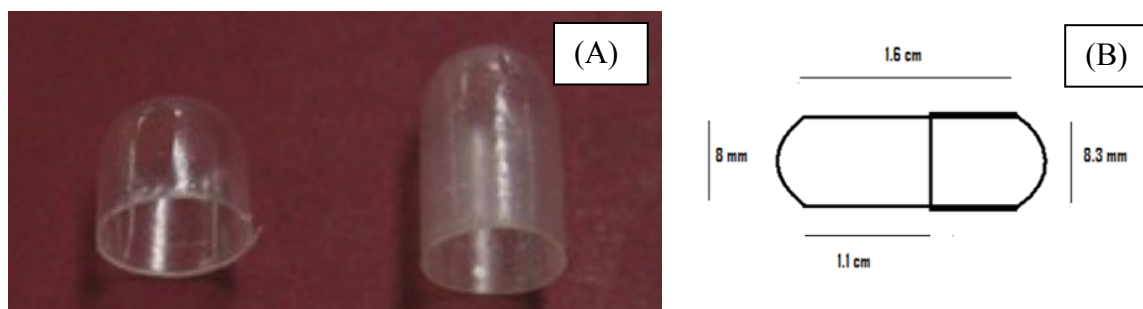


Figure 36: (A) Photograph of regenerated cellulose telescoping capsule halves fabricated using dip coating approach followed by solvent non-solvent phase inversion/precipitation process, and (B) schematic representation of capsule dimensions following assembly of the capsule ‘body’ and ‘cap’

Table 16: Measured capsule cap and body dimensions and estimation of core volume and exterior surface area of an assembled cellulose capsule.

| Length (cylinder) |      | Inner diameter |      | Powder fill volume | External surface area |              |
|-------------------|------|----------------|------|--------------------|-----------------------|--------------|
| Cap               | Body | Cap            | Body |                    | Total                 | Overlap zone |
| (cm)              |      | (cm)           |      | (cm <sup>3</sup> ) | (cm <sup>2</sup> )    |              |
| 0.50              | 1.60 | 0.83           | 0.80 | 1.20               | 2.91                  | 0.55         |

KCl, diphenhydramine HCl, tramadol HCl, niacinamide, acetaminophen and ketoprofen were 198.56, 213.97, 133.97, 133.26, 34.43, 3.82 and 0.038 mg/h, respectively, in 37°C purified water, while their measured solubilities were  $356.81 \pm 6.94$ ,  $739.45 \pm 21.17$ ,  $547.79 \pm 7.23$ ,  $117.36 \pm 4.73$ ,  $21.45 \pm 0.96$  and  $0.25 \pm 0.05$  mg/ml, respectively, in 37°C purified water. The zero order release rates and the solubility data were normalized to the respective API molecular weights. Figure 39 compares the zero order release rates vs. the solubility of the APIs in 37°C purified water. As the solubility of the APIs increased, the zero order release rate also increases. A non-linear increase in zero order rates indicates that as the solubility of the API increases multiple mechanisms may be involved in its release from the capsule core. Since RC films described in the previous chapter were found to transport solutes via pores, it is likely that the water soluble APIs release may be occurring by osmotic as well as diffusive mechanisms. The contributions of these two mechanisms will be further examined in the proceeding sections.

#### Process of API release from capsules

Savastano et al. described the sigmoidal pattern of drug release from porous polymeric-membrane-coated tablets to involve a multi-step process of the external medium accessing the core through hydrated membranes, followed by dissolution of the solid core which eventually results in drug release through the porous pathways [113]. To investigate if a similar process of API release occurred from cellulose capsules, the initial conditions in the capsule core were altered by filling the capsules with different phases of the API (solid, suspension and liquid). Potassium chloride and acetaminophen were chosen in order to examine the release of highly and moderately water soluble APIs from the capsules, respectively. Figure 39 shows the KCl release profiles from capsules filled

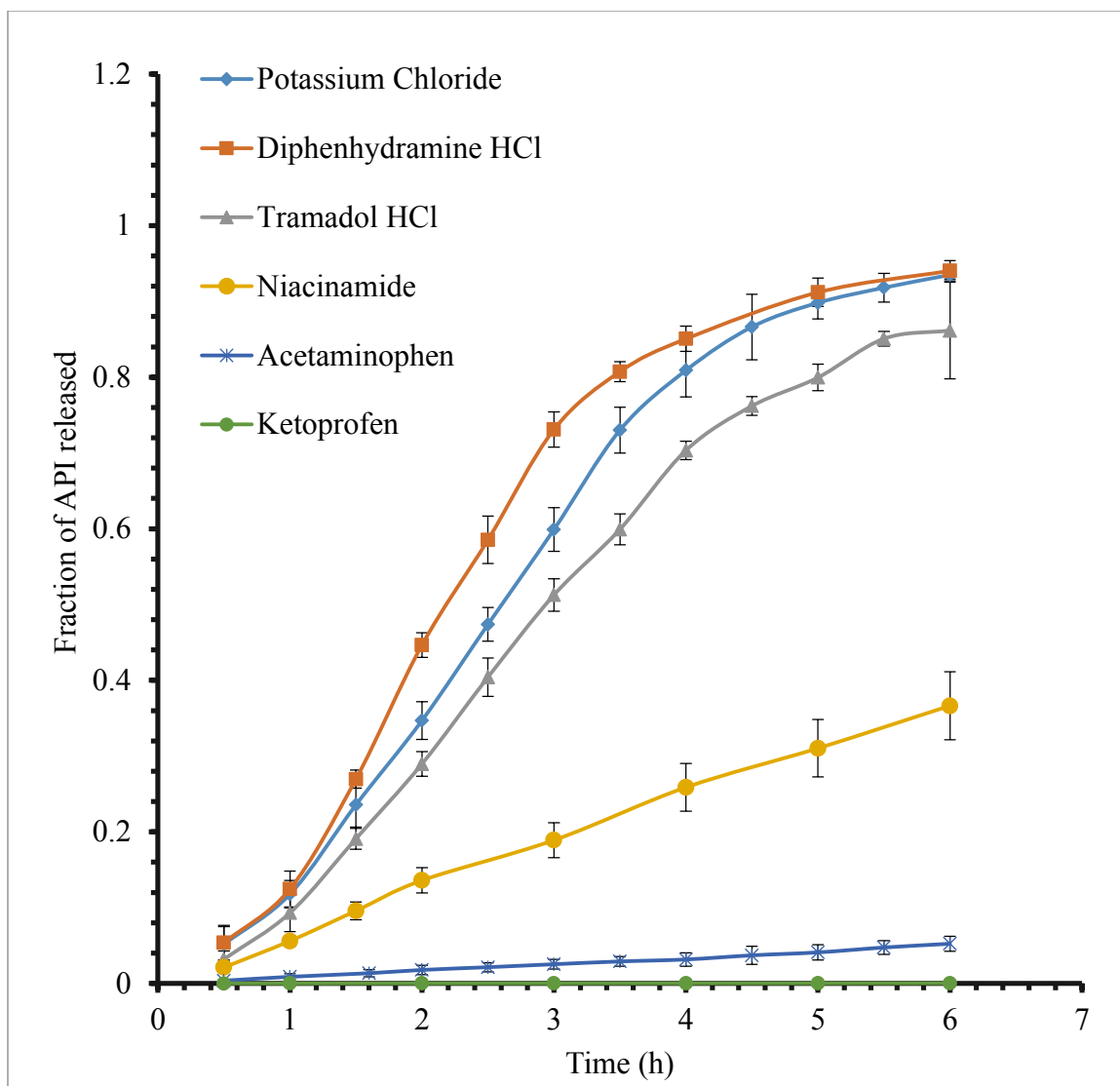


Figure 37: Release profiles of potassium chloride (800 mg), diphenhydramine HCl (700 mg), tramadol HCl (650 mg), niacinamide (550 mg), acetaminophen (450 mg) and ketoprofen (450 mg) from cellulose capsules in purified water at 37 °C.



Table 17: Measured solubility and zero order release rates of the APIs from cellulose capsules, in purified water at 37°C.

| API                 | Molecular weight | Solubility <sup>a</sup> |        | Zero order release rates |                              |
|---------------------|------------------|-------------------------|--------|--------------------------|------------------------------|
|                     | (g/mole)         | (mg/ml, n=3)            | (M)    | (mg/h)                   | (mole/h, x 10 <sup>5</sup> ) |
| Potassium Chloride  | 74.18            | 356.81 ± 6.94           | 4.81   | 198.56                   | 267.67                       |
| Diphenhydramine HCl | 292.63           | 739.45 ± 21.17          | 2.52   | 213.97                   | 73.12                        |
| Tramadol HCl        | 298.44           | 547.79 ± 7.23           | 1.83   | 133.26                   | 44.65                        |
| Niacinamide         | 122.12           | 177.36 ± 4.73           | 1.45   | 34.43                    | 28.19                        |
| Acetaminophen       | 151.17           | 21.45 ± 0.96            | 0.14   | 3.82                     | 2.53                         |
| Ketoprofen          | 254.38           | 0.25 ± 0.05             | 0.0011 | 0.015                    | 0.0059                       |

<sup>a</sup> Measured at 37 °C in purified water

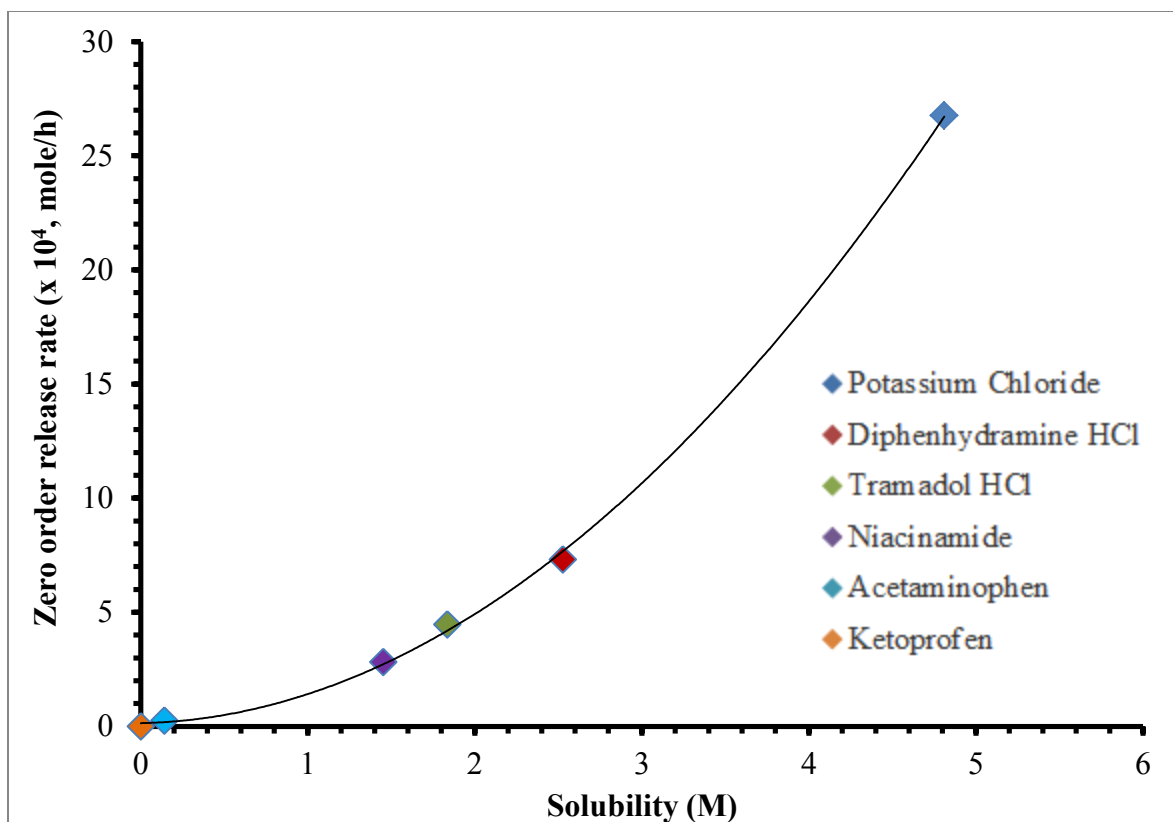


Figure 38: Comparison of API zero order release rates (moles/h) from cellulose capsules vs. their solubility (M) in purified water at 37 °C.

with 800 mg dry KCl powder, suspension containing 650 mg KCl, and solution with 350 mg KCl. The capsules filled with dry KCl powder and a combination of dry powder and solution show an extended zero order release phase with release rates equivalent to 191.66 and 202.61 mg/h, respectively, while the capsule filled with KCl solution showed an initial linear release pattern followed by non-linear release phase for the majority of the release interval. The similarity of drug release rates from solid fill and suspension fill capsules indicates that the presence of a saturated core of API solution is required in order to maintain zero order release phase.

Figure 40 shows acetaminophen release from cellulose capsules filled with 450 mg dry acetaminophen powder, suspension containing 315 mg total acetaminophen, and solution of 15 mg acetaminophen. Analogous to KCl, acetaminophen shows similar zero order release rates between capsules filled with dry powder (3.65 mg/h) and suspension fill (4.10 mg/h). Also, the acetaminophen solution filled capsules show an initial linear release pattern followed by a non-linear release phase. However, unlike KCl, acetaminophen solid fill capsules do not show an initial lag phase, when compared to acetaminophen suspension filled capsules. These results indicate that a very water soluble API, like KCl, possibly draws more water from the external medium than a moderately soluble acetaminophen in order to develop a saturated API core in the capsule, prior to reaching a zero order release phase.

#### Verification of osmotic mechanism for release of water soluble APIs

The hydrophilic nature of cellulose and the pore forming capability of the cellulose films suggests that water soluble API (KCl, diphenhydramine HCl, tramadol

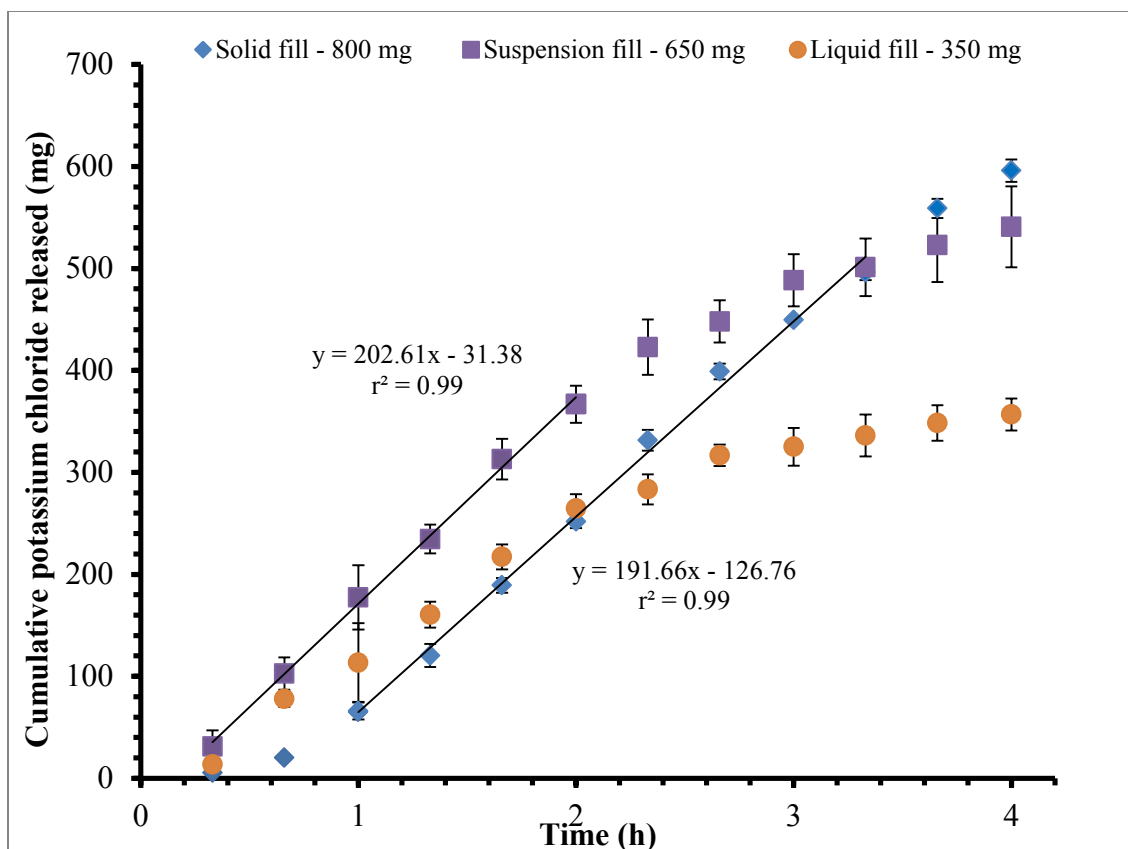


Figure 39: Comparison of potassium chloride release profiles from capsule cores filled with 800 mg dry powder (solid fill), combination of 300 mg dry powder with 1 ml 350 mg/ml solution (suspension fill), and 1 ml of 350 mg/ml solution (liquid fill) in purified water at 37°C.

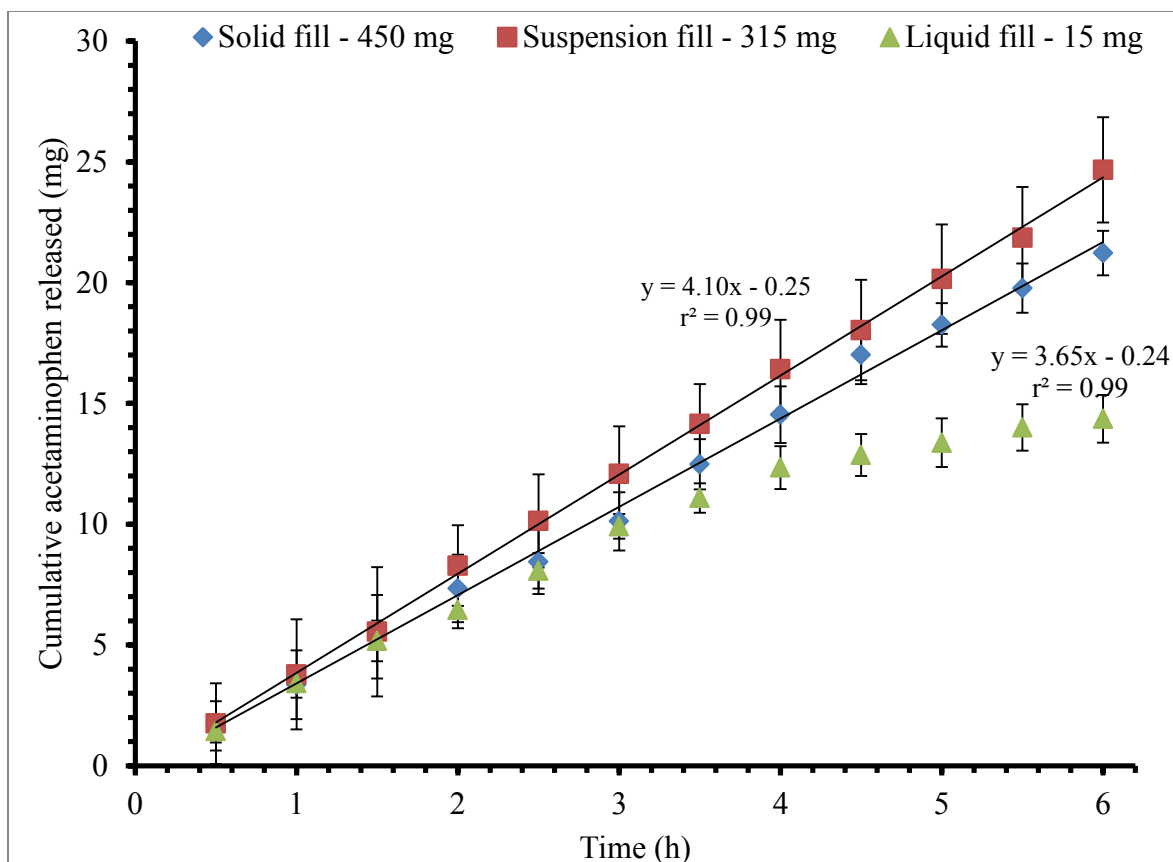


Figure 40: Comparison of acetaminophen release profiles from capsule cores filled with 450 mg dry powder (solid fill), combination of 300 mg dry powder with 1 ml 15 mg/ml solution (suspension fill), and 1 ml of 15 mg/ml solution (liquid fill) in purified water at 37°C.

HCl and niacinamide) release can proceed via osmosis as well as diffusion through the cellulose capsule walls. To determine if the osmotic mechanism contributed to release of these water soluble APIs, their release from cellulose capsules was investigated in release media with varying urea concentrations. Urea solutions were utilized as osmotic pressure modulators in the external medium owing to urea's chemically inert nature. Plots of the cumulative amounts of KCl released in 1.25, 2.51, 3.75 and 4.55 M urea solutions, and diphenhydramine HCl released in 1.25, 2.51 and 3.75 M urea solutions, from cellulose capsules at 37°C are shown in Figure 41. Plots of the cumulative amounts of tramadol HCl released in 0.67, 1.65 and 2.51 M urea solutions and niacinamide released in 0.25, 0.75 and 1.25 M urea solutions from cellulose capsules at 37°C are shown in Figure 42. Zero order release rates were observed in all the API release studies and zero order release rates for all the APIs decreased as the concentration of urea increased in the external medium. Osmotic pressures for the API and urea solutions were determined from water vapor pressures of purified water and water vapor pressure in saturated aqueous API solutions and known concentrations of aqueous urea solutions [70]. Table 18 lists the measured water vapor pressure from saturated aqueous API solutions and known concentrations of aqueous urea solutions, and the estimated osmotic pressures of these solution. The osmotic pressure of the APIs inside the capsule were considered equivalent to the osmotic pressure of the saturated API solutions as the formation of saturated API solution is considered in the capsule core during the zero order phase of its release. The osmotic pressure difference ' $\Delta\pi$ ' across the capsule shell was calculated using the following relationship [114]:

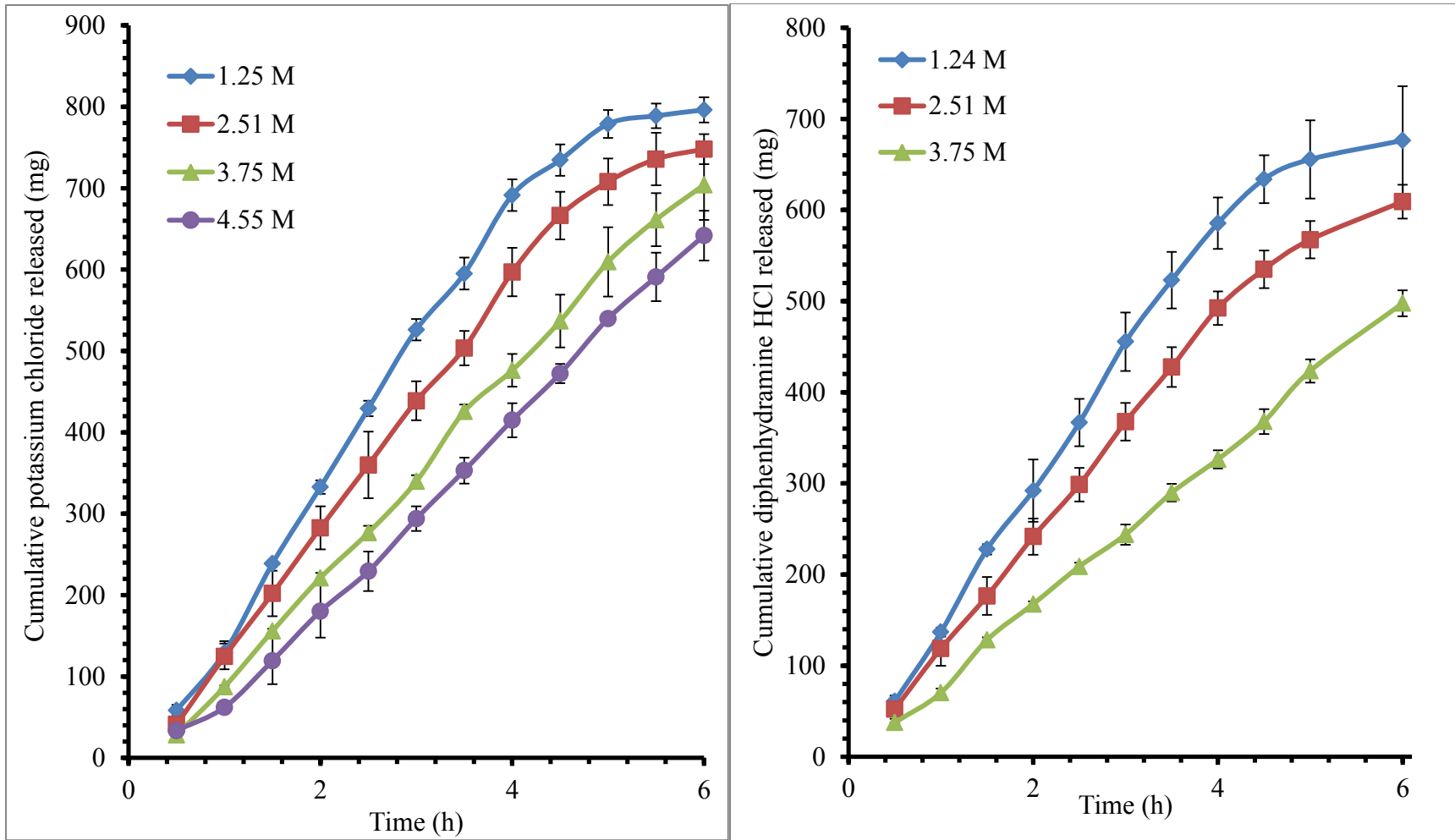


Figure 41: Release profiles of (A) potassium chloride (800 mg) in release media containing 1.25, 2.51, 3.75 and 4.55 M urea solutions and (B) diphenhydramine HCl (750 mg) in release media containing 1.24, 2.51 and 3.75 M urea solutions, at 37°C.

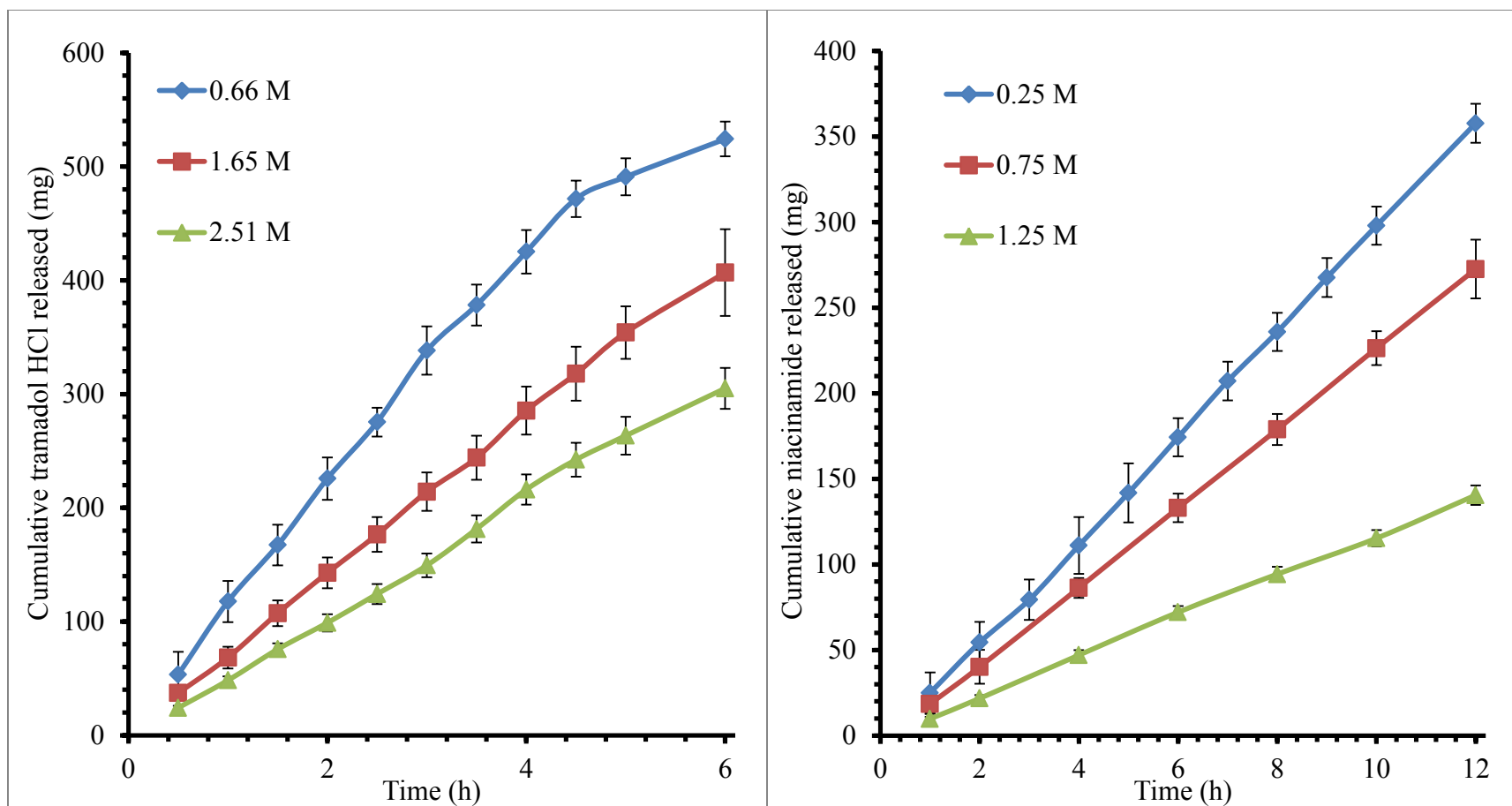


Figure 42: Release profiles of (A) tramadol HCl (650 mg) in release media containing 0.66, 1.65 and 2.51 M urea solutions and (B) niacinamide (550 mg) in release media containing 0.25, 0.75 and 1.25 M urea solutions, at 37°C.



Table 18: Measured vapor pressures of water vapor from saturated API solutions, known concentrations of urea aqueous solutions from three separate experimental runs and the estimated osmotic pressures of these solutions.

|                            | Concentration<br>(M) | Vapor pressure of water vapor in the sample holding flask |       |       |                    | Osmotic pressure<br>of the solution <sup>c</sup><br>$\pi$<br>(atm) |
|----------------------------|----------------------|-----------------------------------------------------------|-------|-------|--------------------|--------------------------------------------------------------------|
|                            |                      | Run 1                                                     | Run 2 | Run 3 | Average $\pm$ S.D. |                                                                    |
|                            |                      | $p$ (mmHg)                                                |       |       |                    |                                                                    |
| <b>Potassium chloride</b>  | 4.81 <sup>a</sup>    | 40.11                                                     | 40.09 | 40.08 | 40.09 $\pm$ 0.02   | 219.31                                                             |
| <b>Diphenhydramine HCl</b> | 2.52 <sup>a</sup>    | 43.15                                                     | 43.16 | 43.15 | 43.16 $\pm$ 0.01   | 116.31                                                             |
| <b>Tramadol HCl</b>        | 1.83 <sup>a</sup>    | 44.39                                                     | 44.36 | 44.38 | 44.38 $\pm$ 0.02   | 77.16                                                              |
| <b>Niacinamide</b>         | 1.45 <sup>a</sup>    | 45.71                                                     | 45.70 | 45.71 | 45.71 $\pm$ 0.01   | 35.79                                                              |
| <b>Urea</b>                | 4.55 <sup>b</sup>    | 43.48                                                     | 43.46 | 43.46 | 43.47 $\pm$ 0.01   | 106.17                                                             |
|                            | 3.75 <sup>b</sup>    | 43.99                                                     | 43.99 | 43.99 | 43.99 $\pm$ 0.00   | 89.41                                                              |
|                            | 2.51 <sup>b</sup>    | 44.89                                                     | 44.87 | 44.87 | 44.88 $\pm$ 0.01   | 61.46                                                              |
|                            | 1.65 <sup>b</sup>    | 45.52                                                     | 45.51 | 45.53 | 45.52 $\pm$ 0.01   | 41.53                                                              |
|                            | 1.25 <sup>b</sup>    | 45.83                                                     | 45.83 | 45.85 | 45.84 $\pm$ 0.01   | 31.82                                                              |
|                            | 0.75 <sup>b</sup>    | 46.26                                                     | 46.26 | 46.25 | 46.26 $\pm$ 0.01   | 19.05                                                              |
|                            | 0.67 <sup>b</sup>    | 46.32                                                     | 46.33 | 46.34 | 46.33 $\pm$ 0.01   | 16.83                                                              |
|                            | 0.25 <sup>b</sup>    | 46.67                                                     | 46.66 | 46.66 | 46.66 $\pm$ 0.01   | 6.79                                                               |

<sup>a</sup> Saturated API solutions

<sup>b</sup> Pre-prepared aqueous urea solutions

<sup>c</sup>  $\pi = \frac{RT}{V^0} \ln \left\{ \frac{p^0}{p} \right\}$ ,  $R = 82.09 \text{ cm}^3 \text{ atm K}^{-1} \text{ mol}^{-1}$ ,  $T = 310.15 \text{ K}$ ,  $V^0 = 18.17 \text{ cm}^3/\text{mol}$ ,  $p^0 = 46.99 \pm 0.02 \text{ mmHg}$

Equation 25

$$\Delta\pi = \pi_{API} - \pi_{urea}$$

where, ' $\pi_{API}$ ' is the osmotic pressure of the API solution inside the capsule core and ' $\pi_{urea}$ ' is the osmotic pressure of urea solution in the external medium. These osmotic pressure difference calculations are absolute values for a system where the API solution is separated from the solvent by a semi-permeable membrane that only allows water to permeate it. The calculated osmotic pressure differences and corresponding observed zero order release rates of potassium chloride, diphenhydramine HCl, tramadol HCl and niacinamide are listed in Table 19. A plot of zero order release rates vs. the osmotic pressure difference for the water soluble APIs is shown in Figure 43. As the osmotic pressure difference across the capsule shell is reduced, the zero order release rates decrease indicating that the release of water soluble APIs from cellulose capsules follows the osmotic mechanism for its release.

Contributions of osmotic and diffusive mechanisms to water soluble API release from capsules during the zero order phase

Theeuwes described the zero order drug release rate from a drug delivery system actuated by osmotic pressure to be the sum of contributions from the osmotic pumping and diffusion mechanisms, by the following equation [114]:

Equation 26

$$\left\{\frac{dM}{dt}\right\}_T = \left\{\frac{dM}{dt}\right\}_O + \left\{\frac{dM}{dt}\right\}_D$$

$$= \frac{A}{h} k \Delta\pi C + \frac{A}{h} C P_{device}$$

where, ' $(dM/dt)_T$ ' is the total zero order drug release rate from the device in purified water, ' $(dM/dt)_O$ ' is the zero order drug release rate due contributed by osmotic

Table 19: Calculated osmotic pressure differences and corresponding zero order release rates of potassium chloride diphenhydramine HCl, tramadol HCl and niacinamide from cellulose capsules in aqueous urea solutions at 37 °C

| API                 | Concentration of API in the core during zero order release phase | Concentration of urea in the external medium | Osmotic pressure difference <sup>a</sup> ' $\Delta\pi$ ' | Zero order release rate ' $\{dM/dt\}_T$ ' |
|---------------------|------------------------------------------------------------------|----------------------------------------------|----------------------------------------------------------|-------------------------------------------|
|                     | (M)                                                              | (M)                                          | (atm)                                                    | (mg/h)                                    |
| Potassium chloride  | 4.81                                                             | 0                                            | 219.31                                                   | 198.56                                    |
|                     |                                                                  | 1.25                                         | 187.49                                                   | 183.94                                    |
|                     |                                                                  | 2.51                                         | 157.85                                                   | 149.63                                    |
|                     |                                                                  | 3.75                                         | 129.90                                                   | 128.19                                    |
|                     |                                                                  | 4.55                                         | 113.14                                                   | 112.08                                    |
| Diphenhydramine HCl | 2.52                                                             | 0                                            | 116.31                                                   | 213.97                                    |
|                     |                                                                  | 1.25                                         | 84.49                                                    | 154.49                                    |
|                     |                                                                  | 2.51                                         | 54.85                                                    | 124.71                                    |
|                     |                                                                  | 3.75                                         | 26.90                                                    | 82.79                                     |
| Tramadol HCl        | 1.83                                                             | 0                                            | 77.16                                                    | 133.26                                    |
|                     |                                                                  | 0.67                                         | 60.33                                                    | 106.61                                    |
|                     |                                                                  | 1.65                                         | 35.63                                                    | 70.68                                     |
|                     |                                                                  | 2.51                                         | 15.70                                                    | 47.99                                     |
| Niacinamide         | 1.45                                                             | 0                                            | 35.78                                                    | 34.43                                     |
|                     |                                                                  | 0.25                                         | 29.00                                                    | 30.22                                     |
|                     |                                                                  | 0.75                                         | 16.74                                                    | 22.85                                     |
|                     |                                                                  | 1.25                                         | 3.97                                                     | 12.80                                     |
|                     |                                                                  |                                              |                                                          |                                           |

<sup>a</sup>  $\Delta\pi = \pi_{API} - \pi_{urea}$ , ' $\pi_{API}$ ' and ' $\pi_{urea}$ ' values were taken from Table 18

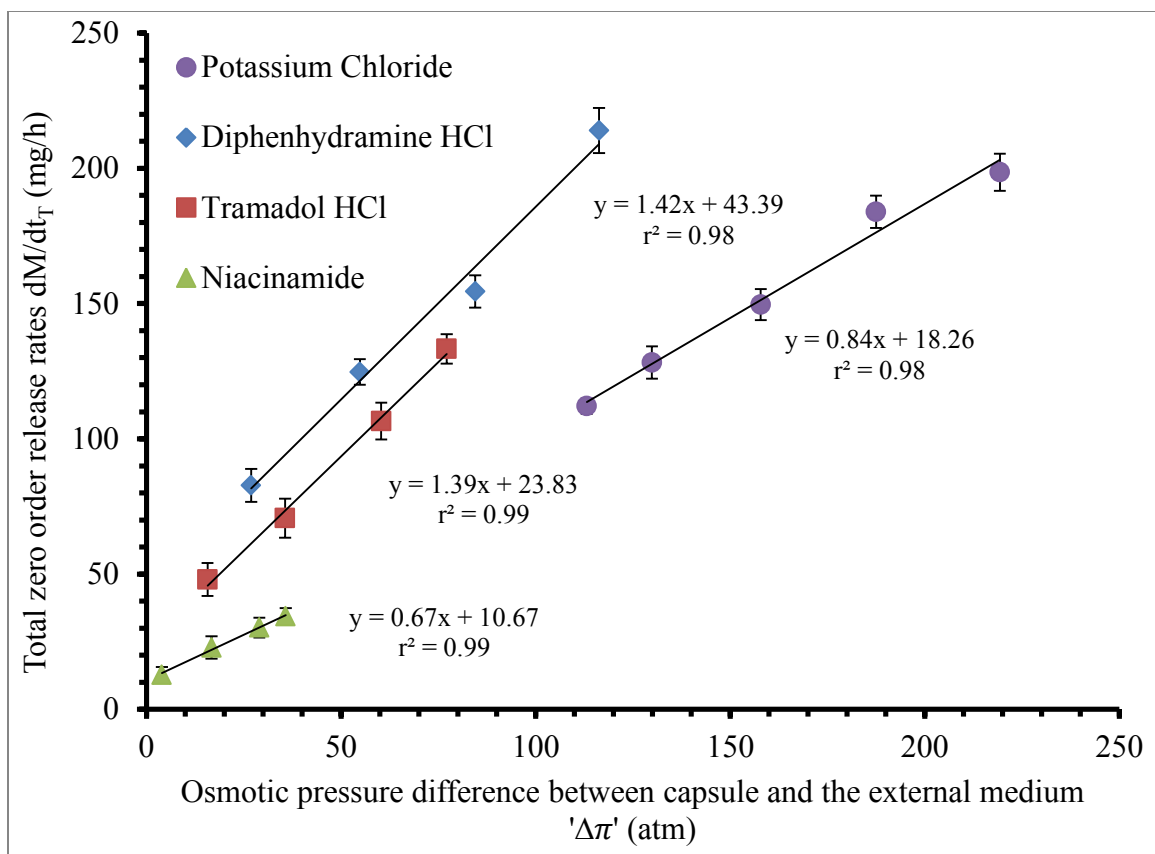


Figure 43: Comparison of total zero order release rates  $(dM/dt)_T$  of potassium chloride, diphenhydramine HCl, tramadol HCl and niacinamide with varying osmotic pressure difference  $'\Delta\pi'$  across cellulose capsule shell, at 37°C.

mechanism and  $(dM/dt)_D$  is the zero order drug release rate contributed by the diffusion mechanism, 'A' is the surface area of the device, 'h' is the thickness of the polymeric coating,  $\Delta\pi$  is the osmotic pressure difference between the device core and the external medium, 'k' is the fluid permeability of the drug solution under a pressure gradient and 'C' is the concentration of the solute in the device, and  $P_{\text{device}}$  is the apparent permeability coefficient of the solute through the membrane. The diffusive component in the above relation is the equivalent to the sum of diffusion occurring through the pores as well as the polymer phase [114]. The data presented in Figure 43 was in agreement with the above equation indicating that osmotic mechanism was involved in the release of water soluble APIs from the capsules. Linear regression was performed on the data presented in this plot, using Microsoft Excel™, and the results summarized in Table 20. Based on Equation 26, the intercept would present the zero order release rate contributed by diffusive mechanism ( $\frac{dM}{dt}_T = \frac{dM}{dt}_D$  when  $\Delta\pi = 0$ ). The diffusive component of the zero order release rates of KCl, diphenhydramine HCl, tramadol HCl and niacinamide were 18.27, 43.39, 28.47 and 9.79 mg/h respectively. By algebraic revision of Equation 26, the osmotic component of total zero order release rates were calculated by the following relation [114]:

Equation 27 
$$\frac{dM}{dt}_O = \left( \left\{ \frac{dM}{dt}_T \right\}_{\text{water}} - \frac{dM}{dt}_D \right)$$

where,  $\left\{ \frac{dM}{dt}_T \right\}_{\text{water}}$  is the zero order release rate of the API in purified water and  $\frac{dM}{dt}_D$  is the intercept from the linear regression of the total zero order release rate vs the osmotic pressure difference across the capsule presented in Figure 43. The osmotic component of

Table 20: Estimation of osmotic component of zero order release rate and fluid permeability, calculated from the linear regression parameters of the total zero order release rate ' $(dM/dt)_T$ ' vs. osmotic pressure difference ' $\Delta\pi$ ' across the capsule shell (Figure 43) when filled with potassium chloride, diphenhydramine HCl, tramadol HCl and niacinamide.

| API                 | Molecular weight | Linear regression parameters (Zero order release rate vs. osmotic pressure difference across the capsule) <sup>a</sup> |                                                |                              |       | Osmotic component of zero order release rate <sup>c</sup> |                              |
|---------------------|------------------|------------------------------------------------------------------------------------------------------------------------|------------------------------------------------|------------------------------|-------|-----------------------------------------------------------|------------------------------|
|                     |                  | Slope                                                                                                                  | Intercept $\left\{ \frac{dM}{dt_D} \right\}^b$ |                              | $r^2$ | (mg/h)                                                    | (x 10 <sup>-4</sup> , mol/h) |
|                     | (g/mole)         | (mg/h-atm)                                                                                                             | (mg/h)                                         | (x 10 <sup>-4</sup> , mol/h) |       |                                                           |                              |
| Potassium chloride  | 74.18            | 0.84                                                                                                                   | 18.27                                          | 2.46                         | 0.98  | 180.29                                                    | 24.30                        |
| Diphenhydramine HCl | 292.63           | 1.42                                                                                                                   | 43.94                                          | 1.49                         | 0.98  | 170.58                                                    | 5.82                         |
| Tramadol HCl        | 298.44           | 1.39                                                                                                                   | 23.84                                          | 0.80                         | 0.98  | 109.42                                                    | 3.66                         |
| Niacinamide         | 122.12           | 0.67                                                                                                                   | 10.67                                          | 0.87                         | 0.99  | 23.76                                                     | 1.94                         |

<sup>a</sup> Linear regression of the data presented in Figure 43

<sup>b</sup> Contribution to total zero order release rate by diffusion mechanism

<sup>c</sup> Osmotic component of zero order release rate where  $\frac{dM}{dt_O} = \left( \left\{ \frac{dM}{dt_T} \right\}_{\text{water}} - \frac{dM}{dt_D} \right)$ , where  $\left\{ \frac{dM}{dt_T} \right\}_{\text{water}}$  values were taken from Table

total zero order release for KCl, diphenhydramine HCl, tramadol HCl and niacinamide were 180.29, 170.58, 104.75 and 24.64 mg/h, respectively and listed in Table 20. All zero order release rates were normalized to the molecular weights of the APIs. Figure 44 compares the total zero order release rate, and the osmotic and diffusive components of zero order release rates for KCl, diphenhydramine HCl, tramadol HCl and niacinamide at 37°C. Both osmotic and diffusive components of zero order release rates from cellulose capsules increased as the aqueous solubility of the enclosed API increased. However, the osmotic component of zero order release rate increases more dramatically than the diffusive component, as the solubility of the enclosed API is increased.

Evaluation of fluid permeability of cellulose capsules and comparison to conventional osmotic systems

The fluid permeability term describes the flow of a solution through a membrane when exposed to an osmotic pressure gradient. The slopes of the linear fitting parameters from Figure 42 were used to determine the fluid permeability ‘k’ of the capsules by the following relationship [114] :

Equation 28 
$$k = \frac{\text{slope} \times h}{A \times C}$$

Using  $h = 0.053$  cm,  $A = 2.91$  cm<sup>2</sup> and  $C =$  solubility of the APIs, the fluid permeability of KCl, diphenhydramine HCl, tramadol HCl and niacinamide were calculated to be  $4.29 \times 10^{-5}$ ,  $3.50 \times 10^{-5}$ ,  $4.62 \times 10^{-5}$  and  $6.88 \times 10^{-5}$  cm<sup>2</sup>/h-atm, respectively. The fluid permeability is the product of the water permeability through the membrane, under a pressure gradient (hydraulic permeability) in the absence of external hydrostatic pressure, and the reflection coefficient of the solute through the membrane. The reflection

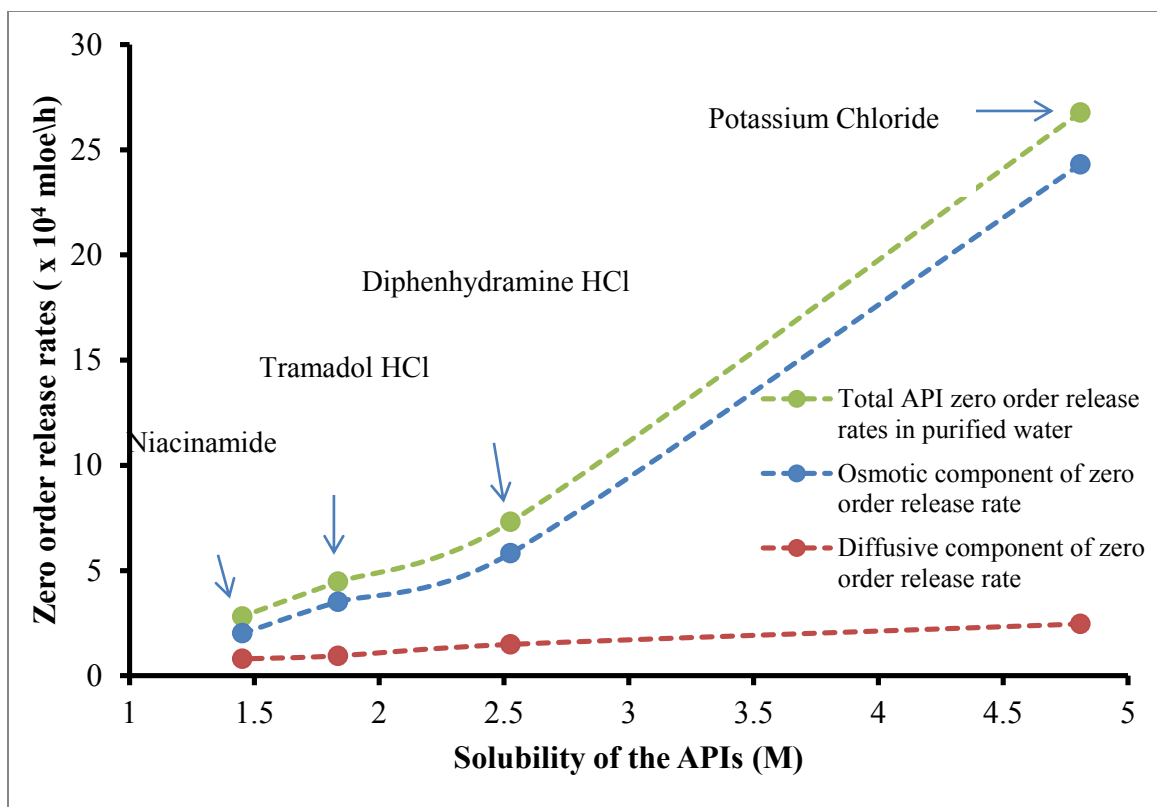


Figure 44: Comparison of total zero order release rate and the osmotic and diffusive components of zero order release rates of potassium chloride, diphenhydramine HCl, Tramadol HCl and niacinamide from cellulose capsules vs. their measured solubility in purified water, at 37°C.



coefficient of these APIs can be assumed to be equal to 1 since solute molecules were found to be permeable through the pores formed *in-situ* in regenerated cellulose films and hence the similarity of the fluid permeabilities is to be expected. Compared to conventional elementary ( $2.81 \times 10^{-6} \text{ cm}^2/\text{h-atm}$ ) [115], controlled porosity ( $7.91 \times 10^{-6} \text{ cm}^2/\text{h-atm}$ ) [114] and asymmetric membrane osmotic drug delivery systems ( $5.32 \times 10^{-6} \text{ cm}^2/\text{h-atm}$ ) [67], the hydraulic permeability of regenerated cellulose capsules was nearly ten times higher ( $\sim 4.66 \times 10^{-5} \text{ cm}^2/\text{h-atm}$ ). The cellulose films used in this investigation were found to absorb large amounts of water, and hence, the higher fluid permeability observed in regenerated cellulose capsules can be attributed to the hydrophilic nature of regenerated cellulose compared to cellulose acetate and ethyl cellulose utilized in conventional osmotic drug delivery systems. Hence, the cellulose capsules developed in this research are better suited for oral osmotic drug delivery systems than the systems previously engineered for this purpose.

#### Influence of osmotic flux on API diffusivity through capsule walls

To determine if the osmotic flux of KCl, diphenhydramine HCl, tramadol HCl and niacinamide had any impact on their transport through the capsule wall, the permeability coefficients of these APIs from capsules ( $P_{\text{capsule}}$ ) were compared with the permeability coefficients of these APIs through RC films determined using diffusion cell flux data. The RC films were prepared using 20 mm diameter glass test tube molds in order to be utilized in diffusion cell experiments. All RC films for these studies were prepared with three coatings of methylolcellulose solution using the same procedure utilized in fabricating cellulose capsules. The permeability coefficients of KCl, diphenhydramine HCl, tramadol HCl and niacinamide through the capsules were

determined from the zero order release rate contributed by diffusive mechanism  $\left\{ \frac{dM}{dt_D} \right\}$ , i.e. the intercept values obtained by linear regression of the data presented in Figure 43, by the following relationship:

$$\text{Equation 29} \quad P_{\text{device}} = \left\{ \frac{dM}{dt_D} \right\} \frac{h}{A C}$$

where, 'C' is the concentration of the API in capsule core, 'h' is the hydrated thickness of the capsule wall and A is the surface area of the capsule wall. Since a saturated API solution is formed in the capsule core during zero order release, the aqueous solubility of the APIs were utilized as their concentration in the capsule core. The permeability coefficients for moderately soluble and poorly soluble acetaminophen and ketoprofen, respectively, were determined from the zero order release rates observed in purified water, using the above relation, assuming that both ketoprofen and acetaminophen were primarily released by the diffusive through the pores in the hydrated capsule wall. The flux profiles of the APIs through RC films in diffusion cell experiments are shown in Figure 45. The permeability coefficients of KCl, diphenhydramine HCl, tramadol HCl and niacinamide through RC films were determined by the steady state flux method using 0.1 M donor cell concentrations in order to limit osmosis mediated solute/solvent flux across the RC films in the diffusion cells. The permeability coefficients of acetaminophen and ketoprofen were determined using the same method, except the donor cell contained saturated solutions of these APIs. The permeability coefficients of the APIs through RC films in diffusion cell experiments were determined by the following relationship:

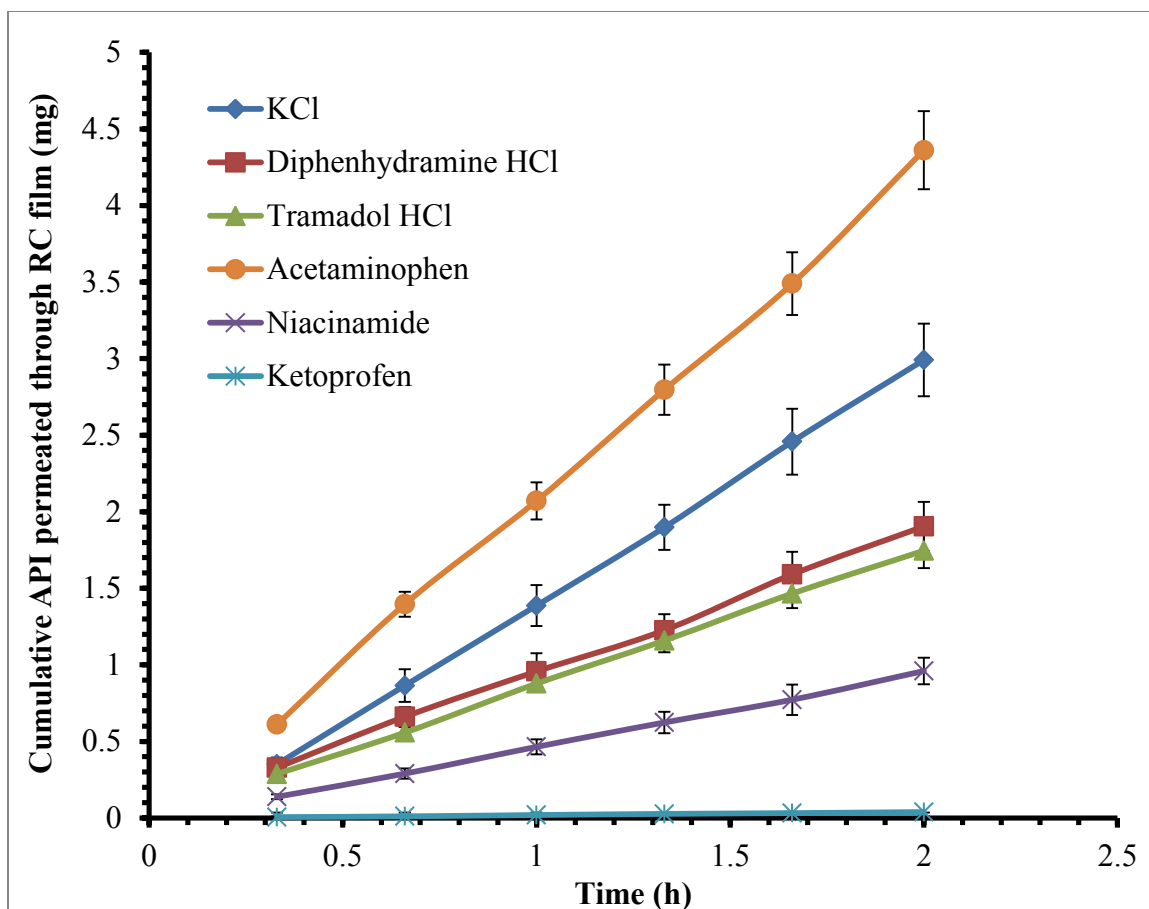


Figure 45: Flux profiles of KCl (0.1 M), diphenhydramine HCl (0.1 M), tramadol HCl (0.1 M), niacinamide (0.1 M), acetaminophen (0.14 M) and ketoprofen (0.0011 M) through RC films (diffusion cell experiments), in purified water at 37 °C.

Equation 30

$$P_{RC \text{ film}} = \left\{ \frac{dM}{dt} \right\} \frac{h}{A C_d}$$

where,  $\left\{ \frac{dM}{dt} \right\}$ , is the flux rate of the API through the RC films in the diffusion cells and 'C<sub>d</sub>' is the concentration of the API in the donor cell. The flux parameters from the diffusion cells and permeability coefficients of the APIs through the capsule and the RC films are summarized in Table 21. The extent of the deviations of the diffusive mechanism of the APIs from cellulose capsules were quantified by the following relationship:

Equation 31 Diffusive mechanism alteration =  $\frac{P_{\text{device}}}{P_{RC \text{ film}}}$

The diffusive mechanism alterations for KCl, diphenhydramine HCl, tramadol HCl, niacinamide, acetaminophen and ketoprofen were 0.15, 0.57, 0.81, 0.90, 0.97 and 0.98, respectively. Figure 46 compares the diffusive mechanism reduction of each API vs. their solubility in purified water at 37°C. As the API solubility increased, its diffusivity through the capsule wall decreased as indicated by a decrease in the diffusive mechanism alteration. In the previous chapter, the flux of KCl as well as the alkyl-p-aminobenzoates through RC films was found to occur through porous channels and hence the diffusivity of these APIs through the capsules can also be assumed to occur through these porous channels formed *in situ*. Based on these results, the API release from cellulose capsules can be regarded as a competitive process between the diffusive mechanism and the osmotic mechanism. A highly soluble API, such as KCl, is primarily released by the osmotic mechanism, which shadows the diffusive flux during the zero order phase of its release. On the other hand, the diffusive flux alteration was nearly 1 for ketoprofen and

Table 21: Permeability coefficients of APIs from cellulose capsules and through RC films obtained from diffusion cell experiments, and the calculated reduction in diffusive mechanism.

| API                        | Capsule                                                                            |                                                                   | RC film flux parameters from diffusion cells |                                                 |                                           |                                                                   | Diffusive mechanism alteration<br>$\left(\frac{P_{\text{device}}}{P_{\text{RC film}}}\right)$ |
|----------------------------|------------------------------------------------------------------------------------|-------------------------------------------------------------------|----------------------------------------------|-------------------------------------------------|-------------------------------------------|-------------------------------------------------------------------|-----------------------------------------------------------------------------------------------|
|                            | Diffusive component of zero order release rate<br>$\left\{\frac{dM}{dt}\right\}_D$ | Permeability coefficient<br>( $P_{\text{capsule}}$ ) <sup>a</sup> | Flux rate<br>$\left\{\frac{dM}{dt}\right\}$  | Concentration of API in donor cell<br>( $C_d$ ) | Thickness of the film <sup>d</sup><br>(h) | Permeability coefficient<br>( $P_{\text{RC Film}}$ ) <sup>e</sup> |                                                                                               |
|                            | (mg/h)                                                                             | ( $\times 10^{-7}$ , $\text{cm}^2/\text{sec}$ )                   | (mg/h)                                       | (mg/ml)                                         | (n=3, cm)                                 | ( $\times 10^{-7}$ , $\text{cm}^2/\text{sec}$ )                   |                                                                                               |
| <b>KCl</b>                 | 18.27                                                                              | 2.59                                                              | 1.53                                         | 7.86 <sup>b</sup>                               | 0.055                                     | 17.5                                                              | 0.15                                                                                          |
| <b>Diphenhydramine HCl</b> | 43.94                                                                              | 3.00                                                              | 1.49                                         | 25.5 <sup>b</sup>                               | 0.055                                     | 5.25                                                              | 0.57                                                                                          |
| <b>Tramadol HCl</b>        | 23.84                                                                              | 2.22                                                              | 0.88                                         | 26.3 <sup>b</sup>                               | 0.051                                     | 2.79                                                              | 0.81                                                                                          |
| <b>Niacinamide</b>         | 10.67                                                                              | 3.04                                                              | 0.48                                         | 12.2 <sup>b</sup>                               | 0.055                                     | 3.54                                                              | 0.90                                                                                          |
| <b>Acetaminophen</b>       | 3.82                                                                               | 9.01                                                              | 2.16                                         | 21.7 <sup>c</sup>                               | 0.059                                     | 9.60                                                              | 0.97                                                                                          |
| <b>Ketoprofen</b>          | 0.038                                                                              | 7.68                                                              | 0.021                                        | 0.25 <sup>c</sup>                               | 0.057                                     | 7.61                                                              | 0.98                                                                                          |

<sup>a</sup>  $P_{\text{capsule}} = \left\{\frac{dM}{dt}\right\}_D \frac{h}{AC}$ ,  $h = 0.053$  cm,  $A = 2.91$   $\text{cm}^2$ ,  $C$  is the solubility of the API

<sup>b</sup> Concentration in donor cell were set to 0.1 M in order to prevent osmotic flux of water from the receiver to donor cell

<sup>c</sup> Aqueous solubility of acetaminophen and ketoprofen as saturated solutions were utilized in diffusion cell experiments

<sup>d</sup> Thickness of the wet film measured at the end of the experiment

<sup>e</sup>  $P_{\text{RC film}} = \left\{\frac{dM}{dt}\right\} \frac{h}{AC_d}$ ,  $A = 1.7$   $\text{cm}^2$ ,  $C_d =$  concentration of the API in the donor cell of the Side-by-Side diffusion cells

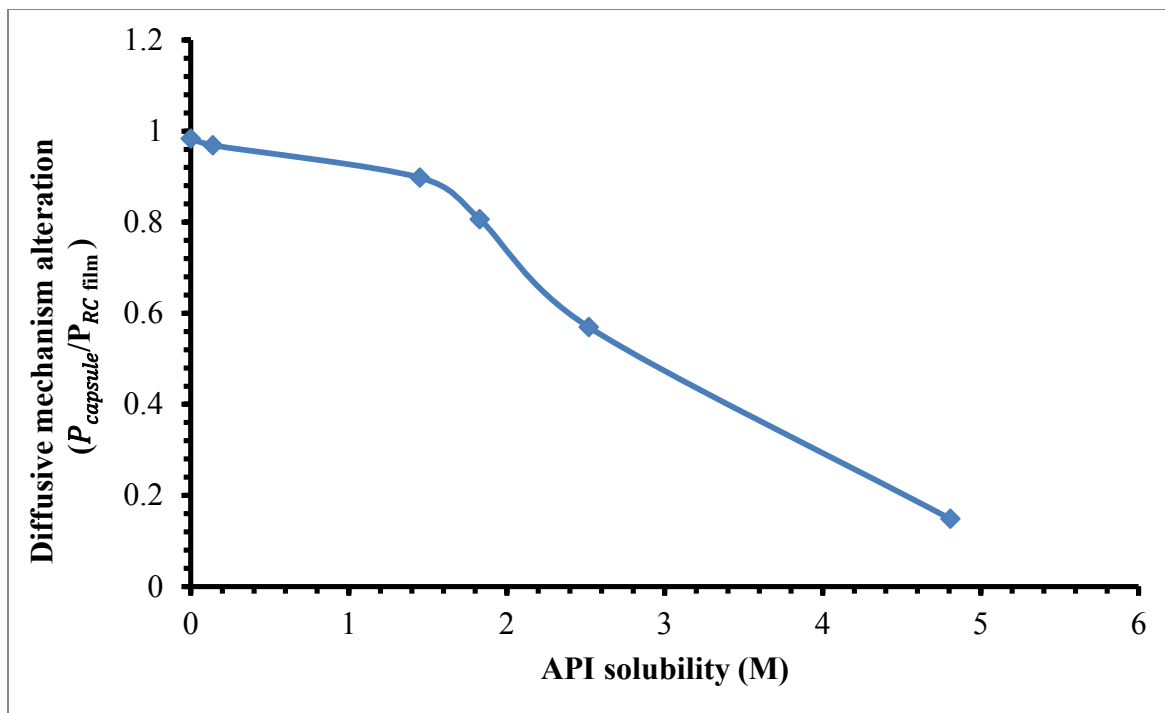


Figure 46: Comparison of diffusive mechanism reduction and solubility of the APIs.

acetaminophen (two moderate to poorly soluble APIs in comparison to KCl, diphenhydramine HCl, tramadol HCl and niacinamide) indicating that their release primarily occurs by the diffusive flux through the pores formed in the hydrated capsule wall.

#### *In-vitro* conditions influencing API release

Drug release from polymeric membrane controlled release devices relies on various physiological factors including the agitation of the gastro intestinal fluids and the environmental pH, based on the physiochemical properties of the API. To characterize the influence of gastro intestinal agitation conditions, the *in-vitro* release of KCl and acetaminophen was examined in release media under varying hydrodynamic conditions. The agitation rate of the paddles was modulated from 150 to 50 rpm and the release medium utilized for these studies was 1 L purified water. Figure 47 shows the release of KCl from capsules with varying stirring rates. As seen from the KCl release profiles, the stirring rate has practically no effect on the release of KCl. Since KCl release occurs via osmotic pumping (convection of fluid under pressure gradient), it is unlikely that the stagnant diffusion layer effects are playing any major role in the release of water soluble APIs from one component fills in the capsule. Gale et al. have shown that osmotic mechanism of release across the porous film coated tablets are not influenced by stirring rates since the drug release from these devices occurs by convection of the drug solution from the device core through the films [116]. Figure 47 shows the release of acetaminophen from cellulose capsules with varying stirring rates. Unlike KCl, APAP does show an agitation effect on its release as the paddle speed decreases from 100 to 50 rpm. However, no significant differences were observed when the paddle speeds was set

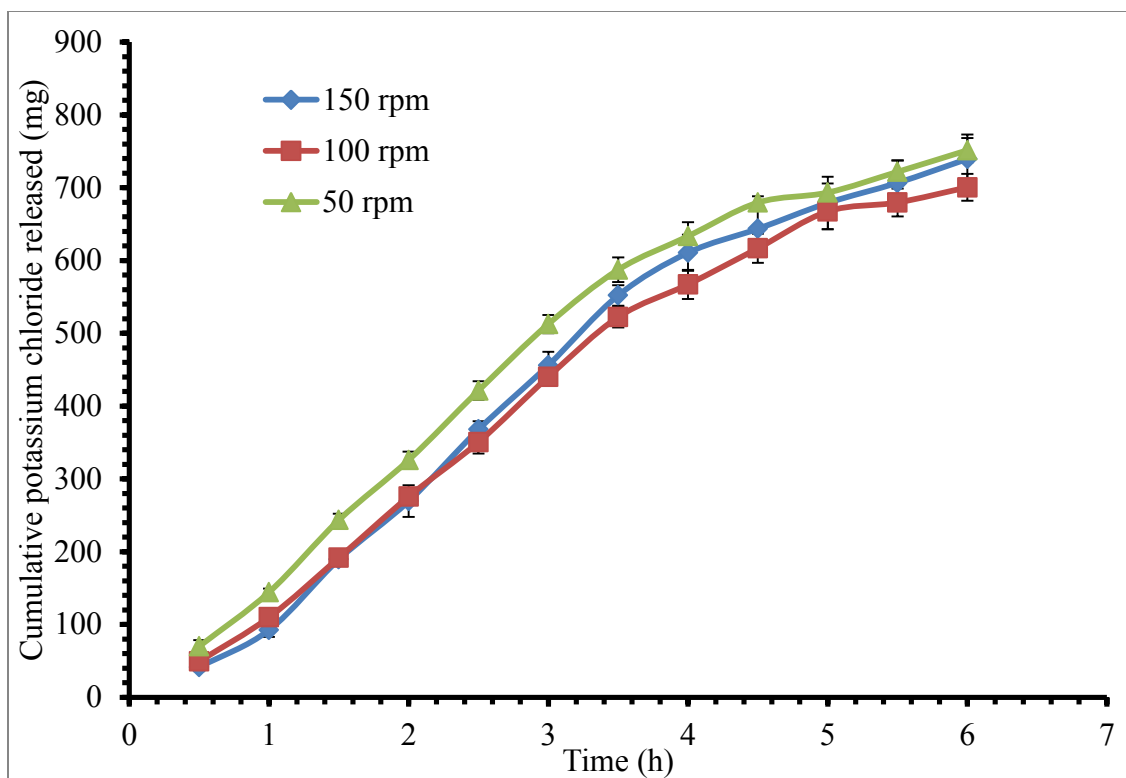


Figure 47: Release of potassium chloride from cellulose capsules in water with varying paddle speeds, at 37 °C.



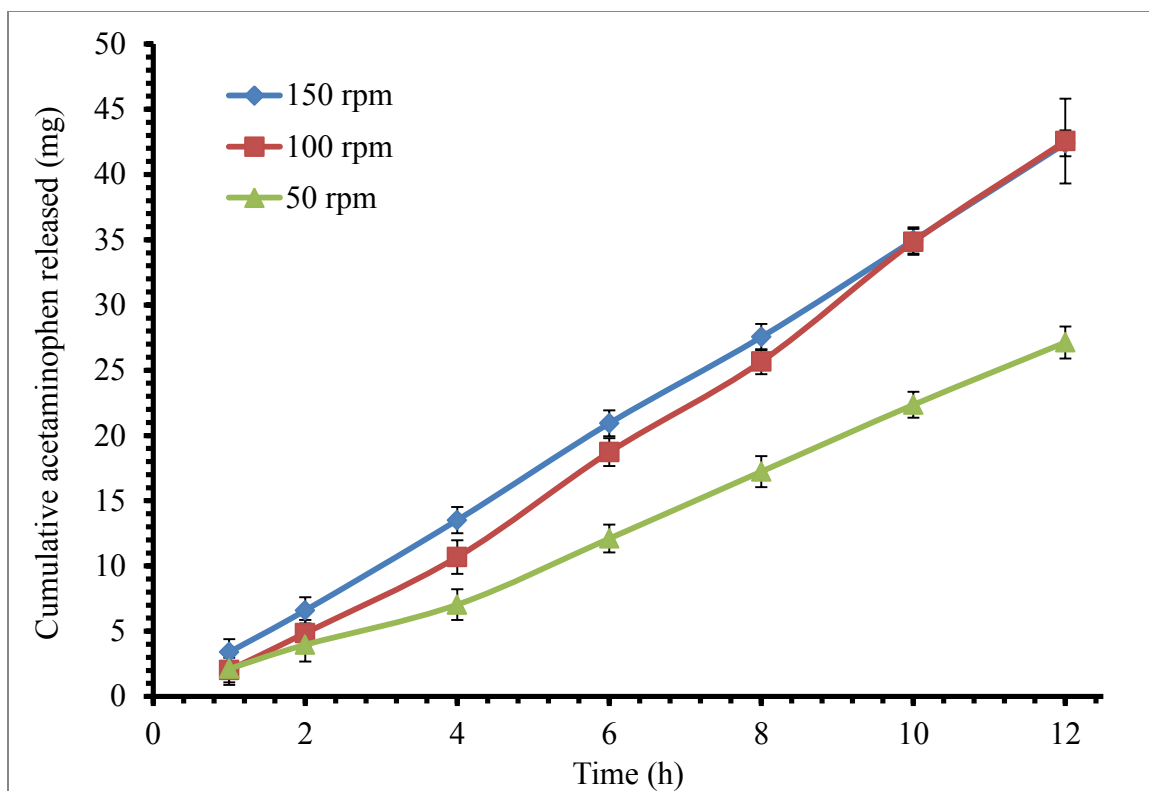


Figure 48: Release of acetaminophen from cellulose capsules in water with varying paddle speeds at 37 °C in purified water.

at 150 rpm, compared to 100 rpm. It is unclear at this point as to whether diffusion layer effects may have played any role in reduced drug release at 50 rpm. It is more likely that the intensive paddle speeds at 100 and 150 rpm may have caused displacement, shaking and/or rocking of the capsule in the dissolution vessel which in turn may have led to faster dissolution of the drug in the core at 150 and 100 rpm paddle speeds.

To analyze the influence of changes in pH of the gastro intestinal tract and its impact on the release of the enclosed API, ketoprofen was chosen as the model drug and its release examined *in-vitro* in pH 1.2 and pH 7.4 buffer medium. Figure 49 shows the release profiles of ketoprofen from cellulose capsules in pH 1.2 and 7.4 medium, at 37 °C. Ketoprofen (pKa 4.76) was chosen as a model API owing to its pH dependent solubility reported by Sheng et al (0.30 mg/ml in pH 1.2 and 40.76 mg/ml in pH 6.8 medium) [111]. All though the bulk environment pH of 7.4 should have theoretically increased the release rate of ketoprofen, the release profile in pH 7.4 was nearly identical to the release profile in pH 1.2. Hence, the pH of the external environment has no impact on the release of a drug with pH dependent solubility, from the capsule core.

### **Conclusions**

Regenerated cellulose capsules were readily formed by immersion precipitation of methylolcellulose solution on Teflon mold pin molds. A multiple dip coating approach was required in order to improve the mechanical stability of the capsule halves. When assembled, these capsules resembled size 000 gelatin capsules in terms of the amount of empty volume of inside the assembled capsules. The release of dry powder

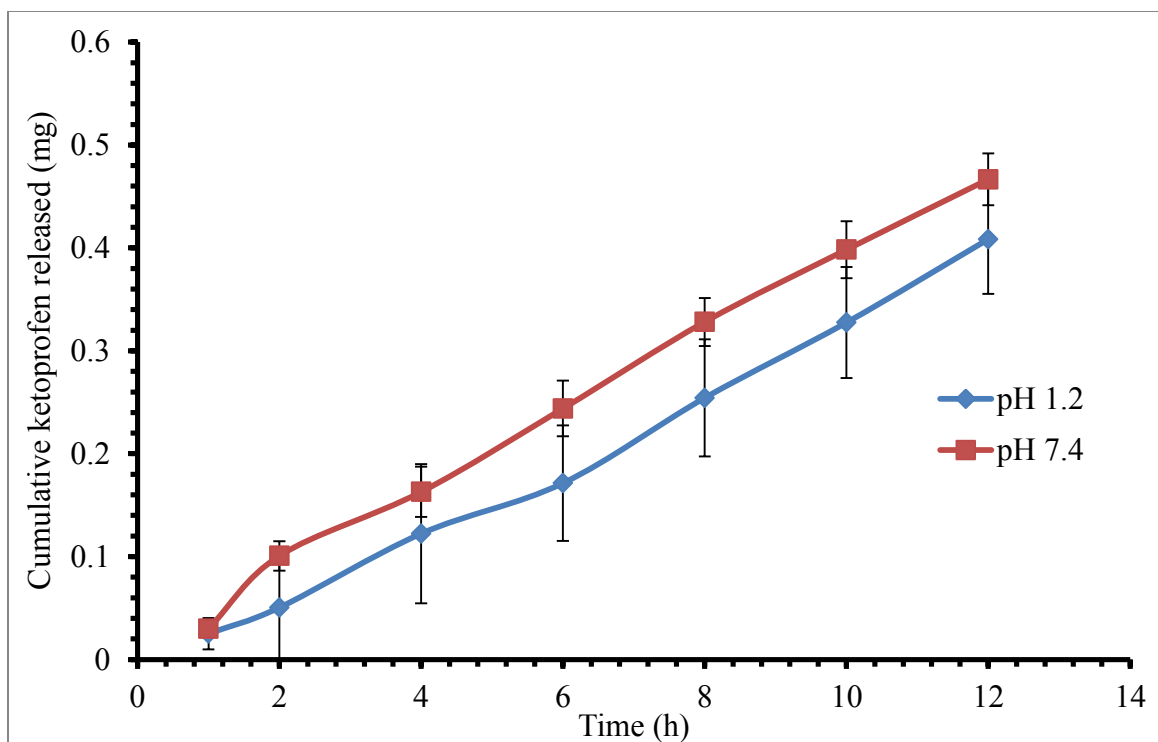


Figure 49: Influence of pH of the release medium on the release of ketoprofen from cellulose capsules at 37 °C.

filled APIs from cellulose capsules depends on water from the external traversing the capsule wall and forming a saturated API solution in the core. Zero order release rates are observed for APIs as long as a saturated solution in the capsules is maintained. Zero order release rates were higher for water soluble APIs and they decreased as the aqueous solubility decreased. The release rate of water soluble APIs also decreased when the osmotic pressure of the external medium was increased. An evaluation of the zero order release rate with varying osmotic pressure differences across the capsule shells indicated that both osmotic and diffusive components were involved in the release of water soluble APIs. Both osmotic and diffusive release rates increased as the aqueous solubility of the enclosed API increases. Comparison of the permeability coefficients of the APIs obtained from the diffusive component of release from cellulose capsules with the permeability coefficients obtained for RC films in Side-by-Side diffusion cell experiments indicates that the diffusivity of the API through the capsule wall decreases as the osmotic component of the release rate increases. The release of water soluble APIs from cellulose capsules is regarded as a process where the osmotic component exceeds the diffusive component as the solubility of the API increases. The influence of stirring rates and pH of the external medium had minimal effects on the release of APIs from cellulose capsules.

## REFERENCES

- [1] Y. Chien, Fundamentals, Development concepts and biomedical assessments, in: Novel Drug Delivery Systems, Dekker, New York, 1982. 43-48
- [2] K. Das, in: An overview of controlled-release technology, A Wiley-Interscience Publication, New York, 1989, 2-10.
- [3] D. Klemm, T. Philipp, U. Heinze, W. Wagenknecht, Comprehensive Cellulose chemistry volume I: Fundamentals and analytical methods, in: Wiley-VCH, New York, 1998, 15-25.
- [4] D. Klemm, H. Schmauder, T. Heinze, Cellulose, Biopolymers. 6 (2002) 275-319.
- [5] J. Blackwell, F. Kolpak, The cellulose microfibril as an imperfect array of elementary fibrils, Macromolecules. 8 (1975) 322-326.
- [6] K. Edgar, C. Buchanan, J. Debenham, P. Rundquist, B. Seiler, M. Shelton, D. Tindall, Advances in cellulose ester performance and application, Progress in Polymer Science. 26 (2001) 1605-1688.
- [7] E. Ford, K. Mendon, F. Thames, W. Rawlins, X-ray diffraction of cotton treated with neutralized vegetable oil-based macromolecular crosslinkers, Journal of Engineered Fibers and Fabrics. 5 (2010) 10-19.
- [8] A. Mittal, R. Katahria, M. Himmel, D. Johnson, Effects of alkaline or liquid-ammonia treatment on crystalline cellulose: changes in crystalline structure and effects on enzymatic digestibility, Biotechnology for Biofuels. 4 (2011), 22-34.
- [9] R. Kirk, D. Othmer, Encyclopedia of Chemical Technology, John Wiley, New York, 1968.
- [10] J. Siepman, H. Kranz, R. Bodmeier, N.A. Peppas, HPMC-matrices for controlled drug delivery: A new model combining diffusion, swelling, and dissolution mechanisms and predicting the release kinetics, Pharmaceutical Research 16 (1999) 1748-1756.
- [11] C. Sánchez-Lafuente, M. Fauci, M. Fernández-Arévalo, J. Álvarez-Fuentes, A. Rabasco, P. Mura, Development of sustained release matrix tablets of didanosine containing methacrylic and ethylcellulose polymers, International Journal of Pharmaceutics. 234 (2002) 213-221.
- [12] B. Lindstedt, M. Sjöberg, J. Hjærtstam, Osmotic pumping release from KCl tablets coated with porous and non-porous ethylcellulose, International Journal of Pharmaceutics. 67 (1991) 21-27.

- [13] V. King, T. Wheatley, Plasticized cellulose acetate latex as a coating for controlled release, in: *Polymeric Delivery Systems*, American Chemical Society, 1993, pp. 80-83.
- [14] S. Vaithiyalingam, M. Nutan, I. Reddy, M. Khan, Preparation and characterization of a customized cellulose acetate butyrate dispersion for controlled drug delivery, *Journal of Pharmaceutical Sciences*. 91 (2002) 1512-1522.
- [15] F. Goodhart, M. Harris, K. Murthy, R. Nesbitt, An evaluation of aqueous film-forming dispersions for controlled release, *Pharmaceutical Technology*. 8 (1984) 64-71.
- [16] K. Edgar, C. Buchanan, J. Debenham, P. Rundquist, B. Seiler, M. Shelton, D. Tindall, Advances in cellulose ester performance and application, *Progress in Polymer Science*. 26 (2001) 1605-1688.
- [17] M. Hirota, N. Tamura, T. Saito, A. Isogai, Oxidation of regenerated cellulose with NaClO<sub>2</sub> catalyzed by TEMPO and NaClO under acid-neutral conditions, *Carbohydrate Polymers*. 78 (2009) 330-335.
- [18] T. Yang, In: Ph.D Thesis, Preparation, characterization and pharmaceutical uses of biodegradable oxidized cellulose and its adduct with chitosan, The University of Iowa, (2002).
- [19] C. Chang, L. Zhang, Cellulose-based hydrogels: Present status and application prospects, *Carbohydrate Polymers*, 84 (2011) 40-53.
- [20] T. Stepanik, S. Rajagopal, D. Ewing, R. Whitehouse, Electron-processing technology: A promising application for the viscose industry, *Radiation Physical Chemistry*, 52 (1998) 505-509.
- [21] H. Zhao, J. Kwak, Y. Wang, J. Franz, J. White, J. Holladay, Interactions between cellulose and N-methylmorpholine-N-oxide, *Carbohydrate Polymers*. 67 (2007) 97-103.
- [22] H.-. Fink, P. Weigel, H.J. Purz, J. Ganster, Structure formation of regenerated cellulose materials from NMMO-solutions, *Progress in Polymer Science*. 26 (2001) 1473-1524.
- [23] T. Rosenau, A. Potthast, H. Sixta, P. Kosma, The chemistry of side reactions and byproduct formation in the system NMMO/cellulose (Lyocell process), *Progress in Polymer Science*. 26 (2001) 1763-1837.
- [24] T. Rosenau, A. Potthast, H. Sixta, P. Kosma, The chemistry of side reactions and byproduct formation in the system NMMO/cellulose (Lyocell process), *Progress in Polymer Science*. 26 (2001) 1763-1837.
- [25] J. Cai, L. Zhang, Unique gelation behavior of cellulose in NaOH/urea aqueous solution, *Biomacromolecules*. 7 (2006) 183-189.

- [26] A. Lue, L. Zhang, D. Ruan, Inclusion complex formation of cellulose in NaOH/thiourea aqueous system at low temperature, *Macromolecular Chemistry and Physics*. 208 (2007) 2359-2366.
- [27] R. Li, L. Zhang, M. Xu, Novel regenerated cellulose films prepared by coagulating with water: Structure and properties, *Carbohydrate Polymers* 87 (2012) 95-100.
- [28] R. Swatloski, S. Spear, J. Holbrey, R. Rogers, Dissolution of cellulose with ionic liquids, *Journal of American Chemical Society* 124 (2002) 4974-4975.
- [29] H. Zhang, J. Wu, J. Zhang, J. He, 1-Allyl-3-methylimidazolium chloride Ionic Liquid: A new and powerful nonderivatizing solvent for cellulose, *Macromolecules*. 38 (2005) 8272-8277.
- [30] S. Zhu, Y. Wu, Q. Chen, Z. Yu, C. Wang, S. Jin, Y. Ding, G. Wu, Dissolution of cellulose with ionic liquids and its application: a mini-review, *Green Chemistry* 8 (2006) 325-327.
- [31] D. Ishii, D. Tatsumi, T. Matsumoto, K. Murata, H. Hayashi, H. Yoshitani, investigation of the structure of cellulose in LiCl/DMAc solution and its gelation behavior by small-angle X-ray scattering measurements, *Macromolecular Bioscience*. 6 (2006) 293-300.
- [32] T. Baker, In Ph.D. Thesis: Formation and reactions of methylol cellulose, Georgia Institute of Technology (1979).
- [33] R. Seymour, E. Johnson, Acetylation of DMSO:PF solutions of cellulose, *Journal of Polymer Science: Polymer Chemistry Edition*. 16 (1978) 1-11.
- [34] L. Schroedera, V. Gentilea, R. Atallaa, Nondegradative preparation of amorphous cellulose, *Journal of Wood Chemical Technology*, 6 (1986) 1-14.
- [35] P. RoyChowdhury, V. Kumar, Fabrication and evaluation of porous 2,3-dialdehydecellulose membrane as a potential biodegradable tissue-engineering scaffold, *Journal of Biomedical Materials Research Part A*. 76A (2006) 300-309.
- [36] C. He, Q. Wang, Studies on the properties of cotton linter membranes, *Advance Polymer Technology*, 10 (1999) 438-441.
- [37] A. Svensson, E. Nicklasson, T. Harrah, B. Panilaitis, D.L. Kaplan, M. Brittberg, P. Gatenholm, Bacterial cellulose as a potential scaffold for tissue engineering of cartilage, *Biomaterials*. 26 (2005) 419-431.
- [38] A. Sokolnicki, R. Fisher, T. Harrah, D. Kaplan, Permeability of bacterial cellulose membranes, *Journal of Membrane Science*. 272 (2006) 15-27.

- [39] G. Serafica, R. Mormino, H. Bungay, Inclusion of solid particles in bacterial cellulose, *Applied Microbiology and Biotechnology*. 58 (2002) 756-760.
- [40] M. Mulder, *Basic Principles of Membrane Technology*, 2nd ed., Kluwer Academic Publishers, The Netherlands, 1996. pp 176-182
- [41] R. Kesting, *Phase Inversion Membranes, Materials Science of Synthetic Membranes*, American Chemical Society, 1985, pp. 131-164.
- [42] J. Fernandes, M. Gil, J. Castro, Hornification—its origin and interpretation in wood pulps, *Wood Science Technology*, 37 (2004) 489-494.
- [43] G. Jayme, G. Hunger, The rearrangement of microfibrils in dried cellulose and the implication of this structure alteration on pulp properties, *Fundamentals of Papermaking Fibers*, Cambridge, 1957, pp. 263-270.
- [44] K. Spence, R. Venditti, O. Rojas, Y. Habibi, J. Pawlak, The effect of chemical composition on microfibrillar cellulose films from wood pulps: water interactions and physical properties for packaging applications, *Cellulose*. 17 (2010) 835-848.
- [45] E. Letková, M. Letko, M. Vrška, Influence of recycling and temperature on the swelling ability of paper, *Chemical Papers*. 65 (2011) 822-828.
- [46] A. Streitwieser, C. Heathcock, *Introduction to organic chemistry*, 3rd ed., Macmillan, New York, 1989, pp. 859-860
- [47] P. Sinko, Y. Singh, *Martin's Physical Pharmacy and Pharmaceutical Sciences*, 6th ed., Lippincott Williams & Wilkins, Baltimore, 2011., pp 1656-1670.
- [48] V. Yasnovsky, D. Macdonald, Prevention of hornification of dissolving pulp, US. Patent No. 4,385,172 (1980)
- [49] H. Higgins, A McKenzie, The structure and properties of paper XIV: Effects of drying on cellulose fibers and the problems maintaining pulp strength, *Appita Journal*. 16 (1963) 145-161.
- [50] L. Lachman, H. Lieberman, J. Kanig, *Capsules, The Theorey and Practice of Industrial Pharmacy*, 2nd ed., Lea & Febiger, 1976, pp. 293-295.
- [51] G. Digenis, T. Gold, V. Shah, Cross-linking of gelatin capsules and its relevance to their in vitro-in vivo performance, *Journal of Pharmaceutical Science* 83 (1994) 915-921.
- [52] T. Ogura, Y. Furuya, S. Matsuura, HPMC capsules - An alternative to gelatin, *Pharmaceutical Technology Europe*. 10 (1998) 32-42.



- [53] L. Felton, M. Haase, N. Shah, G. Zhang, M. Infeld, A. Malick, J. McGinity, Physical and enteric properties of soft gelatin capsules coated with eudragit® L 30 D-55, , 113 (1995) 17-24.
- [54] E. Cole, R. Scott, A. Connor, I. Wilding, H. Petereit, C. Schminke, T. Beckert, D. Cadé, Enteric coated HPMC capsules designed to achieve intestinal targeting, *International Journal of Pharmaceutics*. 231 (2002) 83-95.
- [55] H. Brøndsted, C. Andersen, L. Hovgaard, Crosslinked dextran — a new capsule material for colon targeting of drugs, *Journal of Controlled Release*. 53 (1998) 7-13.
- [56] C.J. Kenyon, E.T. Cole, I.R. Wilding, The effect of food on the in vivo behaviour of enteric coated starch capsules, *International Journal of Pharmaceutics*. 112 (1994) 207-213.
- [57] F. Theeuwes, Delivery of drug to colon by oral disage form, US. Patent No. 4,904,474 (1990).
- [58] L. Dong, P. Wong, P. Espinal, L-OROS Hardcap: A new osmotic delivery system for controlled release of liquid formulation, In: *International Symposium on Controlled Release of Bioactive Materials*, (2001).
- [59] L. Dong, P. Wong, P. Espinal, A novel osmotic delivery system: L-OROS Soft cap, In: *International Symposium on Controlled Release of Bioactive Materials*, (2000).
- [60] P. Wong, Osmotic device with delayed activation of drug delivery, US. Patent No. 5,223,265 (1993).
- [61] P. Wong, F. Theeuwes, S. Larsen, L. Dong, Osmotic device for delayed delivery of agent, US. Patent No.5,531,736 (1996).
- [62] M. Mcneill, Dispensing device, US. Patent No.5,342,246, (1994).
- [63] H. Stevens, C. Wilson, P. Welling, M. Bakhshae, J. Binns, A. Perkins, M. Frier, E. Blackshaw, M. Frame, D. Nichols, M. Humphrey, S. Wicks, Evaluation of Pulsincap™ to provide regional delivery of dofetilide to the human GI tract, *International Journal of Pharmaceutics*, 236 (2002) 27-34.
- [64] M. Pina, A. Sousa, A. Brojo, Enteric coating of hard gelatin capsules. Part 1. Application of hydroalcoholic solutions of formaldehyde in preparation of gastro-resistant capsules, *International Journal of Pharmaceutics*, 133 (1996) 139-148.
- [65] A. Thombre, J. Cardinal, A. DeNoto, S. Herbig, K. Smith, Asymmetric membrane capsules for osmotic drug delivery: I. Development of a manufacturing process, *Journal of Controlled Release*, 57 (1999) 55-64.

- [66] S. Herbig, J. Cardinal, R. Korsmeyer, K. Smith, Asymmetric-membrane tablet coatings for osmotic drug delivery, *Journal of Controlled Release*, 35 (1995) 127-136.
- [67] A. Thombre, J. Cardinal, A. DeNoto, D. Gibbes, Asymmetric membrane capsules for osmotic drug delivery II. In vitro and in vivo drug release performance, *Journal of Controlled Release*, 57 (1999) 65-73.
- [68] Y. Chen, D. Flanagan, *Theory of Diffusion and Pharmaceutical Applications, Developing Solid Oral Dosage Forms*, Academic Press, San Diego, 2009, pp. 147-162.
- [69] S. Ghebre, R. Gordon, R. Nesbitt, M. Fawzi, Evaluation of acrylic-based modified-release film coatings, *International Journal of Pharmaceutics*, 37 (1987) 211-218.
- [70] E. Washburn, The Fundamental Law For a General Theory of solutions, *Journal of American Chemical Society*, 32 (1910) 653-670.
- [71] G. Lewis, The osmotic pressure of concentrated solutions and the law of perfect solutions. *Journal of American Chemical Society*, 30 (1908) 668-683.
- [72] R. Rose, J. Nelson, A continuous long term injector, *Australian Journal of Experimental Biological and Medical Sciences*. 33 (1955) 415-421.
- [73] O. Kedem, A. Katchalsky, A physical interpretation of the phenomenological coefficients of membrane permeability, *Journal of General Physiology*. 45 (1961) 143-179.
- [74] F. Theeuwes, Elementary osmotic pump, *Journal of Pharmaceutical Sciences* 64 (1975) 1987-1991.
- [75] F. Theeuwes, Osmotically powered agent dispensing device with filling means, US. Patent No. 3,760,984 (1973).
- [76] R. Rowe, P. Sheskey, M. Quinn, P. American, *Handbook of Pharmaceutical Excipients*, Pharmaceutical Press ; American Pharmacists Association, Washington, DC, 2009.
- [77] O. Battista, Hydrolysis and crystallization of cellulose, *Industrial & Engineering Chemistry*. 42 (1950) 502-507.
- [78] *The American Standard Test Methods, Standard Test Methods for Intrinsic Viscosity of Cellulose*, American Society for Testing and Materials, 1994, pp. 1795-1794.
- [79] A.W. Craig, D.A. Henderson, A viscometer for dilute polymer solutions, *Journal of Polymer Science*. 19 (1956) 215-218.

- [80] N. Patil, N. Dweltz, T. Radhakrishnan, X-Ray measurements of crystallinity and crystallite size in swollen and hydrolyzed cottons, *Textile Research Journal*. 32 (1965) 460-471.
- [81] United States Pharmacopeia and National Formulary, United States Pharmacopeial Convention, 2008.
- [82] R. Grouls, E. Ackerman, H. Korsten, L. Hellebrekers, D. Breimer, Partition coefficients (n-octanol/water) of N-butyl-p-aminobenzoate and other local anesthetics measured by reversed-phase high-performance liquid chromatography, *Journal of Chromatography B: Biomedical Sciences and Applications*. 694 (1997) 421-425.
- [83] S. Zhou, K. Tashiro, T. Hongo, H. Shirataki, C. Yamane, T. Ii, Influence of water on structure and mechanical properties of regenerated cellulose studied by an organized combination of infrared spectra, x-ray diffraction, and dynamic viscoelastic data measured as functions of temperature and humidity, *Macromolecules*. 34 (2001) 1274-1280.
- [84] H. Higgins, C. Stewart, K. Harrington, Infrared spectra of cellulose and related polysaccharides, *Journal of Polymer Science*. 51 (1961) 59-84.
- [85] Y. Kataoka, T. Kondo, FT-IR microscopic analysis of changing cellulose Crystalline structure during wood cell wall formation, *Macromolecules*. 31 (1998) 760-764.
- [86] C. Yamane, M. Mori, M. Saito, K. Okajima, Structures and mechanical properties of cellulose filament spun from cellulose/aqueous NaOH solution System, *Polymer Journal*. 28 (1996) 1039-1047.
- [87] D. Xing, N. Peng, T. Chung, Formation of cellulose acetate membranes via phase inversion using ionic liquid, [BMIM]SCN, as the Solvent, *Industrial Engineering and Chemistry Research*, 49 (2010) 8761-8769.
- [88] P. Kleinebudde, M. Jumaa, F. Saleh, Influence of degree of polymerization on behavior of cellulose during homogenization and extrusion/spheronization, *The AAPS Journal*. 2 (2000) 18-27.
- [89] E. Nagy, O. Borlai, A. Ujhidy, Membrane permeation of water—alcohol binary mixtures, *Journal of Membrane Science*. 7 (1980) 109-118.
- [90] N. Nambu, T. Nagai, H. Nogami, Permeation of phenothiazines through cellulose membrane, *Chemical and Pharmaceutical Bulletin*. 19 (1971) 802-812.
- [91] N. Peppas, D. Meadows, Macromolecular structure and solute diffusion in membranes: An overview of recent theories, *Journal of Membrane Science*. 16 (1983) 361-377.

- [92] M. Nakagaki, N. Koga, S. Iwata, Bio-physico-chemical studies on phenoxazone compounds. I. Diffusion constant and degree of association, Japanese journal of pharmacology. 82 (1962) 1134-1138.
- [93] Y. Oh, D. Flanagan, Diffusional properties of zein membranes and matrices, Drug Development in. Industrial Pharmacy, 36 (2010) 497-507.
- [94] M. Antwi, A. Myerson, W. Zurawsky, Diffusion of lysozyme in buffered salt solutions, Industrial Engineering and Chemical Research, 50 (2011) 10313-10319.
- [95] A. Gaigalas, J. Hubbard, M. McCurley, S. Woo, Diffusion of bovine serum albumin in aqueous solutions, Journal of Physical Chemistry, 96 (1992) 2355-2359.
- [96] R. Fisher, Diffusion with immobilization in membranes: Transport and failure mechanisms, PART II— Transport Mechanisms Biological and Synthetic Membranes, Alan R. Liss Co, 1989.
- [97] E. Achter, I. Swan, Conformation of lysozyme and  $\hat{I}\pm$ -lactalbumin in solution, Biochemistry , 10 (1971) 2976-2978.
- [98] R. Gavillon, T. Budtova, Kinetics of cellulose regeneration from cellulose/NaOH/Water gels and comparison with cellulose N-Methylmorpholine-N-Oxide\water solutions, Biomacromolecules. 8 (2007) 424-432.
- [99] N. Isobe, U. Kim, S. Kimura, M. Wada, S. Kuga, Internal surface polarity of regenerated cellulose gel depends on the species used as coagulant, Journal of Colloid Interface Science, 359 (2011) 194-201.
- [100] C. Kaewprasisit, E. Hequet, N. Abidi, J. Gourelot, Application of methylene blue adsorption to cotton fiber specific surface area measurement: Part I. Methodology, The Journal of Cotton Science. 2 (1998) 164-173.
- [101] G. Annadurai, R. Juang, D. Lee, Use of cellulose-based wastes for adsorption of dyes from aqueous solutions, Journal of Hazardous Materials, 92 (2002) 263-274.
- [102] F. Podczeczek, B.E. Jones, The History of Medicinal Capsules, Pharmaceutical Capsules, Pharmaceutical Press, London U.K., 2004, pp. 1-22.
- [103] S. Frisbee, K. Mehta, J. McGinity, Processing factors that influence the in vitro and in vivo performance of film-coated drug delivery systems, Drug Development. 2 (2002) 43-55.
- [104] T. Bussemer, R. Bodmeier, Formulation parameters affecting the performance of coated gelatin capsules with pulsatile release profiles, International Journal of Pharmaceutics. 267 (2003) 59-68.

- [105] T. Dahl, I. Sue, A. Yum, The effect of pancreatin on the dissolution performance of gelatin-coated tablets exposed to high-humidity conditions, *Pharmaceutical Research*, 8 (1991) 412-414.
- [106] T. Bussemer, R. Bodmeier, Formulation parameters affecting the performance of coated gelatin capsules with pulsatile release profiles, *International Journal of Pharmaceutics*, 267 (2003) 59-68.
- [107] M. Pina, A. Sousa, A. Brojo, Enteric coating of hard gelatin capsules. Part 2 — Bioavailability of formaldehyde treated capsules, *International Journal of Pharmaceutics* 148 (1997) 73-84.
- [108] M.J. O'Neil, *The Merck Index : An Encyclopedia of Chemicals, Drugs, and Biologicals* / Maryadele J. O'Neil, Merck, Whitehouse Station, N.J., 2006.
- [109] R. Hendrickson, P. Beringer, J.P. Remington, *Remington : The Science and Practice of Pharmacy*, Lippincott Williams & Wilkins, Philadelphia, PA, 2005.
- [110] USP, Acetaminophen monograph, in: Anonymous *The United States Pharmacopeia* 2008, pp. 1269.
- [111] J. Sheng, N. Kasim, R. Chandrasekharan, G. Amidon, Solubilization and dissolution of insoluble weak acid, ketoprofen: Effects of pH combined with surfactant, *European Journal of Pharmaceutical Sciences*. 29 (2006) 306-314.
- [112] L. Haar, J. Gallagher, G. and Kell, *NBS/NRC Steam Tables*, Hemisphere Publishing Corporation, New York, 1984 pp 1349-1352.
- [113] L. Savastano., H. Leuenberger, H. Merkle., Membrane modulated dissolution of oral drug delivery systems, *Pharmaceutica Acta Helvetia*, 70 (1995) 117-124.
- [114] F. Theeuwes, Elementary osmotic pump, *Journal of Pharmaceutical Sciences* 64 (1975) 1987-1991.
- [115] G. Zentner, G. Rork, K. Himmelstein, The controlled porosity osmotic pump, *Journal of Controlled Release*, 1 (1985) 269-282.
- [116] R. Gale, S. Chandrasekaran, D. Swanson, J. Wright, Use of osmotically active therapeutic agents in monolithic systems, *Journal of Membrane Science*, 7 (1980) 319-331.